

Investigation of the interaction of PRMT6 and LEF1/ β -catenin in hematopoiesis

Untersuchung der Zusammenwirkung von PRMT6 und LEF1/ β -Catenin in der Hämatopoese

von der Fakultät für Energie-, Verfahrens- und Biotechnik (Fakultät 4)
der Universität Stuttgart zur Erlangung der Würde eines Doktors der
Naturwissenschaften (Dr. rer. nat.) genehmigte Abhandlung

Vorgelegt von

Lucas Schneider

aus Bad Säckingen

Hauptberichter: Prof. Dr. Jörn Lausen

Mitberichter: Prof. Dr. Monilola Olayioye

Tag der mündlichen Prüfung: 29.03.2021

Institut für Industrielle Genetik der Universität Stuttgart

2021

Table of contents

Summary	1
Zusammenfassung.....	3
1 Introduction.....	5
1.1 Hematopoiesis.....	5
1.1.1 Adult hematopoiesis.....	5
1.1.2 Megakaryopoiesis and platelet production	6
1.1.3 Erythropoiesis.....	8
1.2 Chromatin and transcription	9
1.2.1 Chromatin organization.....	9
1.2.2 Posttranslational histone modifications.....	9
1.3 Protein Arginine Methyltransferases	11
1.3.1 Protein domain structures of PRMTs	11
1.3.2 The mechanism and function of arginine methylation of PRMTs.....	12
1.3.3 PRMT6	13
1.4 Hematopoietic transcription factors	16
1.4.1 RUNX1.....	16
1.4.2 TCF/LEF family	16
1.5 Wnt signaling pathway.....	18
1.5.1 β -catenin (CTNNB1).....	19
1.5.2 Wnt-signaling pathway in hematopoiesis	19
1.5.3 Wnt-signaling in megakaryopoiesis.....	20
1.6 The PRMT family in LEF1/Wnt/ β -catenin-signaling	20
1.7 Aim of this study.....	22
2 Materials and Methods	23
2.1 Material	23
2.1.1 Cell lines.....	23
2.1.2 Cell culture media and supplements.....	23
2.1.3 Chemicals, Reagents and Enzymes.....	24
2.1.4 Plasmids.....	26

2.1.5	Oligonucleotides.....	30
2.1.6	Antibodies.....	32
2.1.7	Equipment	33
2.2	Molecular biology techniques	34
2.2.1	Preparation of Calcium Competent Cells	34
2.2.2	Transformation of Competent Cells	34
2.2.3	Mini Plasmid DNA Preparation.....	34
2.2.4	Midi Plasmid DNA Preparation.....	34
2.2.5	Sequencing	34
2.2.6	Agarose Gel Electrophoresis.....	35
2.2.7	Polymerase Chain Reaction (PCR)	35
2.2.8	Cloning of lentiviral plasmids	35
2.2.9	RNA isolation	36
2.2.10	cDNA synthesis	36
2.2.11	Gene Expression analysis / quantitative real-time PCR (qPCR).....	36
2.3	Cell culture methods	37
2.3.1	Thawing and freezing of cells	37
2.3.2	Cell quantification with Neubauer counting chamber	37
2.3.3	Passaging of the cells.....	37
2.3.4	Isolation of primary hCD34 ⁺ cells	37
2.3.5	Differentiation of primary human CD34 ⁺ cells	38
2.3.6	Transient Transfection.....	38
2.3.7	Concentration of lentiviral particles.....	38
2.3.8	Gene knockdown and overexpression via lentiviral transduction	38
2.3.9	Cell cycle analysis	39
2.3.10	Multicolor Flow Cytometry.....	39
2.4	Protein biochemistry	39
2.4.1	Luciferase assay	39
2.4.2	Protein labeling	40
2.4.3	Whole cell lysates	40
2.4.4	Nuclear extraction	40
2.4.5	Co-Streptavidin precipitation	41

2.4.6	SDS-PAGE and Western blotting	41
2.4.7	Chromatin immunoprecipitation (ChIP).....	42
2.4.8	ChIP sequencing analysis.....	43
2.5	Identification of novel PRMT6 interaction partners.....	44
3	Results	46
3.1	PRMT6 is important in megakaryocytic and erythroid differentiation	46
3.2	Identification of novel PRMT6 interaction partners.....	46
3.3	PRMT6 interactome functional annotation	51
3.4	Network analysis of protein interaction data	53
3.5	Verification of the LEF1-PRMT6 protein interaction with Co-Streptavidin Precipitation	53
3.6	PRMT6 TOP-flash assay	57
3.7	LEF1 expression in different leukemia cell lines.....	58
3.8	LEF1 ChIP-Seq analysis in K562 cells.....	60
3.9	Verification of the identified LEF1 peaks.....	65
3.10	LEF1 knockdown in K562 cells	69
3.11	LEF1 overexpression in K562 cells	71
3.12	β -catenin overexpression in K562 cells	74
3.13	Verification of LEF1 binding sites in megakaryocytic cells	77
3.14	β -catenin overexpression in megakaryocytic cells.....	79
3.15	Expression analysis of erythroid and megakaryocytic cells	81
3.16	PRMT6 Knockdown shows a direct influence on the cell cycle.....	85
4	Discussion	87
4.1	PRMT6 interactome.....	87
4.2	LEF1 is a new interaction partner of PRMT6	89
4.3	LEF1 and PRMT6 in myeloid cells	89
4.4	Identification of target genes of LEF1 and PRMT6.....	90
4.5	Verification of LEF1-PRMT6 target genes.....	92
4.6	LEF1 participates in the megakaryocytic differentiation.....	92
4.7	LEF1-PRMT6 interaction in megakaryocytic cells.....	93
4.8	PRMT6 targets the cell cycle regulator CCND1	94
4.9	The bone marrow microenvironment (BMM).....	94
4.10	Implications and outlook.....	97

5	Supplements.....	98
6	References.....	104
7	List of tables.....	117
8	List of figures	118
9	Abbreviations	120
	Publications	124
	Curriculum vitae	125
	Acknowledgements.....	126
	Ehrenwörtliche Erklärung.....	127

Summary

Transcription factors and histone-modifying enzymes are important regulators of hematopoietic gene expression and cell differentiation. The hematopoietic differentiation is regulated by a regulatory network of various transcription factors, such as GATA1, RUNX1, KLF1, FLI1 and TAL1. (Hattangadi et al., 2011; Tijssen et al., 2011). Together, these factors control the cell fate decision of the megakaryocytic-erythroid differentiation.

PRMT6 was identified as an important factor in erythroid and megakaryocytic differentiation (Herglotz et al., 2013; Herkt et al., 2018). PRMT6 fulfills its function by being recruited by transcription factors such as RUNX1 to promoter regions of target genes, where it catalyzes the asymmetric dimethylation on H3R2. As a result, PRMT6 controls the expression of the megakaryocytic marker CD41 and the erythroid marker glycophorin A.

PRMT6 was used in this thesis to identify yet unknown transcription factors of the cell fate decision at the megakaryocytic-erythroid bifurcation. Stable isotope labeling of amino acids in cell culture was used to identify new interaction partners of PRMT6 by mass spectrometry. For this purpose, erythroleukemic K562 cells were lentivirally transduced with a biotin-coupled PRMT6 gene, and the tagged protein complexes were isolated by streptavidin precipitation. The subsequent proteome analysis identified the known interaction partners RUNX1 and PRMT1.

In addition, the transcription factor LEF1 was identified as a new interaction partner of PRMT6. This interaction was confirmed by co-streptavidin precipitation in HEK293T cells. LEF1 belongs to a family of transcription factors that are involved in the Wnt signaling pathway. This factor recruits the co-activator β -catenin to target genes in order to increase their expression. The interaction was confirmed by using the luciferase TOPflash detection system. Here it was shown that PRMT6 competes with β -catenin for binding to LEF1.

LEF1 is an important factor in lymphoid differentiation. An influence of this transcription factor on myeloid cells and on the cell fate decision of megakaryocytic-erythroid differentiation is unknown at the current state of research. To investigate this influence, LEF1 ChIP-Seq datasets from erythroleukemic K562 cells from the ENCODE database were evaluated (ENCODE Project Consortium, 2012; Davis et al., 2018). It was shown that LEF1 binds to promoter and enhancer regions of megakaryocytic genes. The target genes CD41, RUNX1 and CCND1 were confirmed by ChIP assay. The expression of these genes is also controlled by PRMT6 (Herglotz et al., 2013; Bao et al., 2018), confirming the interaction of PRMT6 and LEF1.

Inhibition of LEF1 expression in K562 cells by the RNA interference method with small hairpin RNA also reduced the expression of CD41 and CCND1. The overexpression of the LEF1 protein, however, led to an activation of the CCND1 expression, the CD41 and RUNX1 expression remained unchanged. The overexpression of the constitutively active co-activator β -catenin (Kolligs et al., 1999) in K562 cells activated the LEF1 expression and also increased the expression of the megakaryocytic genes CD41 and RUNX1. The expression of the erythroid genes TAL1, KLF1 and BCL6 remained unchanged.

The binding of LEF1 together with PRMT6 to the CD41 promoter was confirmed in TPO differentiated primary human CD34⁺ cells with CHIP assays. The overexpression of the constitutively active β -catenin protein also activated the LEF1, CD41 and RUNX1 genes in megakaryocytic cells. An expression analysis of various differentiated human CD34⁺ cells showed that LEF1 and PRMT6 are highly expressed in megakaryocytes.

The described study shows that the transcription factor LEF1 and the methyltransferase PRMT6 play an important role in the myeloid differentiation. LEF1 enables the recruitment of PRMT6 and β -catenin to megakaryocytic target genes. This shows that PRMT6 and the Wnt signaling pathway are important for the production of platelets. The obtained data support a model in that the Wnt signal transduction has a controlling function on the maturation of megakaryocytes in the bone marrow microenvironment. The LEF1/ β -catenin/Wnt signaling is a well-studied pathway in the hematopoietic stem cell niche, there it controls the maintenance and quiescence of the stem cells (Fleming et al., 2008). The pathway controls a great part of the lymphocyte development, controlling the maturation of B- and T-Lymphocytes (van Genderen et al., 1994; Verbeek et al., 1995). Different studies showed that several members of the PRMT family have a direct regulatory influence on the Wnt/ β -catenin signaling pathway (Cha and Jho, 2012). PRMT6 was identified in this work as a LEF1 interaction partner and thus also as a direct regulator of the Wnt/ β -catenin signaling pathway.

This thesis shows that PRMT6 and the Wnt signaling pathway have a regulating effect on megakaryopoiesis and platelet production. The cells of the bone marrow microenvironment which control this differentiation through Wnt signaling are still unknown. Elucidating this process will help to investigate and treat platelet production disorders such as thrombocytopenia and thrombocytopenia.

Zusammenfassung

Transkriptionsfaktoren und Histon-modifizierende Enzyme sind wichtige Regulatoren der hämatopoetischen Genexpression sowie der Zelldifferenzierung. Die hämatopoetische Differenzierung wird durch ein regulatorisches Netzwerk verschiedener Transkriptionsfaktoren, wie beispielsweise GATA1, RUNX1, KLF1, FLI1 und TAL1 reguliert. (Hattangadi et al., 2011; Tijssen et al., 2011). Diese Faktoren steuern gemeinsam die Linienentscheidung der megakaryozytär-erythroiden Differenzierung.

PRMT6 wurde als ein wichtiger Faktor in der erythroiden sowie der megakaryozytären Differenzierung identifiziert (Herglotz et al., 2013; Herkt et al., 2018). PRMT6 erfüllt seine Funktion indem es von Transkriptionsfaktoren wie beispielsweise RUNX1 zu Promotorregionen von Zielgenen rekrutiert wird und dort eine asymmetrische Dimethylierung an H3R2 katalysiert. Hierdurch beeinflusst PRMT6 die Expression des megakaryozytären Markers CD41 und des erythroiden Markers Glykophorin A.

In der vorliegenden Arbeit wurde PRMT6 verwendet um noch ungekannte Transkriptionsfaktoren dieser Linienentscheidung zu identifizieren. Mittels stabiler Isotopenmarkierung von Aminosäuren in Zellkultur wurden neue Interaktionspartner von PRMT6 durch Massenspektrometrie ermittelt. Hierfür wurden erythroleukämische K562 Zellen mit einem Biotin gekoppelten PRMT6 Gen lentiviral transduziert, und die markierten Proteinkomplexe mittels Streptavidin Präzipitation isoliert. Die nachfolgende Proteomanalyse konnte die bekannten Interaktionspartner RUNX1 und PRMT1 identifizieren.

Darüber hinaus wurde der Transkriptionsfaktor LEF1 als neuer Interaktionspartner von PRMT6 identifiziert. Diese Interaktion konnte mittels Co-Streptavidin Präzipitation in HEK293T Zellen bestätigt werden. LEF1 gehört zu einer Familie von Transkriptionsfaktoren, die am Wnt-Signalweg beteiligt sind. Dieser Faktor rekrutiert den Koaktivator β -Catenin zu Zielgenen, um deren Expression zu verstärken. Die Interaktion konnte durch Anwendung des Luciferase TOPflash Nachweissystems bestätigt werden, hier zeigte sich, dass PRMT6 zusammen mit β -Catenin um die Bindung an LEF1 konkurriert.

LEF1 ist ein wichtiger Faktor der lymphoiden Differenzierung. Ein Einfluss dieses Transkriptionsfaktors auf myeloische Zellen und auf die Linienentscheidung der megakaryozytär-erythroiden Differenzierung ist nach Stand der jetzigen Forschung unbekannt. Um diesen Einfluss zu untersuchen, wurden LEF1 ChIP-Seq Daten von erythroleukämische K562 Zellen aus der ENCODE Datenbank ausgewertet (ENCODE Project Consortium, 2012; Davis et al., 2018). Hierbei konnte gezeigt werden, dass LEF1 in den Promoter und Enhancer Regionen von megakaryozytären Genen bindet. Die Zielgene CD41, RUNX1 und CCND1 wurden mittels ChIP-Experimente bestätigt. Die Expression dieser Gene wird ebenfalls von PRMT6 kontrolliert (Herglotz et al., 2013; Bao et al., 2018) was die Interaktion von LEF1 und PRMT6 bestätigt.

Die Inhibierung der LEF1 Expression in K562 Zellen durch die RNA-Interferenz Methode reduzierte ebenfalls die Expression von CD41 und CCND1. Die Überexpression des LEF1 Proteins führte zu einer

Aktivierung der CCND1 Expression, die CD41 und RUNX1 Expression blieb hingegen unverändert. Die Überexpression des konstitutiv aktiven Coaktivators β -Catenin (Kolligs et al., 1999) in K562 Zellen führte nicht nur zur Aktivierung der LEF1 Expression sondern verstärkte auch die Expression der megakaryozytären Gene CD41 und RUNX1. Die Expression der erythroiden Gene TAL1, KLF1 und BCL6 blieben hingegen unverändert.

In TPO differenzierten primären human CD34⁺ Zellen konnte die Bindung von LEF1 zusammen mit PRMT6 auf dem CD41 Promoter mittels CHIP-Experimente bestätigt werden. Die Überexpression des konstitutiv aktiven β -Catenin Proteins führte in megakaryozytären Zellen ebenfalls zur Aktivierung der Gene LEF1, CD41 und RUNX1. Eine Expressionsanalyse verschiedener differenzierter humaner CD34⁺ Zellen zeigte, dass LEF1 zusammen mit PRMT6 auch in Megakaryozyten verstärkt exprimiert wird.

Die beschriebene Untersuchung zeigt, dass der Transkriptionsfaktor LEF1 und die Methyltransferase PRMT6 eine wichtige Rolle in der myeloiden Differenzierung spielen. LEF1 ermöglicht hier die Rekrutierung von PRMT6 und β -Catenin zu megakaryozytären Zielgenen. Dies zeigt, dass PRMT6 und der Wnt-Signalweg eine bedeutende Rolle in der Produktion von Blutplättchen innehaben. Die hier gewonnenen Daten unterstützen ein Modell, dass die Wnt Signaltransduktion im Mikromilieu des Knochenmarks eine steuernde Funktion auf die Ausreifung von Megakaryozyten hat. Die LEF1/ β -Catenin Signaltransduktion ist ein gut untersuchter Signalweg in der hämatopoetischen Stammzellnische und steuert dort die Aufrechterhaltung der Stammzellpopulation (Fleming et al., 2008). Des Weiteren kontrolliert der Signalweg einen großen Teil der Lymphozytenentwicklung und kontrolliert die Reifung von B- und T-Lymphozyten (van Genderen et al., 1994; Verbeek et al., 1995). Verschiedene Studien konnten zeigen, dass einige Mitglieder der PRMT-Familie einen direkten regulatorischen Einfluss auf den Wnt/ β -Catenin Signalweg haben (Cha and Jho, 2012). PRMT6 wurde in dieser Arbeit als LEF1 Interaktionspartner und damit auch als direkter Regulator des Wnt/ β -Catenin Signalwegs, identifiziert.

Diese Arbeit zeigt, dass der Wnt-Signalweg zusammen mit PRMT6 einen regulierenden Effekt auf die Megakaryopoese und die Thrombozytenproduktion hat. Die Zellen des Knochenmark- Mikromilieus, die diese Differenzierung durch Wnt-Signalübertragung steuern, sind jedoch noch unbekannt. Die Aufklärung dieses regulatorischen Prozesses kann dazu beitragen Störungen der Produktion von Thrombozyten, wie Thrombozythämien und Thrombozytopenien zu untersuchen und zu behandeln.

1 Introduction

1.1 Hematopoiesis

Hematopoiesis describes the formation of all blood cells from pluripotent hematopoietic stem cells (HSCs). Most mature blood cells are short lived and need to be continuously regenerated. Hematopoietic stem cells have the potential to differentiate into mature blood cells like erythrocytes, megakaryocytes, myeloid and lymphoid cells (Orkin and Zon, 2008). These processes of differentiation are carefully regulated by transcription factors, miRNAs, growth factors, cytokines and other chemical modulators (Zhu and Emerson, 2002; Bissels et al., 2012). In adult mammals the majority of these differentiation steps take place in a local tissue microenvironment, the hematopoietic stem cell niche of the bone marrow (Morrison and Scadden, 2014).

During embryogenesis, the primitive hematopoiesis initiates extra-embryonic in the yolk sac (Lancrin et al., 2009; Lancrin et al., 2010). The definitive hematopoiesis begins in the aorta-gonad-mesonephros region (Medvinsky and Dzierzak, 1998). These definitive HSCs move to the placenta and fetal liver and form the late fetal hematopoiesis. Finally hematopoiesis relocates to the bone marrow where it resides permanently (Balazs et al., 2006).

1.1.1 Adult hematopoiesis

The human adult hematopoiesis is modeled as a hierarchical system (Figure 1). Long-term repopulating hematopoietic stem cells (LT-HSCs) represent the immature cells and are capable of long-term self-renewal. During differentiation, these cells lose gradually the ability for self-renewal, called short-term (ST)-HSCs. This potential is further reduced in multipotent progenitors (MPPs). The MPPs bifurcate to common myeloid erythroid progenitors (CMEPs) or common lymphoid progenitors (CLPs). The later differentiate to mature lymphocytes represented by T- and B-cells. The CMEPs further differentiate into megakaryocytic-erythroid progenitors (MEPs) and granulocyte-macrophage progenitors (GMPs). The GMPs give rise to mature granulocytes, monocytes and macrophages. The MEPs bifurcate into erythroid progenitors (EP) or megakaryocytic progenitors (MkPs). An overview of this hierarchical model is shown in Figure 1 (Psaila and Mead, 2019).

The fate decision in hematopoietic differentiation is determined by transcription factors. An array of these factors is necessary for the long-term repopulating capability of HSCs. An example of the factors are RUNX1, GATA2, TAL1 and LEF1; see Figure 1 (Skokowa et al., 2006; Orkin and Zon, 2008). The branching points of differentiation are controlled by antagonizing transcription factors like FLI1 and KLF1 which control the megakaryocytic/erythroid bifurcation point (Starck et al., 2003).

The maintenance and differentiation of this system is also assured by different extrinsic factors like cytokines and growth factors. Examples are the hormone erythropoietin (EPO) which is the primary regulator of the definitive erythropoiesis (Jelkmann, 2007); the hormone thrombopoietin (TPO) instead stimulates the production and stimulation of megakaryocytes (Kaushansky, 1997). Furthermore differentiation and self-renewal of HSCs is controlled by the family of Wnt proteins (Luis et al., 2012). It has been shown that regulation of hematopoiesis with Wnt proteins is highly dosage

dependent. HSCs require a low Wnt dosage for self-renewal and T-Cell progenitors on the other hand require high dosages (Luis et al., 2011).

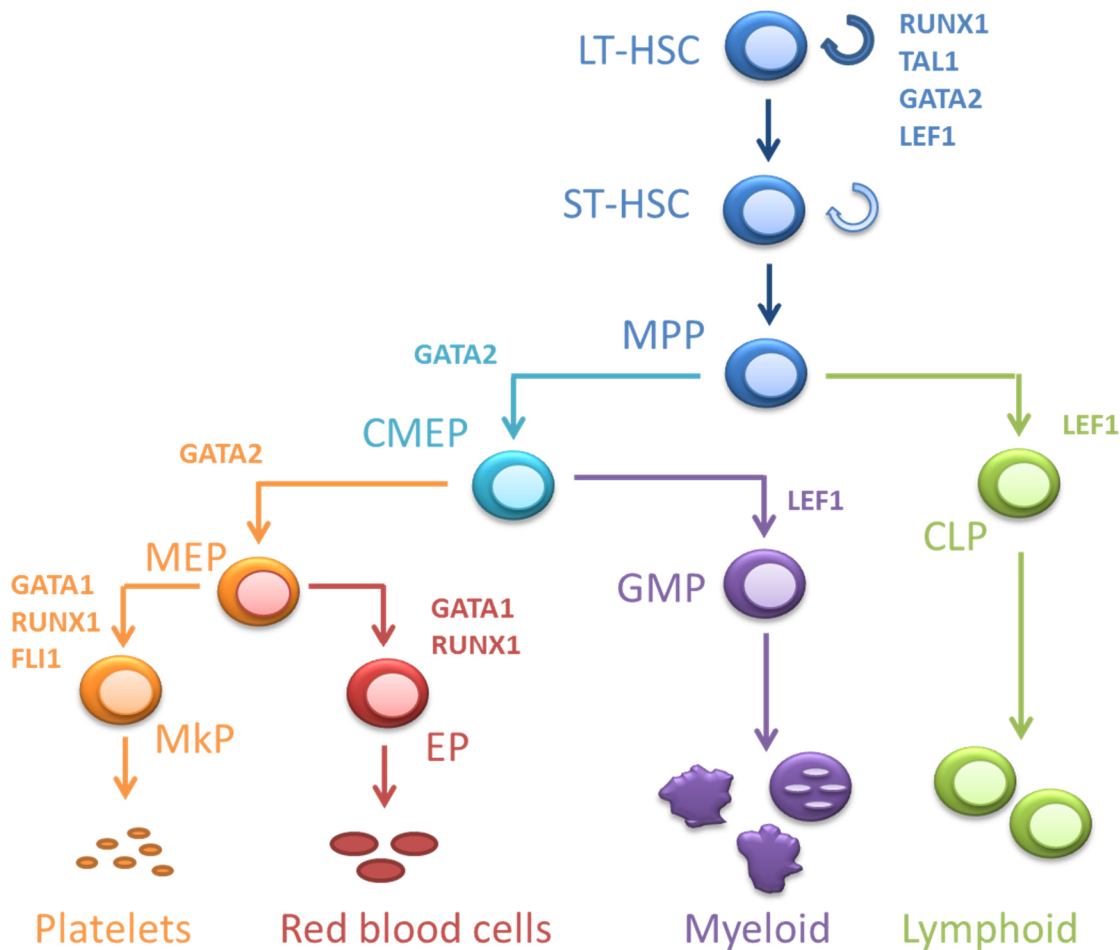


Figure 1: Hierarchical model of human hematopoiesis; Long-term repopulating hematopoietic stem cells are capable of long-term self-renewal and have the highest differentiation potential. Multipotent progenitors give rise to myeloid or lymphoid cells. Myeloid differentiation finally leads to the production of platelets, erythrocytes or other myeloid cells. Examples of hematopoietic transcription factors necessary for these processes are shown. LT-HSC: Long-term repopulating hematopoietic stem cells; ST-HSC: short-term repopulating hematopoietic stem cell; MPP: multipotent progenitor; CMEP: common myeloid erythroid progenitors; CLP: common lymphoid progenitor; GMP: granulocyte-macrophage progenitor; MEP: megakaryocytic-erythroid progenitor; EP: erythroid progenitor; MkP: megakaryocytic progenitor (Skokowa et al., 2006; Orkin and Zon, 2008; Songdej and Rao, 2017; Psaila and Mead, 2019).

1.1.2 Megakaryopoiesis and platelet production

Platelets produced by megakaryocytes are important in hemostasis, thrombosis and inflammation. The production of platelets is a multi-stage process called megakaryopoiesis. The pluripotent HSC differentiates under the stimulus of the megakaryocytic growth factor thrombopoietin (TPO), which leads to lineage commitment and maturation (Figure 2). The development of the mature megakaryocytes occurs in the bone marrow, the proplatelet formation and platelet release occurs directly into the blood stream (Songdej and Rao, 2017).

TPO activates during the megakaryocytic differentiation process characteristic cell surface molecules like integrin alpha-IIb (ITGA2B), also known as CD41; integrin beta-3 (ITGB3) also known as CD61. Later the glycoprotein Ib (GPIb), also known as CD42 is expressed on the surface (Kaushansky et al., 1994).

The maturation of megakaryocytes is controlled by an orchestra of transcription factors. A genome-wide analysis in megakaryocytes identified the simultaneous binding of GATA1, GATA2, RUNX1, FLI1 and TAL1 to promoters of several megakaryocytic genes (Doré and Crispino, 2011; Tijssen et al., 2011). Loss of GATA1 leads to impaired polyploidization and cytoplasmic maturation (Shivdasani et al., 1997). The restored expression of GATA1 target genes like *CCND1* leads back to increased megakaryocyte size, but does not rescue the proplate formation (Muntean et al., 2007). The *RUNX1* knockout shows similar effects observed with GATA1, the polyploidization and cytoplasmic maturation is also impaired (Heller et al., 2005). *RUNX1* directly targets the megakaryocytic genes *ITGA2B*, *GPIb* and *TSP1* (Herglotz et al., 2013). *FLI1* is critical during the megakaryocytic differentiation, the *FLI1* knockout in mice leads to embryonic lethality. The mice die of embryonic hemorrhaging and defects in fetal megakaryopoiesis (Spyropoulos et al., 2000). The transcription factor regulates in megakaryocytic cells genes which are essential for terminal megakaryocytic maturation, like *ITGA2B* and *GPIb* (Wang et al., 2002). Conditional knockout of *TAL1* shows a specific decrease of megakaryocytes (Schlaeger et al., 2005). The knockdown leads to a reduction of polyploidization and reduced platelet numbers. The functionality of the platelets is not affected (Chagraoui et al., 2011).

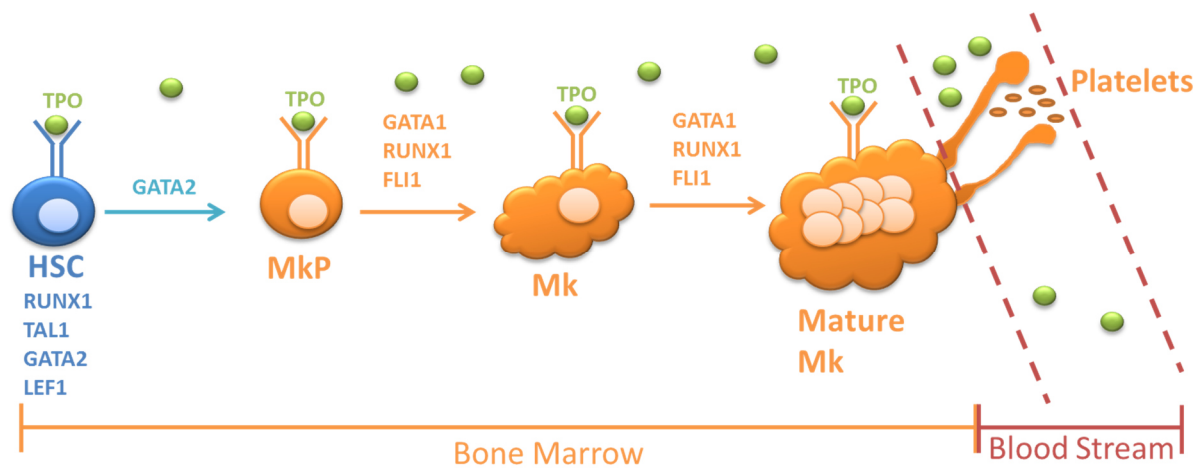


Figure 2: Schematic representation of megakaryopoiesis and platelet production. Hematopoietic stem cells differentiate after treatment with TPO to megakaryocytic progenitors. A set of TFs like GATA1, RUNX1 and FLI1 promote the differentiation process of the megakaryocytic maturation. The cytoplasm of the mature megakaryocyte continues to expand, and the cell becomes polyploid. The complete differentiation leads to proplatelet formation and platelet release into the blood stream. HSC: hematopoietic stem cell; MkP: megakaryocytic progenitor; Mk: megakaryocyte; TPO: Thrombopoietin; modified after (Songdej and Rao, 2017).

1.1.3 Erythropoiesis

The predominant function of red blood cells (RBCs) is the transport of oxygen and carbon dioxide. The bone marrow is able to produce 2 million erythrocytes per second. The life span of a typical erythrocyte is 120 days before they are recycled in the spleen and liver (Higgins, 2015). Erythropoiesis is regulated by the cytokine erythropoietin (EPO). This cytokine is induced under hypoxic conditions and is produced in the kidney. It stimulates the terminal differentiation of erythroid progenitors. The final step of enucleation produces the reticulocytes which are released into the blood stream. There they develop into the disk shape mature red blood cells. (Hattangadi et al., 2011)

The differentiation process is controlled by transcription factors like GATA1, TAL1 and EKLF1. The GATA1 knockout is lethal, causing severe anemia. The knockout mice die at embryonic day 10.5 and 11.5. The erythroid cells arrested at a proerythroblast-like state (Fujiwara et al., 1996). The erythroid differentiation and development is directly regulated by GATA1, which binds directly to promoters of alpha- and beta globin (Evans et al., 1988) and heme biosynthesis enzymes (Orkin, 1992). Deletion of TAL1 in adult mice led to impaired erythropoiesis. Progenitor cells and hematocrit levels were reduced (Hall et al., 2003). ChIP-seq of TAL1 identified 80 genes with known erythroid functions which are directly regulated by this transcription factor (Kassouf et al., 2010). The embryos of EKLF1 deficient mice die of anemia during fetal liver erythropoiesis with beta-globin deficiency (Perkins et al., 1995). The EKLF1 transcription factor binds directly to the human beta-globin promoter. Co-transfection experiments in erythroleukemic K562 cells showed increased beta-globin promoter activity after overexpression of EKLF1 (Donze et al., 1995). EKLF1 ChIP-seq revealed that the transcription factor directly regulates most aspects of terminal erythroid differentiation (Tallack et al., 2010). This includes the heme biosynthesis or production of alpha- and beta-globin protein chains.

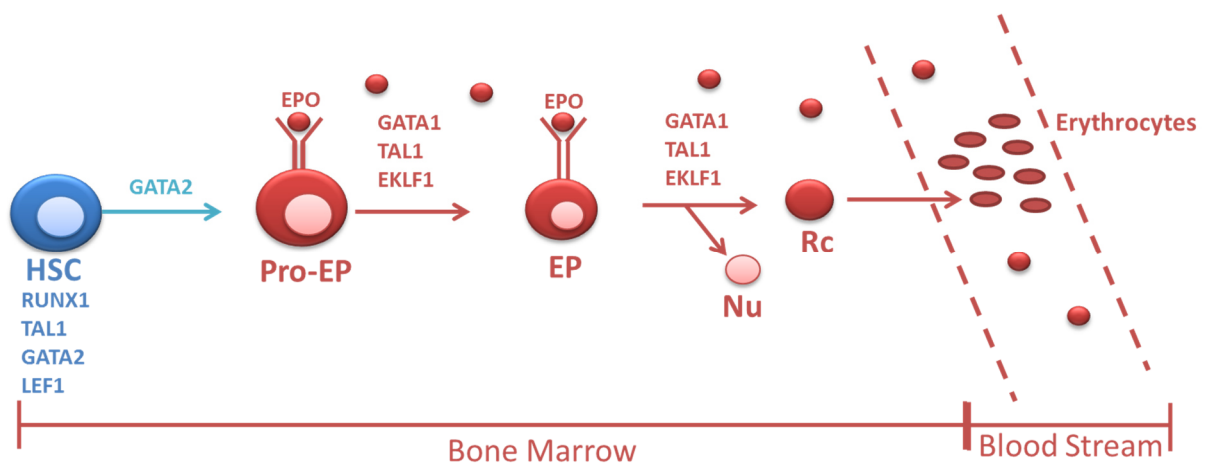


Figure 3: Schematic representation of erythropoiesis. Hematopoietic stem cells differentiate into proerythroblasts. Treatment with EPO leads to the finale differentiation into erythrocytes. Enucleation leads to the formation of reticulocytes which are released into the bloodstream and form mature erythrocytes. HSC: hematopoietic stem cell; Pro-EP: Proerythroblast; EP: Erythroblast; Nu: Nucleus; Rc: Reticulocytes; modified after (Hattangadi et al., 2011).

1.2 Chromatin and transcription

The genetic heritage of eukaryotes is packaged in chromatin localized in the nucleus. The efficient packaging structure allows the use of little storage space, but the DNA has also to be accessible for complex biological processes. This dynamic regulation is a key component of gene expression.

1.2.1 Chromatin organization

The eukaryotic DNA is packaged in chromatin that is composed of DNA, RNA and different histone proteins. The smallest packaging unit of chromatin is the nucleosome containing eight histones. Each histone is wrapped with 147 base pairs of DNA strand. The nucleosome is composed of two copies each of four core histones H2A, H2B, H3 and H4 (Luger et al., 1997). The linker region of the DNA strand between the nucleosome is connected to the fifth histone H1, which controls the distances between the nucleosomes. Furthermore, the histone H1 mediates the packaging of the nucleosomes into 30-nm chromatin fibers (Felsenfeld and Groudine, 2003). The formation of larger loops leads to a denser condensation, with the entire mitotic chromosome as highest condensation; see Figure 4.

Chromatin can be distinguished in two different configurations, the euchromatin and the heterochromatin. Euchromatin possesses a loosened structure, which makes it more accessible for RNA-polymerases and transcription factors. Heterochromatin is densely packed and is therefore characterized as silenced transcriptional inactive chromatin. These configurations of chromatin and the subsequent transcriptional regulation is cell type specific. These configurations are controlled by post-translational histone modifications (Bowman and Poirier, 2014).

1.2.2 Posttranslational histone modifications

The central domains of the histone proteins as also the C-termini are located in the inner of the nucleosome and therefore inaccessible for modifications. The arginine and lysine rich N-terminal histone tails instead protrude from the nucleosome which makes them accessible to modifications. N-terminal histone tails can be modified through different processes like methylation, phosphorylation, acetylation and other processes (Luger and Richmond, 1998) These modifications influence the accessibility of the promoters and genes for transcription.

Histone modifications are performed by different groups of enzymes. The writers catalyze the post-translational modifications (PTMs). This dynamic, reversible modifications can be removed by eraser enzymes. The reader enzymes recognize the specific PTMs and recruit other cofactors for transcriptional modifications (Gillette and Hill, 2015).

Writers for example are histone acetyltransferases (HATs) which catalyze an acetyl group onto a lysine in a histone tail. The positive charge of the histone gets neutralized and the loosened structure makes the DNA more accessible for transcription. These writers are most prominently found in promoter and enhancer regions (Zhang et al., 1998). Acetylations are removed by histone deacetylases (HDACs). These modifications are associated with the repression of gene expression (Pazin and Kadonaga, 1997). The histone methylation is performed by methyltransferases. These comprise of lysine methyltransferases and protein-arginine-methyltransferases (PRMTs). The later will be described in detail.

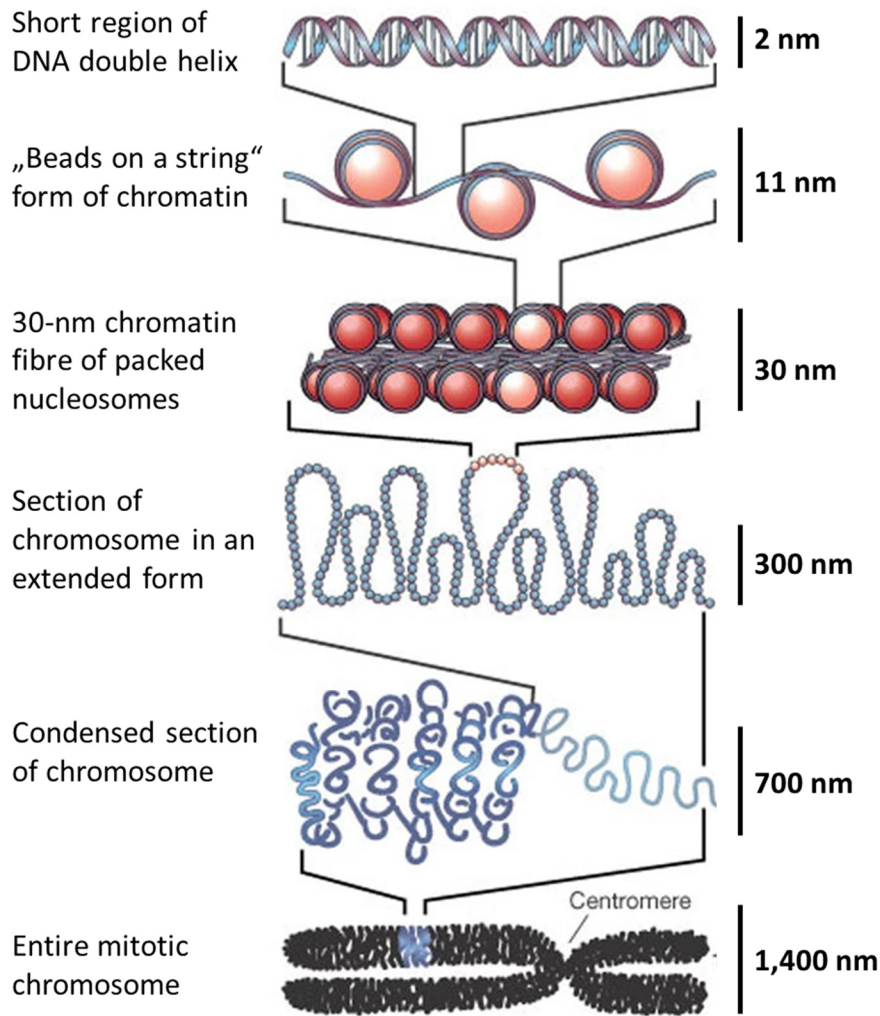


Figure 4: Different assembly levels of chromatin packaging. The DNA double helix is wound around the histone octamer. Two super helical turns of double stranded DNA correspond to 147 base pairs. The histone H1 couples the nucleosome to a 30-nm chromatin fibre. Several further condensation steps lead to the densest backpacking, the entire mitotic chromosome. Modified after (Gary and Clarke, 1998)

1.3 Protein Arginine Methyltransferases

Protein arginine methyltransferases are a small family of enzymes which perform post translational modifications on proteins by catalyzing the transfer of methyl groups at arginine residues. PRMTs are essential for transcriptional regulation, signal transduction, DNA repair and RNA processing (Bedford and Richard, 2005).

1.3.1 Protein domain structures of PRMTs

A family of nine PRMTs is encoded in the mammalian genome (Yang and Bedford, 2013; Yang et al., 2015). The nine PRMTs and their histone substrates are shown in Figure 5. The length of the enzymes varies from 316 to 843 amino acids. They share a conserved catalytic domain which methylate glycine- and arginine-rich (GAR) motifs. They catalyze the transfer of the methyl group to the guanidine nitrogen via the cofactor S-Adenosyl methionine (SAM) (Rakow et al., 2019). Several PRMTs target different arginine residues of histone 3 and histone 4 for methylation (Yang and Bedford, 2013). The N- and C- terminal parts are specific for every PRMT. The N-terminus of PRMT2 contains an additional SH3 domain. This domain binds heterogeneous nuclear ribonucleoproteins (hnRNPs) (Kzhyshkowska et al., 2001). The N-terminus of PRMT3 contains a zink finger motive, which is necessary for the recognition and methylation of RNA-binding substrates (Frankel and Clarke, 2000). PRMT7 and PRMT9 contain two catalytic domains. The N-terminus of PRMT9 harbors a tetratricopeptide repeat domain (TPR) and two putative AdoMet-binding motifs (Bedford, 2007).










PRMT	Protein domain structure	Histone substrates
PRMT1	 316	H4R3
PRMT2	 433	H3R8
PRMT3	 531	
CARM1	 608	H3R2; H3R17
PRMT5	 637	H4R3; H3R8
PRMT6	 375	H3R2
PRMT7	 692	H4R3
PRMT8	 394	
PRMT9	 843	

Figure 5: Family of mammalian PRMT enzymes; Protein arginine methyltransferases constitute a small family of nine enzymes that share a conserved catalytic domain (marked in purple). The histone substrates of several PRMTs are shown. Olive: SH3-Domain; Orange: Zink finger domain; Aquamarine: Putative AdoMet-binding motifs (Litt et al., 2009; Yang and Bedford, 2013).

The protein arginine methyltransferases are evolutionary conserved in yeast, nematodes, drosophila, plants and mammals. The enzymes are unknown in prokaryotes (Gary and Clarke, 1998; Boulanger et al., 2005).

1.3.2 The mechanism and function of arginine methylation of PRMTs

Protein arginine methyltransferases consist of four conserved motives (I, post-I, II and III), a double E loop structure and a THW-loop structure (Katz et al., 2003). The highly conserved S-Adenosyl methionine (SAM) binding domain consists of the four conserved motives and the double E loop structure. It contains the part which binds the methyl group donor in the Rossman fold (see Figure 6). The substrate binding site is located in the β -sheet domain and contains the THW-loop.

The first determined X-ray crystal structure of a protein arginine methyltransferases was PRMT3 (Zhang et al., 2000) The crystal structure of PRTM1 was identified in 2003 (Zhang and Cheng, 2003). PRMT6 is composed of two domains, the N-terminal Rossmann fold shown in blue and the C-terminal β -sheet domain shown in gold. Between both domains is a dimerization arm embedded, shown in green. The dimerization arm from one monomer binds to the Rossmann fold of the second monomer and forms a ring-like dimer. This is shown in the crystal structure of the full length human PRMT6 in Figure 6 (Wu et al., 2016). The S-adenosyl-L-homocysteine (SAH) molecule bind into a pocket in the Rossmann fold. The N-terminus which is variable in different PRMTs is shown in white.

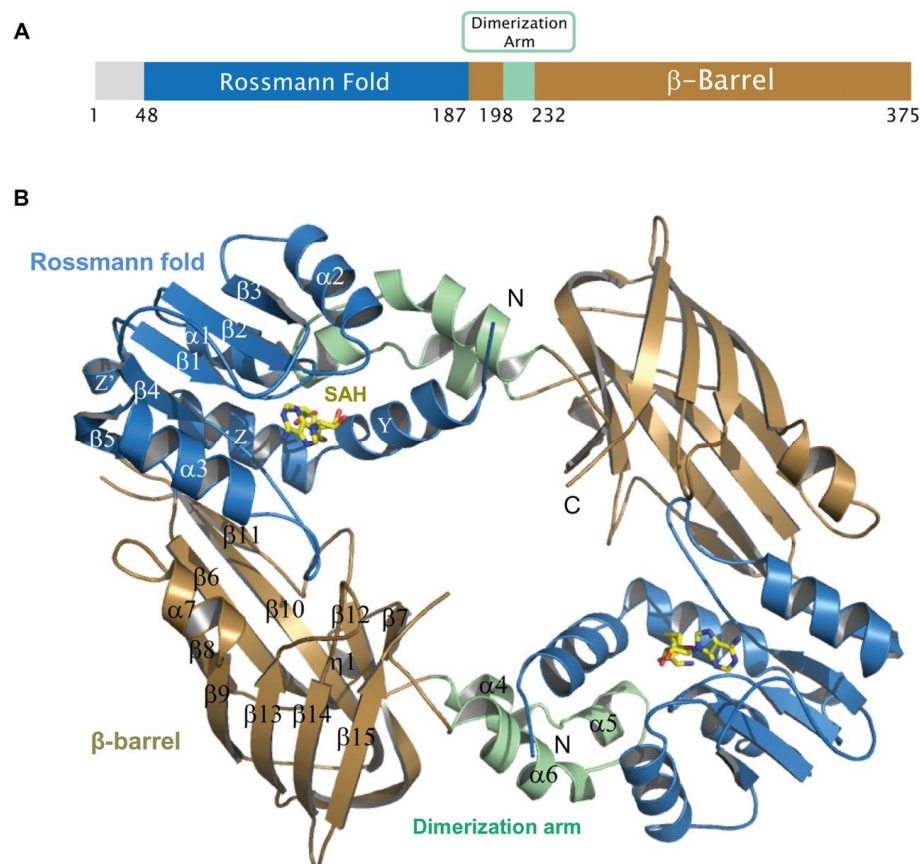


Figure 6: (A) Schematic representation of the protein domain structure of PRMT6. The variable N-terminus is shown in white, the Rossmann fold in blue, the dimerization arm in green and the β -barrel sheet in gold. (B) Crystal structure of the full length human PRMT6. The homodimerized PRMT6 is in complex with its substrate S-adenosyl-L-homocysteine (SAH). (Wu et al., 2016).

The protein arginine methyltransferases are classified in three different types. All three types show the ability to produce monomethyl-arginine (MMA). Type I enzymes (PRMT1, PRMT2, PRMT3, CARM1, PRMT6 and PRMT8) produce an asymmetric dimethyl-arginine (ADMA), by adding a second methyl group to the same guanidine nitrogen. They have a seven stranded β -sheet structure. Type II enzymes (PRMT5 and PRMT9) catalyze the production of symmetric dimethyl-arginine (SDMA). PRMT7 is a Type III enzyme; the enzymatic activity is limited to mono-methylation (Rakow et al., 2019). The molecular mechanism of the methylation is shown in Figure 7. The methylation of the arginine groups changes the binding properties of these amino acids. This changes the hydrogen bonds and hydrophobic and steric properties of the target protein (Hughes and Waters, 2006).

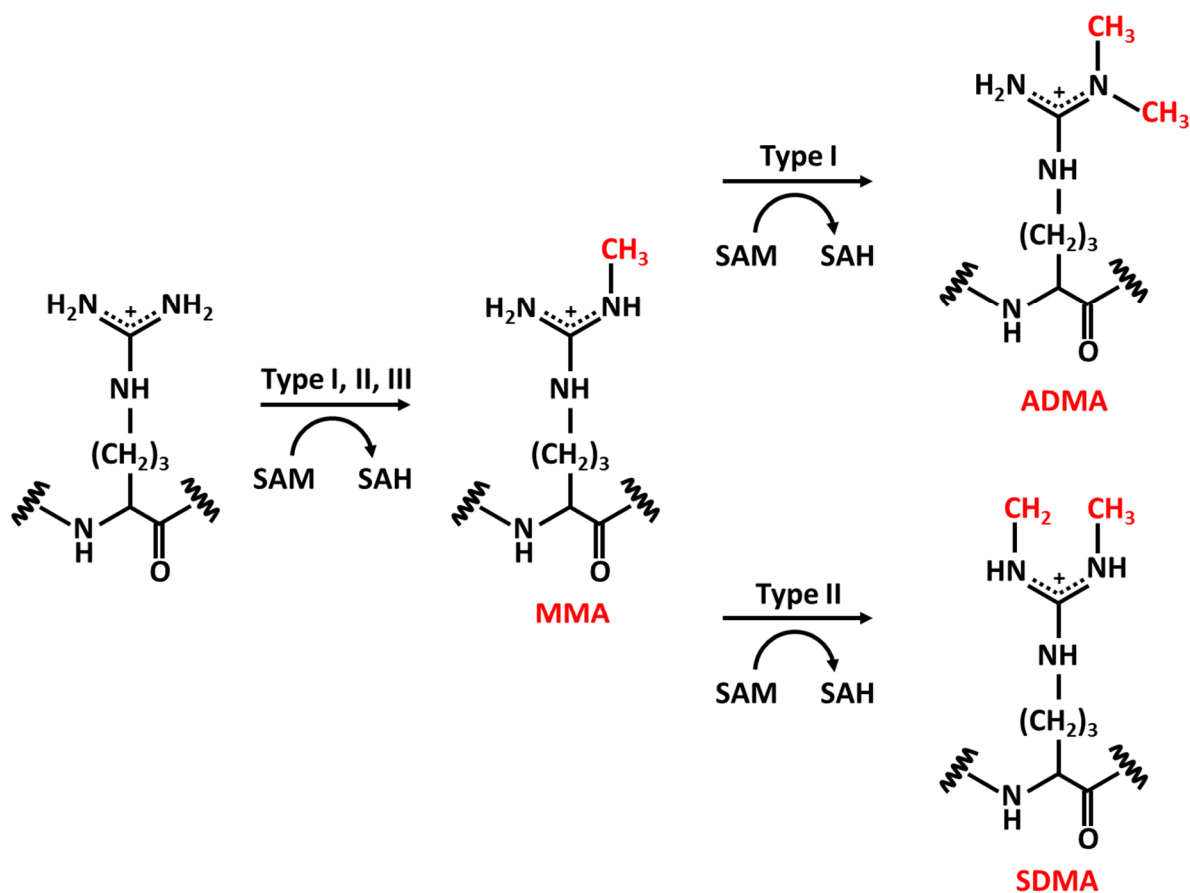


Figure 7: Mechanisms of arginine methylation of PRMTs. PRMTs of Type I, II and III catalyze the production of monomethylarginine (MMA) by the transfer of a methyl group from the donor S-Adenosyl-Methionin (SAM). The type II proteins PRMT5 and PRMT9 produce symmetric dimethylarginine (SDMA) by adding a second methyl group to the second terminal guanidine nitrogen. The Type I proteins (PRMT1, PRMT2, PRMT3, CARM1, PRMT6 and PRMT8) produce asymmetric dimethyl-arginine (ADMA) by methylation of the same guanidine nitrogen. SAH: S-Adenosyl-Homocystein. Modified after (Bedford, 2007).

1.3.3 PRMT6

The protein arginine methyltransferases 6 is solely localized in the nucleus and shows automethylation capacity, which enhances its stability (Singhroy et al., 2013). A know target of PRMT6 is the DNA polymerase beta, which is methylated *in vitro* and *in vivo*. The methylation enhanced the DNA polymerase activity. These findings link PRMT6 with DNA base excision repair (El-Andaloussi et al., 2006).

One of the main substrates of PRMT6 are the histones H3 and H4. Both are methylated *in vitro*. PRMT6 catalyzes the asymmetric dimethylation of histone H3 arginine 2 (H3R2me2a). This modification is associated with downregulated genes. H3R2me2a inhibits the trimethylation of H3K4 through the MLL1-complex, which on the other hand is associated with increased gene expression (Guccione et al., 2007); (Hyllus et al., 2007).

H3R2me2a co-occurs with histone H3 lysine 27 trimethylation (H3K27me3) on a genomic level. This repressive mark is produced by the Polycomb repressive complex 2 (PRC2). It has been shown that PRMT6 directly interacts with the PRC2 subunits (Stein et al., 2016). The cooperation with the Polycomb complex leads to the repression of HOXA genes in a cellular model of neuronal differentiation.

Several studies have shown that PRMT6 influences the hematopoietic differentiation. PRMT6 suppresses the expression of *thrombospondin 1 (TSP1)*, which was first isolated from platelets (Michaud-Levesque and Richard, 2009). It was demonstrated that PRMT6 is recruited via the transcription factor RUNX1 to the promoters of megakaryocytic genes. The RUNX1/PRMT6 corepressor complex is exchanged with a RUNX1 activator complex upon megakaryocytic differentiation. *CD41*, *miR27a*, *CD42b*, *TSP-1*, *PU.1* and *NF-E2* were identified as direct RUNX1/PRMT6 targets (Herglotz et al., 2013).

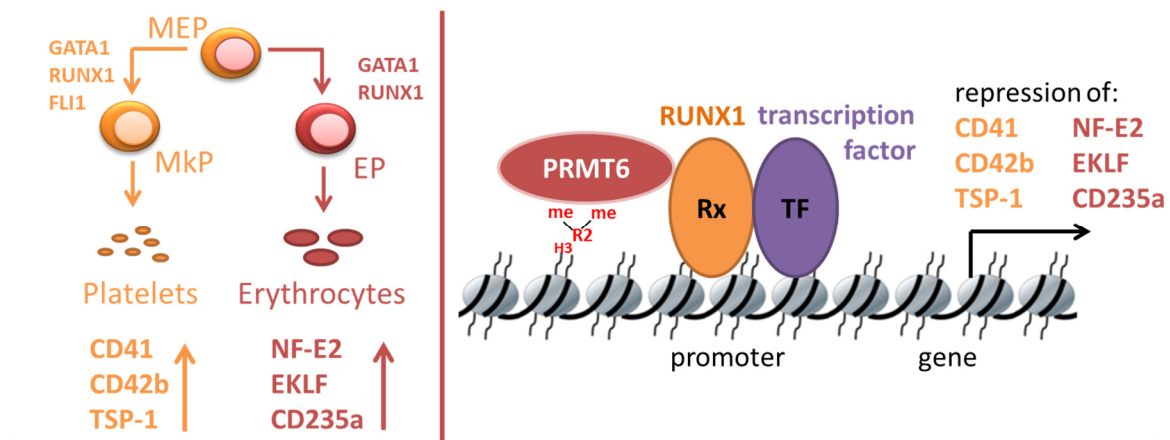


Figure 8: The transcription factor RUNX1 recruits PRMT6 to genes involved in the regulation of erythroid and megakaryocytic differentiation. PRMT6 controls the repression of these genes at the megakaryocytic-erythroid bifurcation. Megakaryocytic genes comprise of *CD41*, *CD42b* and *TSP-1*. Erythroid genes comprise of *NF-E2*, *EKL* and *CD235a* (Michaud-Levesque and Richard, 2009; Herglotz et al., 2013; Kuvardina et al., 2015; Herkt et al., 2018).

In addition, PRMT6 is also recruited by RUNX1 to the promoter of erythroid master regulator *KLF1* during megakaryocytic differentiation. Upon the recruitment of PRMT6 to the promoter, H3R2 is methylated and the *KLF1* gene expression is downregulated (Kuvardina et al., 2015). Furthermore, the erythroid gene *glycophorin A (GYPA)* is a direct target of RUNX1/PRMT6. This repression complex is recruited to the promoter of *GYPA* during the megakaryocytic differentiation and represses its expression. During erythroid differentiation PRMT6 dissociates from the promoter and the expression is activated (Herkt et al., 2018).

These studies prove that PRMT6 controls the repression of genes at the megakaryocytic-erythroid bifurcation. Figure 8 shows the recruitment of PRMT6 to promoter regions by transcription factors like RUNX1.

A global ChIP-Seq analysis of H3R2me2a identified that this histone modification is highly PRMT6 dependent. Surprisingly it was shown that the H3R2me2a modification associates mostly with highly transcribed genes (Bouchard et al., 2018). PRMT6 and H3R2me2a are generally associated with silenced genes (Kuvardina et al., 2015; Herkt et al., 2018). These opposing effects are still under investigation.

PRMT6 has a potential role in oncogenesis. Overexpression of the enzyme was observed in a wide range of solid tumor. The knockdown of PRMT6 reduced the growth of bladder and lung cancer cells significantly (Yoshimatsu et al., 2011). The tumor suppressor genes p21 and p27, two cyclin-dependent kinase inhibitors were identified as direct targets of PRMT6. Knockdown of PRMT6 leads to upregulation of these suppressors (Kleinschmidt et al., 2012). As PRMT6 prevents senescence and promotes cell growth it is a therapeutic target for different types of cancer (Stein et al., 2012).

1.4 Hematopoietic transcription factors

The development of hematopoietic stem cells like self-renewal, differentiation and lineage commitment decisions is controlled by lineage-specific transcription factors. On top of this hierarchy are the HSC transcription factors which maintain the population of HSCs in the bone marrow. Such factors are RUNX1, GATA2, TAL1 and LEF1; see Figure 1 (Skokowa et al., 2006; Orkin and Zon, 2008). Antagonizing transcription factors are important at the branching points of hematopoietic differentiation (Graf and Enver, 2009). Examples are the krueppel-like factor 1 (KLF1) and friend of leukemia integration 1 (FLI1) which cross antagonize at the megakaryocytic/erythroid bifurcation point (Starck et al., 2003). KLF1 is indispensable for erythroid differentiation, FLI1 instead for the megakaryocytic differentiation. Another important factor of the megakaryocytic/erythroid differentiation is RUNX1 (Kuvardina et al., 2015).

1.4.1 RUNX1

Studies have shown that RUNX1 expression is maintained during megakaryocytic differentiation, but is reduced during erythroid development (North et al., 2004). RUNX1 controls the lineage fate decision at the megakaryocyte/erythroid branching point (Kuvardina et al., 2015). It binds during megakaryocytic development to the *KLF1* promoter and recruits corepressors like PRMT6 which lead to the downregulation of *KLF1* expression. Another target of RUNX1 is *ITGA2B* (CD41) expressed in megakaryocytes and thrombocytes. RUNX1 recruits coactivators to the CD41 promoter and upregulates the gene expression (Herglotz et al., 2013). The *RUNX1* conditional knockout leads to impaired polyploidization and cytoplasmic maturation in megakaryocytes (Heller et al., 2005).

Furthermore it has been demonstrated that RUNX1 interacts with the transcription factor LEF1, which binds to the Runt homology domain (RHD) of RUNX1 (residues 50–179) (Kahler and Westendorf, 2003). Both factors work as transcriptional repressors, recruiting specifically the TLE/Groucho corepressor complex. The T cell receptor (TCR) enhancers alpha and beta contain functional RUNX1 binding sites. These lead to a RUNX1 depended inhibition through the TLE/Groucho corepressor complex (Levanon et al., 1998). RUNX1 itself is able to interact with the Wnt coactivator beta-Catenin. RUNX1 can activate the Wnt/ β -catenin pathway in colorectal cancer (CRC). Here it directly recruits β -catenin to the promoter and enhancer regions of the proto-oncogene c-KIT. This gives RUNX1 a crucial role in the Wnt signaling pathway (Li et al., 2019).

1.4.2 TCF/LEF family

The TCF/LEF gene family is a group of transcription factors with diverse functions in cell fate decision and embryonic development. In most vertebrates, four members are known: LEF1, TCF7 (TCF1), TCF7L1 (TCF3) and TCF7L2 (TCF4) are shown in Figure 9 (Arce et al., 2006). These factors undergo a transcriptional switch from repressor to activator in response to Wnt signaling. All these members show a high affinity to bind the DNA sequence WWCAAAG, known as the Wnt-responsive element (WRE). TCF/LEF1 acts as a transcriptional repressor by recruiting TLE/Groucho corepressors to promoters. After stimulation with Wnt factors, activator complexes like β -catenin are recruited by

displacing the corepressors (see also Figure 10) (Daniels and Weis, 2005). Target genes of LEF1 are *Cyclin D1 (CCND1)*, *Myc* and *Survivin (BIRC5)* (He et al., 1998; Tetsu and McCormick, 1999; Skokowa et al., 2006).

All TCF/LEF proteins share several conserved domains. The N-terminus harbors the β -catenin binding domain. Dominant negative isoforms (dnLEF1 and dnTCF1), which are missing the β -catenin domain are produced through alternative splicing. The high-mobility group (HMG) DNA-binding domain is responsible for binding the DNA sequence WWCAAAG. The context-dependent regulatory domain (CRD) recruits the corepressor and the nuclear localization signal (NLS) ensures the nuclear import (Arce et al., 2006).

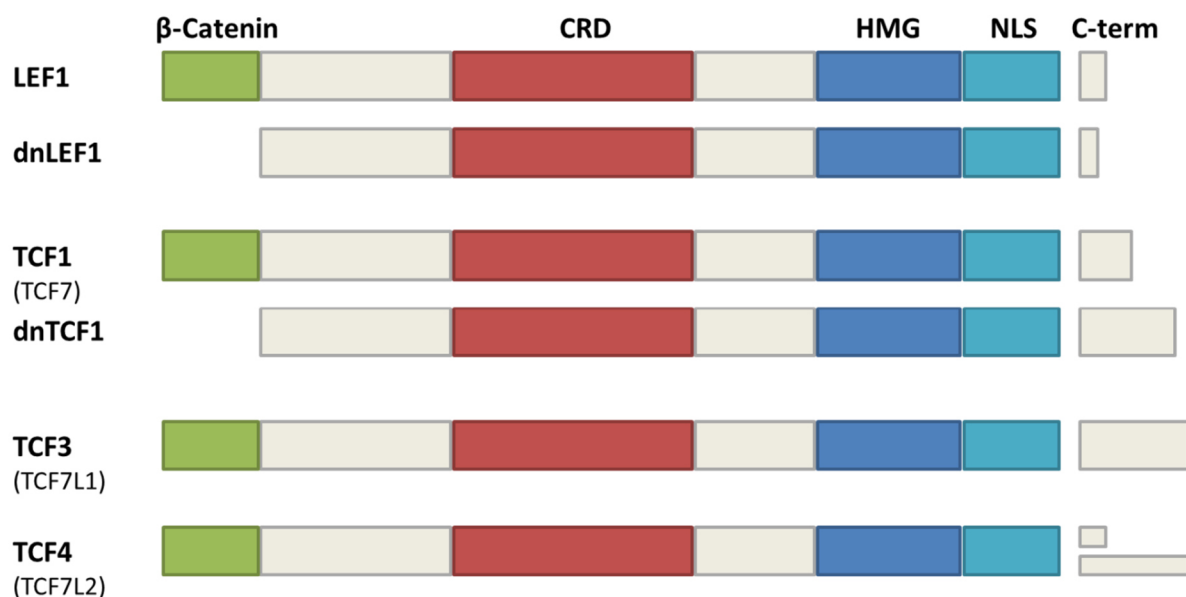


Figure 9: Family of mammalian TCF/LEF transcription factors; all factors share several conserved protein domains. The β -catenin-binding domain is located at the N-terminus (green); alternative splicing produces dominant negative isoforms (dnLEF1 and dnTCF1) in which the β -catenin-binding domain is missing. The Context-dependent regulatory domain (CRD) recruits the TLE/Groucho corepressors (red); the high-mobility group (HMG) DNA-binding domain recognizes the double stranded DNA sequence WWCAAAG (Blue); the nuclear localization signal (NLS) is shown in aquamarine. The C-terminal tails are variable and are subject to alternative splicing (C-term). Modified after (Arce et al., 2006).

TCF/LEF transcription factors play a crucial role in lymphopoiesis, by being essential for T- and B-cell differentiation. LEF1 is expressed in pre-B and T lymphocytes in adult mice (van Genderen et al., 1994). LEF1 and TCF1 are expressed during T cell differentiation. They regulate the T cell receptor alpha (TCRalpha) and show a redundancy for the regulation of T cell differentiation (Okamura et al., 1998). B lymphocyte proliferation is regulated through a LEF1 dependent mechanism (Reya et al., 2000). LEF1 is critical for neutrophil granulocytopenesis; here it controls the proliferation and differentiation of granulocyte progenitor cells (Skokowa et al., 2006). An involvement of TCF/LEF transcription factors in other myeloid lineages is not explored. Likewise, the impact on erythropoiesis and megakaryopoiesis and platelet production is not described in literature. It has been shown that LEF1 is expressed in the human erythroleukemia cell lines HEL and K562. Both cell lines are described

as Wnt-responsive which accumulate high amounts of LEF1 in the nucleus (Morgan et al., 2019). The impact of Wnt signaling on megakaryocytic/erythroid differentiation is unknown.

1.5 Wnt signaling pathway

The canonical Wnt pathway (Wnt/ β -catenin pathway) is evolutionary highly conserved. It is involved in several important mechanisms like cell differentiation and proliferation, embryogenesis, homeostasis, tissue repair and apoptosis (Clevers, 2006). Wnt proteins are a family of secreted glycolipoproteins consisting of 19 Wnt proteins in mammals. The absence of a Wnt signaling protein defines the Wnt-off state (Figure 10).

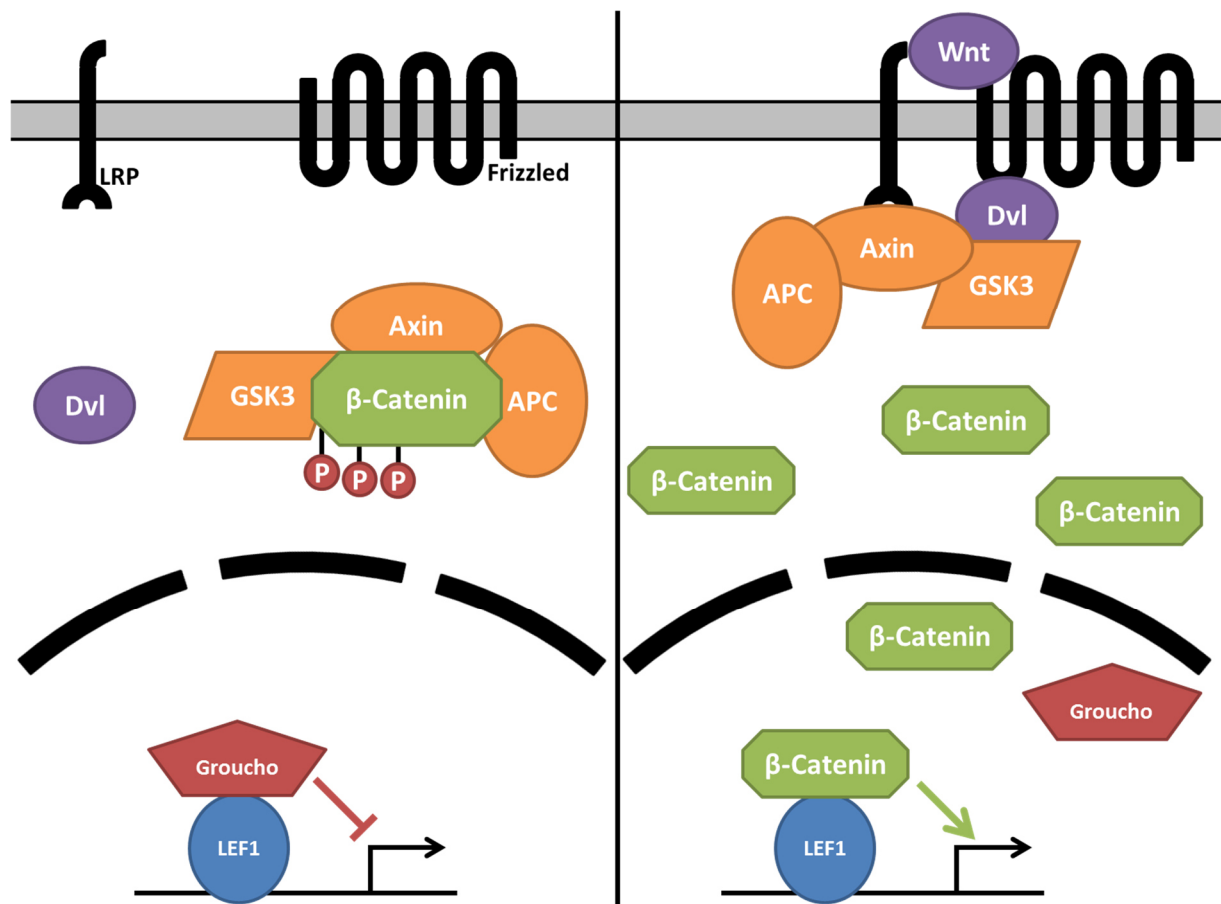


Figure 10: Schematic representation of the canonical Wnt signaling pathway. Left: Wnt-off state; The Wnt ligand is absent. β -catenin is phosphorylated by the β -catenin destruction complex (formed by the tumor suppressor APC, the scaffolding protein Axin and the kinase GSK3 β). GSK3 β phosphorylates Ser33, Ser37, and Thr41 at the N-terminus of β -catenin. These modifications are recognized by ubiquitinating proteins and β -catenin is targeted for degradation. β -catenin is not able to enter the nucleus and TCF/LEF1 acts as a transcriptional repressor by recruiting TLE/Groucho corepressors. Right: Wnt-on state; The Wnt ligand binds to the lipoprotein receptor proteins (LRP) and the transmembrane Frizzled proteins. This co-receptor complex recruits Dvl and Axin and inhibits the destruction complex. β -catenin is stabilized and translocates into the nucleus. The TLE/Groucho corepressors get displaced and β -catenin directly binds to TCF/LEF1 and activates gene expression (MacDonald et al., 2009).

Here the β -catenin protein is constantly degraded by the Axin complex. The tumor suppressor adenomatous polyposis coli (APC), the scaffolding protein Axin and the glycogen synthase kinase 3 beta (GSK3 β) are forming this destruction complex. The N-terminus of β -catenin is phosphorylated by GSK3 β at Ser33, Ser37, and Thr41. This leads to the recognition of β -catenin by ubiquitinating

proteins targeting it for proteasomal degradation. The continuous removal of the protein prevents β -catenin from entering the nucleus. Wnt/ β -catenin target genes are repressed by the TCF/LEF transcription factors which recruit TLE/Groucho corepressors. The Wnt/ β -catenin pathway is activated (Wnt-on), when Wnt proteins bind to the transmembrane Frizzled receptor and its co-receptor the low-density lipoprotein receptor related protein (LRP). This complex recruits the scaffolding protein Dishevelled (Dvl) and the Axin complex. The destruction complex gets inactivated and GSK3 β is no longer phosphorylating β -catenin, which gets stabilized, accumulates in the cytosol and translocates into the nucleus. β -catenin binds to the TCF/LEF transcription factors at Wnt target genes. The TLE/Groucho corepressors get displaced and the gene expression is activated (MacDonald et al., 2009).

1.5.1 β -catenin (CTNNB1)

β -catenin is an evolutionary conserved protein, being present in a wide range of metazoa (animals) from porifera (sponges) to insects and vertebrates (Valenta et al., 2012). β -catenin consists of a central region with 12 armadillo repeats. The central region serves as scaffold for several binding partners like TCF/LEF transcription factors, APC and Axin. The carboxy-terminal domain serves as transactivation domain by recruiting transcriptional co-activators. The amino-terminal domain contains the GSK3 β phosphorylation sites (Kolligs et al., 1999). The protein structure is shown in Figure 11.

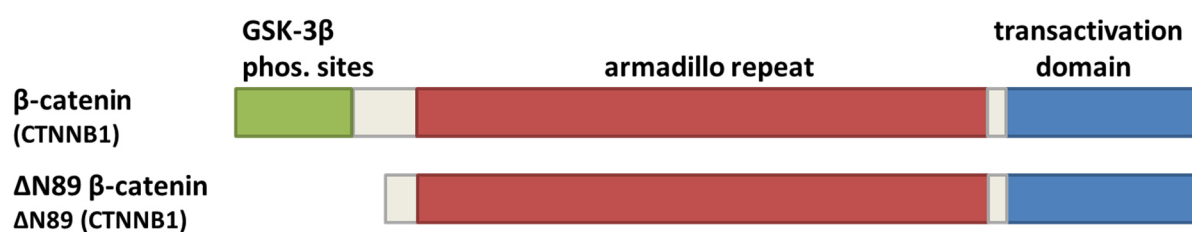


Figure 11: Protein structure of β -catenin: The GSK-3 β phosphorylation sites are located at the N-terminus (green). The armadillo repeats bind to TCF/LEF, APC and Axin (red). The C-terminal transactivation domain recruits transcriptional co-activators (blue). The truncated Δ N89 β -catenin lacks the GSK-3 β phosphorylation site and acts as dominant active β -catenin (Kolligs et al., 1999).

1.5.2 Wnt-signaling pathway in hematopoiesis

Wnt signaling influences hematopoietic stem cells and many differentiated blood cells (Lento et al., 2013). Wnt proteins are expressed in the microenvironment of HSCs and progenitor cells (van den Berg et al., 1998). Moreover, Wnt proteins promote the proliferation in HSCs, shown in human embryonic stem cell culture (Corrigan et al., 2009; Goessling et al., 2009). The expression of dominant active β -catenin in the HSCs of transgenic mice increases proliferation and enhances reconstitution *in vivo* (Reya et al., 2003).

Enforced expression of the dominant active β -catenin leads to impaired myeloid commitment and blocked erythrocyte differentiation and the loss of stem cell repopulation (Kirstetter et al., 2006). Constitutive activation of β -catenin in mice blocked the hematopoietic differentiation process, with a

lethal phenotype. HSCs repopulation was impaired by enforced cell cycle entry leading to the exhaustion of the HSC pool (Scheller et al., 2006).

Wnt signaling is a very important pathway in the lymphocyte development, controlling the maturation of B- and T-lymphocytes (van Genderen et al., 1994; Verbeek et al., 1995). β -catenin controls the late stages of T cell development. Transgenic overexpression enhances the production of mature thymocytes (Mulroy et al., 2003). The deletion of β -catenin in T cells showed impaired development of the cell population, resulting in a decrease of the splenic T cells (Xu et al., 2003).

1.5.3 Wnt-signaling in megakaryopoiesis

In vitro studies in the human megakaryocytic cell line UT-7/TPO showed that treatment with TPO leads to the inhibition of GSK3 β . Furthermore, the accumulation of total cellular β -catenin was stimulated by this (Soda et al., 2008). *Ex vivo* treatment of murine fetal liver megakaryocytes with Wnt3a stimulates the production of proplatelets. Fetal liver cells from low-density lipoprotein receptor-related protein 6 (LRP6) deficient mice show reduced numbers of megakaryocytes. LRP6 is part of Frizzled co-receptor group and acts as Wnt activator (Macaulay et al., 2013). Activated Wnt-signaling in hematopoietic cells was studied in a double transgenic mouse model. β -catenin was stabilized in cells which express the platelet derived growth factor b (PDGFb). This growth factor is expressed in megakaryocytes and platelets. Activated Wnt-signaling led to enhanced development of megakaryocytes. These megakaryocytic cells with stabilized β -catenin showed increased levels of RUNX1 expression (Yalcin, 2018).

1.6 The PRMT family in LEF1/Wnt/ β -catenin-signaling

The PRMT family enzymes were identified as regulators of the LEF1/Wnt/ β -catenin-signaling in several studies (Cha and Jho, 2012). An overview of these regulations is shown in Figure 12. PRMT1 methylates the scaffolding protein Axin in the absence of Wnt activation. The methylation increases the stability of Axin and therefore stabilizes the binding to the glycogen synthase kinase 3 beta (GSK3 β) (Figure 10). PRMT1 stabilizes the β -catenin destruction complex and functions as a negative regulator of Wnt signaling (Cha et al., 2011). PRMT2 is directly recruited by β -catenin to Wnt target loci. PRMT2 performs asymmetric dimethylation at histone H3R8 at promoter regions and enhancer, increasing the gene expression of the target genes of LEF1/Wnt/ β -catenin-signaling (Blythe et al., 2010).

CARM1/PRMT4 is an important positive modulator of β -catenin mediated gene expression. CARM1 is also directly recruited by β -catenin to Wnt target loci and performs asymmetric dimethylation of histone H3R17 at Wnt promoter regions, increasing the gene expression (Ou et al., 2011). The knockdown of CARM1 reduces the expression of β -catenin target genes, supporting the findings (Ou et al., 2011). PRMT5 stabilizes the activation of the LEF1/Wnt/ β -catenin-signaling by the direct epigenetic silencing of the pathway antagonists. ChIP-seq data revealed that PRMT5 performs symmetric dimethylation at histone H3R8 at the promoter regions of AXIN1 and AXIN2. The modification leads to the reduced expression of the β -catenin antagonists, enhancing the Wnt signaling (Chung et al., 2019).

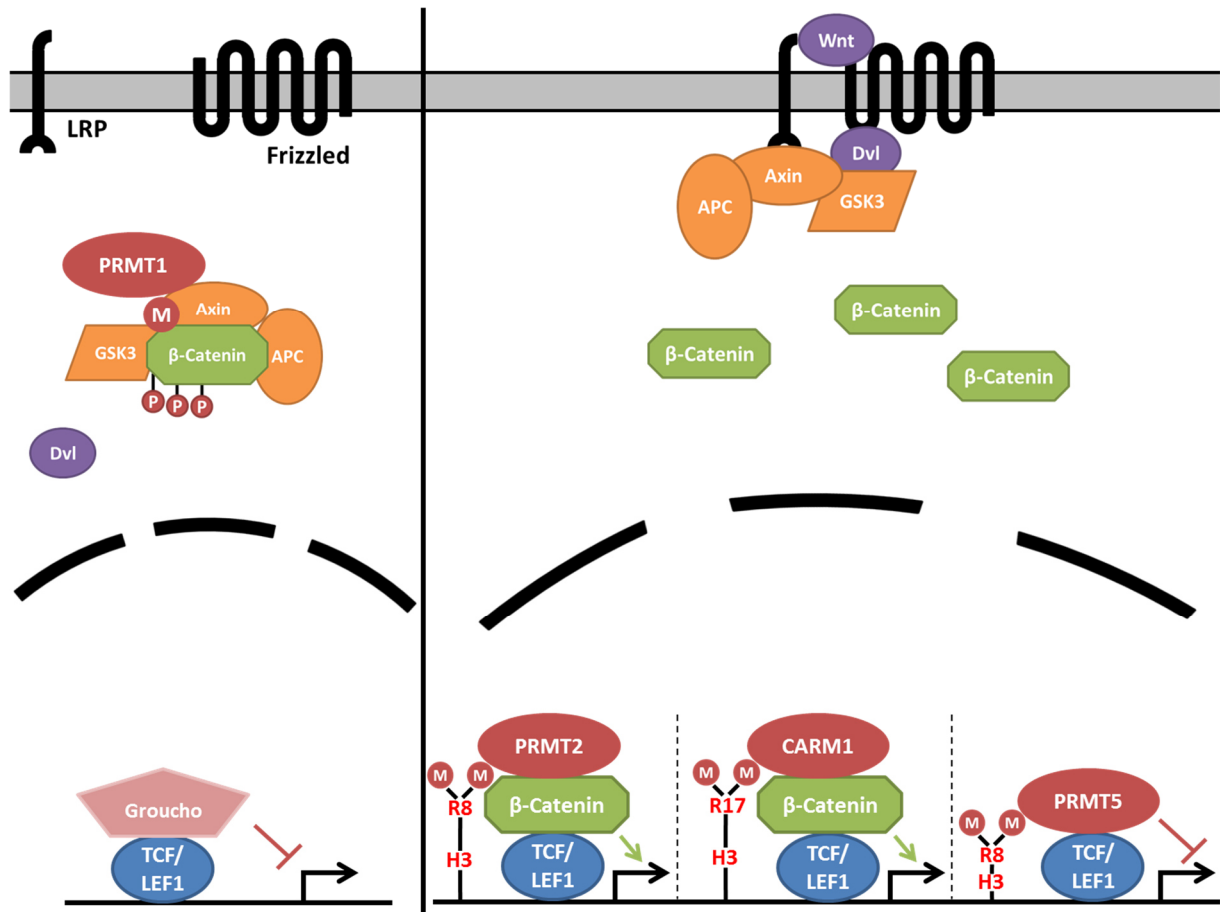


Figure 12: Schematic representation of PRMT family enzymes regulating the Lef1/Wnt/ β -catenin-signaling pathway. PRMT1 methylates and stabilizes Axin, negatively regulating the Wnt signaling pathway (Cha et al., 2011). PRMT2 is recruited by β -catenin and increases gene expression of Wnt target loci by asymmetric dimethylation at histone H3R8 (Blythe et al., 2010). CARM1 is recruited by β -catenin and also increases gene expression of Wnt target loci by asymmetric dimethylation at histone H3R17 (Ou et al., 2011). PRMT5 is recruited by TCF/LEF1 transcription factors to the promoter regions of AXIN1 and AXIN2, repressing their transcription and enhancing the Wnt signaling (Chung et al., 2019). PRMT methylation is illustrated with a red M; modified after (Cha and Jho, 2012).

These publications show that several members of the PRMT family play an important role in the Lef1/Wnt/ β -catenin-signaling. The interaction of PRMT6 with this pathway is currently unknown. Do to the fact that PRMT6 is recruited to target genes by hematopoietic transcription factors like RUNX1 (Herglotz et al., 2013), which are also involved in the recruitment of β -catenin (Li et al., 2019), it is likely that other hematopoietic transcription factors like TCF/LEF1 recruit PRMT6 to Wnt target genes.

1.7 Aim of this study

PRMT6 is a very important regulator in the hematopoietic system. Several studies link PRMT6 to the megakaryocytic-erythroid bifurcation. The transcription factor RUNX1 recruits PRMT6 to megakaryocytic promoters like CD41 and TSP-1 (Herglotz et al., 2013). The erythroid master regulator KLF1 is therefore repressed during megakaryocytic differentiation (Kuvardina et al., 2015). In a similar way, the RUNX1/PRMT6 complex represses the expression of the erythroid gene glycophorin A. (Herkt et al., 2018). These studies show a versatile and overarching role of PRMT6 in the megakaryocytic-erythroid bifurcation. RUNX1 recruits PRMT6 to act as a transcriptional repressor. Here it catalyzes the asymmetric dimethylation of histone H3 residue arginine 2 (H3R2). A global ChIP-seq analysis of this histone mark showed in contrast, that PRMT6 is mostly associated with highly transcribed genes (Bouchard et al., 2018). These differences suggest that PRMT6 interacts with a wide range of proteins, performing various modifications of gene expression. The hematopoietic differentiation is controlled by a regulatory network of various transcription factors. (Hattangadi et al., 2011; Tijssen et al., 2011). Therefore, PRMT6 is of interest to identify currently unknown interaction partners connected to the megakaryocytic-erythroid bifurcation.

The aim of this work was to identify a new transcription factor interacting with PRMT6 using affinity purification coupled with stable isotope labeling by amino acids in cell culture. The erythroleukemic K562 cell line was used to specially identify a new megakaryocytic-erythroid transcription factor. The interaction was verified by various different experimental studies. In order to identify target genes of this factor, ChIP-sequencing data of K562 cells were analyzed. The target genes were verified with chromatin immunoprecipitation. Small hairpin RNA knockdown and overexpression of the transcription factor were utilized to analyze the gene expression of the target genes. These findings were verified by the overexpression of another cofactor of the newly identified transcription factor. Finally, these factors were analyzed on their impact of gene expression of megakaryocytic target genes in TPO treated primary human hematopoietic stem cells in more detail.

2 Materials and Methods

2.1 Material

2.1.1 Cell lines

The cell lines used in this study are described in Table 1.

Table 1: Cell lines

Name	Cell line	Medium
HEK293T	Human embryonic kidney 293 cells	DMEM
K562	Erythroleukemic cell line	RMPI 1640
HEL	Erythroleukemic cell line	RMPI 1640
TF-1	Erythroleukemic cell line	RMPI 1640
Jurkat	T lymphocyte cell line	RMPI 1640
U937	Myelogenous leukemia cell line	RMPI 1640
Kasumi	Myelogenous leukemia cell line	RMPI 1640

All cells were supplemented with 1% Pen/Strep and 10% FBS

2.1.2 Cell culture media and supplements

The following cell culture media and supplements were used for the axenic cultivation of human primary cells and cell lines.

Table 2: Cell culture media and supplements

Media or supplement	Supplier
Dulbecco's Modified Eagle Medium (DMEM)	Thermo Fisher Scientific
Dulbecco's phosphate-buffered saline (DPBS)	Thermo Fisher Scientific
Fetal bovine serum (FBS)	PAA-Laboratories
Ficoll® Paque	Sigma Aldrich
L-Glutamine	Thermo Fisher Scientific
Penicillin/Streptomycin	Thermo Fisher Scientific
RPMI 1640 Medium for SILAC	Thermo Fisher Scientific
RPMI 1640 Medium, GlutaMAX™	Thermo Fisher Scientific
SFEM I media	StemCell Technologies
SFEM II media	StemCell Technologies
StemSpan CC100	StemCell Technologies
StemSpan Erythroid Expansion Supplement	StemCell Technologies
StemSpan Megakaryocyte Expansion Supplement	StemCell Technologies
Trypsin-EDTA (0.05%)	Thermo Fisher Scientific

2.1.3 Chemicals, Reagents and Enzymes

The chemicals and reagents used in this study are described in Table 3.

Table 3: Chemicals, Reagents

Chemical	Supplier
Acetic acid, 100%	Carl Roth
Agarose	Lonza
Adenosin-5'-triphosphate disodium salt (ATP)	Carl Roth
Albumin Fraction V, endotoxin-tested	Carl Roth
Ammonium peroxydisulphat (APS)	Carl Roth
Ampicillin sodium salt (Amp)	Carl Roth
Calcium chloride (CaCl ₂)	Carl Roth
Deoxycholic acid sodium salt (DOC)	Carl Roth
Dimethylsulphoxide (DMSO)	Carl Roth
1,4-Dithiothreitol (DTT)	Carl Roth
Ethylenediaminetetraaceticacid (EDTA)	Carl Roth
Ethylene glycol tetraacetic acid (EGTA)	Carl Roth
Ethanol, 96%	Carl Roth
Ethidiumbromide solution, 1 %	Carl Roth
Formaldehyde solution, 37 %	Carl Roth
Glycerol	Carl Roth
Glycine	Carl Roth
Glycylglycine	AppliChem
N-2-Hydroxyethylpiperazine-N'-2-ethane sulphononic acid (HEPES)	Carl Roth
Lysogeny broth (LB)	Carl Roth
LB agar	Carl Roth
D-Luciferin	Carl Roth
Methanol	Carl Roth
β-Mercaptoethanol	Carl Roth
Magnesium chloride (MgCl ₂)	Carl Roth
Magnesium sulphate (MgSO ₄)	Carl Roth
Nonidet P-40 (NP-40)	AppliChem
2-Nitrophenyl-β-D-galactopyranoside (ONPG)	Carl Roth
dNTP-Set	Carl Roth
2-Propanol	Carl Roth
Polyethylenimine (PEI)	Polysciences
Powdered milk	Carl Roth
Potassium chloride (KCl)	Carl Roth
Potassium dihydrogenphosphate (KH ₂ PO ₄)	Carl Roth
Protamine sulfate	Sigma Aldrich
Protease Inhibitor Cocktail 5 Mamm Cell/Tissue	AppliChem
Proteinase K	AppliChem
RNAse A	Invitrogen
Roti®-Block	Carl Roth
ROTIPHORESE®Gel 30 (37,5:1)	Carl Roth
D(+)-Saccharose	Carl Roth

Sodiumchloride (NaCl)	Carl Roth
Sodiumdodecylsulfate (SDS)	Carl Roth
Monosodiumphosphate	Carl Roth
Disodiumphosphate	Carl Roth
Sodiumbicarbonate (NaHCO ₃)	Carl Roth
Tetramethylethylenediamine (TEMED)	Carl Roth
Tris-(hydroxymethyl)-amino methane (TRIS)	Carl Roth
TRIS hydrochloride (TRIS-HCl)	Carl Roth
Triton® X-100	Carl Roth
Trypan blue solution	Sigma Aldrich
Tween 20	Carl Roth

Table 4: Enzymes

The enzymes used in this study are described in Table 4.

Enzymes	Cat. #	Supplier
Q5® High-Fidelity DNA Polymerase	M0491L	New England BioLabs
T4 DNA Ligase	M0202L	New England BioLabs
Micrococcal Nuclease	10011S	Cell Signaling
BamHI-HF	R3136S	New England BioLabs
NotI-HF	R3189S	New England BioLabs
AgeI-HF	R3552S	New England BioLabs
MluI-HF	R3198S	New England BioLabs
EcoRI-HF	R3101S	New England BioLabs

2.1.4 Plasmids

Overexpression vectors were used for Co-Streptavidin precipitation and luciferase assay experiments. Lentiviral vectors were inserted in K562 cells.

Table 5: Plasmids

Overexpression vectors

Insert	Vector	Cloning Site	Tag	Resistance
hPRMT1	pcDNA3	-	Myc-His	Amp
hPRMT6	pcDNA3	-	HA	Amp
hLEF1	pcDNA3	-	-	Amp
hN89- β -Catenin	pcDNA3	BamHI/NotI	3xFlag	Amp
hRUNX1-HA	pcDNA3	EcoRV/XhoI	2HA	Amp

Lentiviral overexpression vectors

Insert	Vector	Cloning Site	Tag	Resistance
AVI-hPRMT6	pRRlsAviMCS	AgeI/MluI	AVI	Amp
hLEF1	LeGOiG2	BamHI/EcoRI	-	Amp
hN89- β -Catenin	LeGO iG2	BamHI/NotI	3xFlag	Amp
hRUNX1-AVI	pRRlsMCSAvi	MluI/AgeI	AVI	Amp
AVI-hRUNX1	pRRlsAviMCS	MluI/AgeI	AVI	Amp

Lentiviral knockdown vectors

Insert	Vector	ID	Tag	Resistance
shLEF1_A	pGIPZ	V2LHS_115192	-	Amp
shLEF1_B	pGIPZ	V2LHS_224400	-	Amp
shPRMT6_A	pGIPZ	V2LHS_155923	-	Amp
shPRMT6_B	pGIPZ	V2LHS_408221	-	Amp

Luciferase vectors

Insert	Vector	Cloning Site	Tag	Resistance
Super 8x TOPFlash	pGL3	MluI	-	Amp
Super 8x FOPFlash	pGL3	Asp718/XmaI	-	Amp

The pGL3-Basic vector (Promega, Madison) was used for transient transfection in luciferase assays. The vector is suited for the use in eukaryotic cells. The firefly luciferase gene was cloned after a multiple cloning site without promoter. The artificial promoters Super 8x TOPFlash and Super 8x FOPFlash were cloned in front of the luciferase gene. The empty vector is shown in Figure 13.

The pcDNA3 plasmid was used as expression vector for proteins in human cell lines. Overexpression is driven by the human cytomegalovirus (CMV) immediate early enhancer and promoter. The empty vector is shown in Figure 14.

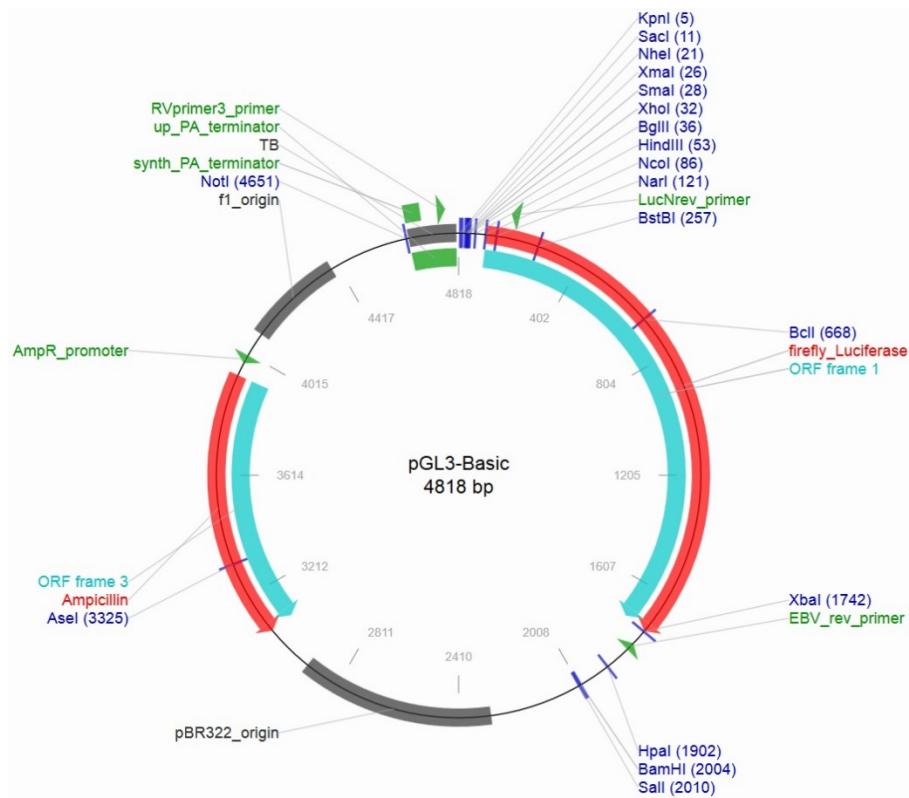


Figure 13: Plasmid vector map of the pGL3-Basic vector. The vector contains an ampicillin resistance and the gene of the firefly luciferase fused to a multiple cloning site without promoter. The enzymatic restriction sites are shown in dark blue.

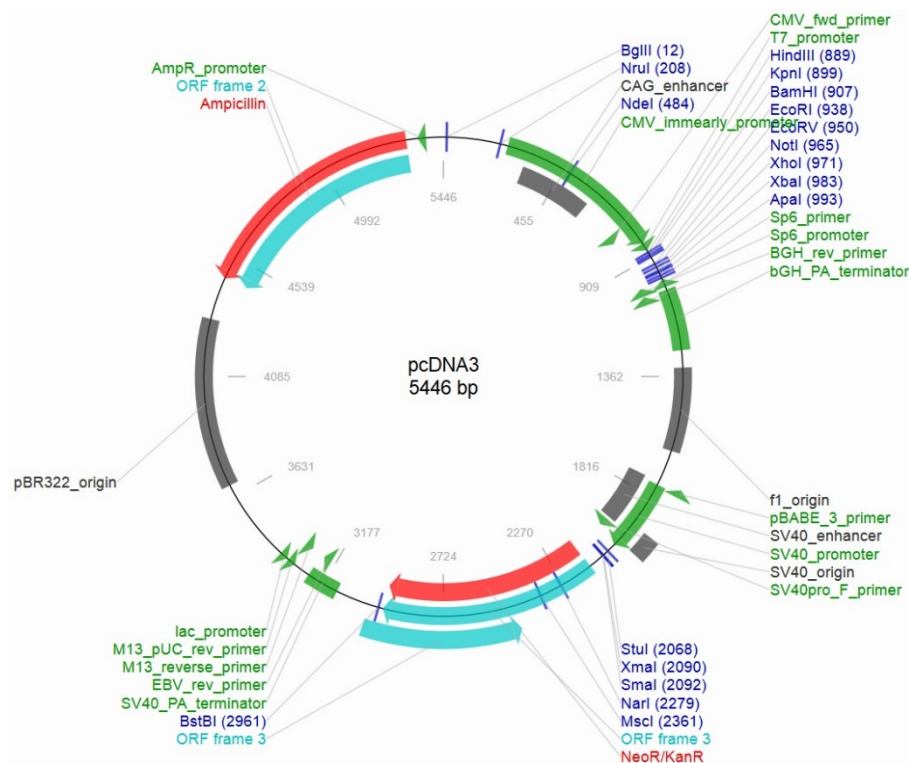


Figure 14: Plasmid vector map of the pcDNA3 vector. The vector contains an ampicillin resistance and the human cytomegalovirus (CMV) immediate early enhancer and promoter for strong gene expression cloned in front of the multiple cloning site. The enzymatic restriction sites are shown in dark blue.

The LeGO-iG2 vector was used for the stable transduction in mammal cells. The protein expression is driven by a spleen focus-forming virus (SFFV) promoter in front of the multiple cloning site. The expression of the enhanced green fluorescent protein (EGFP) is fused to the internal ribosomal entry site (IRES2) and thereby coupled to the expression of the inserted gene (Weber et al., 2008). The empty vector is shown in Figure 15.

Created with SnapGene®

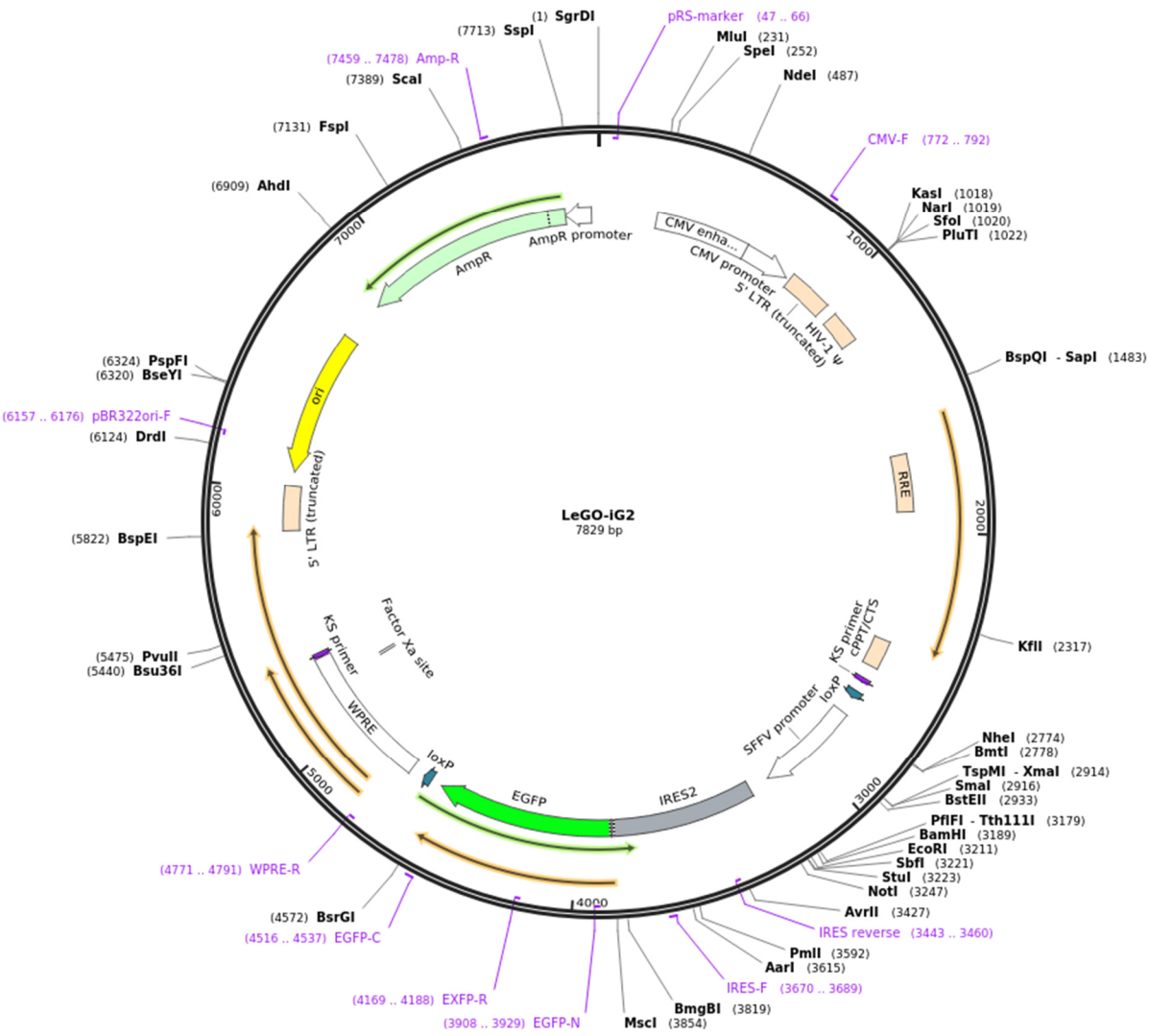


Figure 15: Plasmid vector map of the LeGO-iG2 vector. The vector contains an ampicillin resistance and the spleen focus-forming virus (SFFV) promoter for strong gene expression cloned in front of the multiple cloning site. The enhanced green fluorescent protein (EGFP) is coupled through the internal ribosomal entry site (IRES2) to the target expression (Weber et al., 2008). The enzymatic restriction sites are shown in black.

The pRRLsAVI-MCS-iGFP-BirA vector was used for Co-Streptavidin precipitation. The vector was used for transient transfection and stable transduction in cell lines. The expression cassette is similar to the LeGO-iG2 vector. The vector additionally contains a BirA ligase which biotinylates the AVI-tagged inserted gene (Rodriguez et al., 2005). The empty vector is shown in Figure 16.

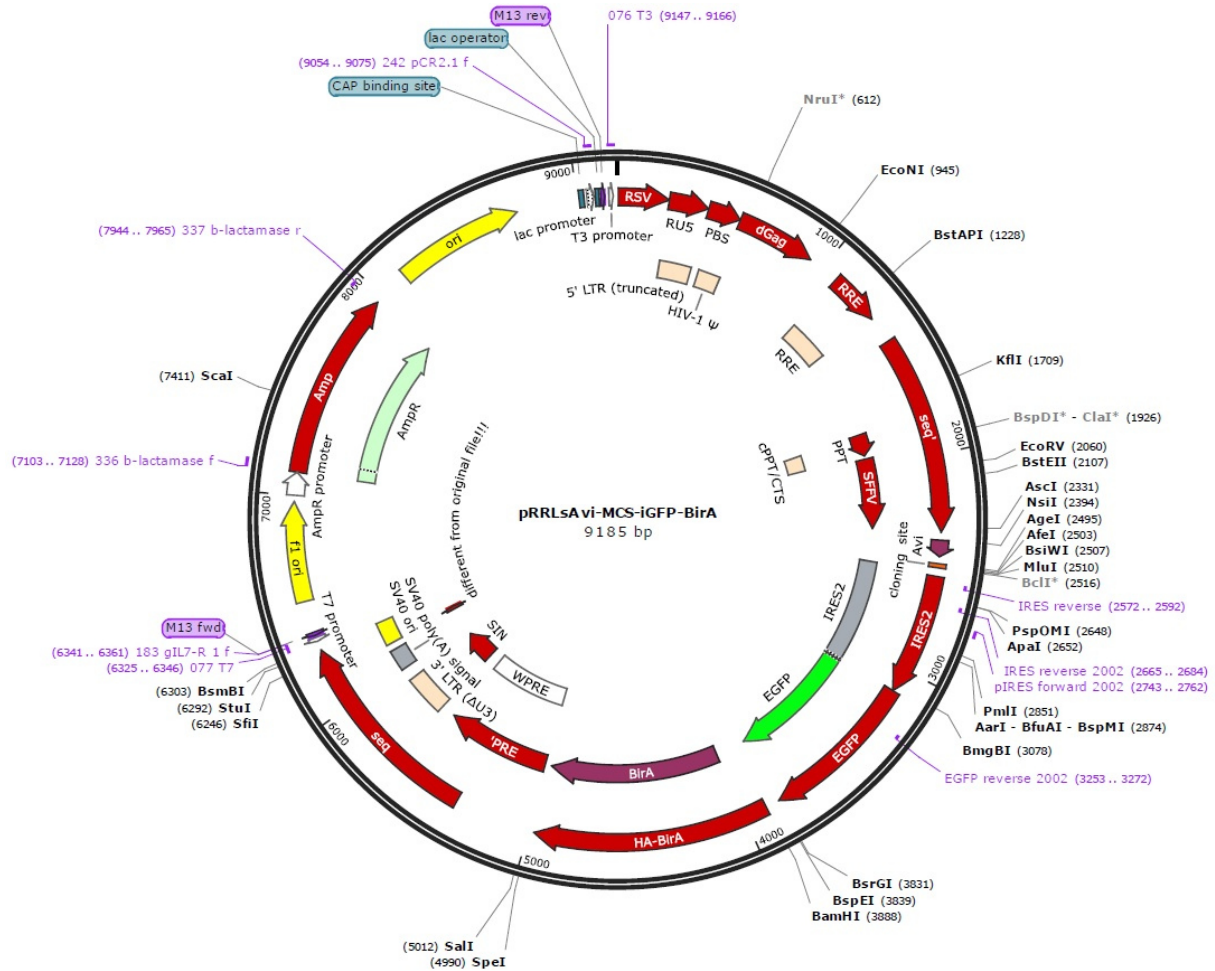


Figure 16: Plasmid vector map of the pRRLsAVI-MCS-iGFP-BirA vector. The vector contains an ampicillin resistance and the spleen focus-forming virus (SFFV) promoter for strong gene expression cloned in front of the multiple cloning site. The enhanced green fluorescent protein (EGFP) is coupled through the internal ribosomal entry site (IRES2) to the target expression. Additionally, the BirA ligase is expressed, which biotinylates AVI-tagged inserted gene. The enzymatic restriction sites are shown in black.

The pGIPZ vector was used for gene knockdown in mammal cells. The vector was inserted with stable virus transduction. The vector contains a specific microRNA adapted shRNA which is based on miR-30. The empty vector is shown in Figure 17.

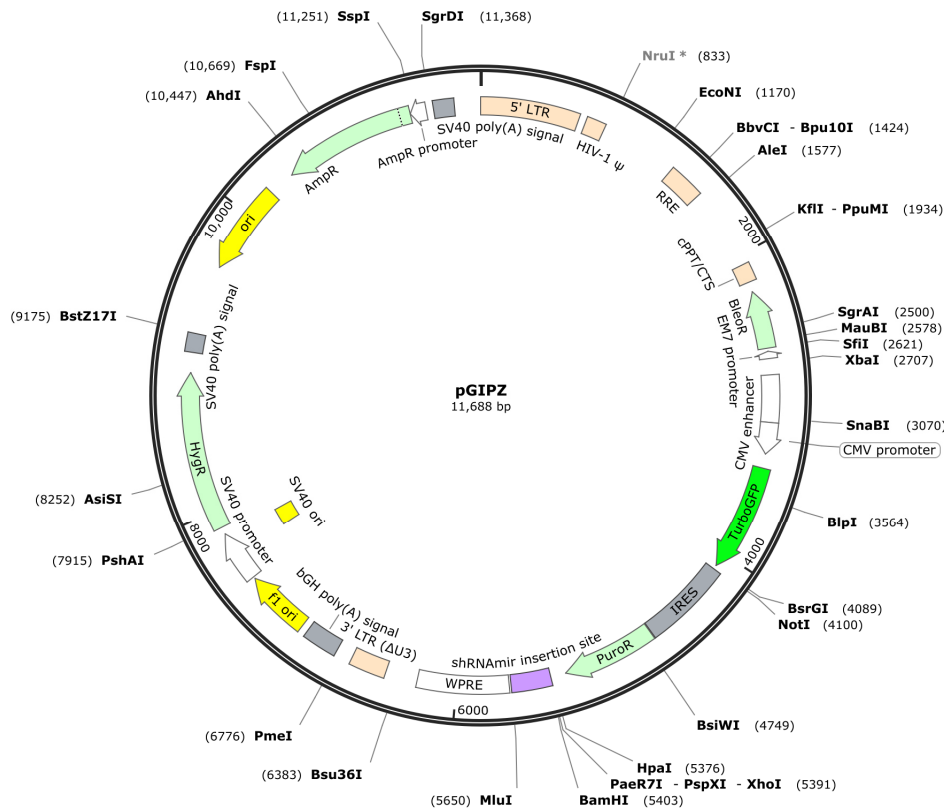


Figure 17: Plasmid vector map of the pGIPZ vector. The vector contains an ampicillin resistance and the green fluorescent protein (GFP) for positive selection. It allows for the constitutive expression of an microRNA adapted shRNA which is based on miR-30.

2.1.5 Oligonucleotides

The Oligonucleotides used in this study are described in Table 6.

Table 6: Oligonucleotides

cloning primers

Name	Sequence 5' → 3'
hLEF1 BamHI fwd	ATAGGATCCACCATGCCCAACTCTCCGG
hLEF1 EcoRI rev	ATATGAATTCTCAGATGTAGGCAGCTGTCA
hPRMT6 AgeI fwd	CCGGACCGGTTTCGAGCCCAAGAAAAGAAA
hPRMT6 MluI rev	CGCGACGCGTTCAGTCTCCATGGCAAAGTC
hRUNX1 MluI fwd	ATATACGCGTACCATGCGTATCCCCGTAGA
hRUNX1 AgeI rev	ATATACCGGTGTAGGGCCTCCACACGGCCT
hRUNX1 AgeI fwd	ATATACCGGTTCGTATCCCCGTAGATGCCAG
hRUNX1 MluI rev	ATATACGCGTTCAGTAGGGCCTCCACACGG

ChIP primers

Name	Sequence 5' →3'
CCND1 TSS fwd	CTCTGCCGGGCTTTGATCTT
CCND1 TSS rev	AAACTCCCCTGTAGTCCGTG
CCND1 -4,000 fwd	TAAGGGGTCCGAATCCGAGT
CCND1 -4,000 rev	GGAAACGGGTTGCGTACCTA
CD41 TSS fwd	AAGCTTGGCTCAAGACGGAG
CD41 TSS rev	CTGCCCCGATAAAACCTGA
CD41 -5,000 fwd	TGTTGCCCATCCACTCAA
CD41 -5,000 rev	TTGCGTAGCCTGAGCTTTCA
RUNX1 enh fwd	AAGACTTCTGCTGCAAGCCA
RUNX1 enh rev	TTGGGAAAGCAGGACTTGGG
RUNX1 -800 fwd	CCCGAAACAGTGGCTGATCT
RUNX1 -800 rev	AAACGGCTCTTGGAGGAGTG

real time primers

Name	Sequence 5' →3'
Axin2 RT fwd	CTGGCTCCAGAAGATCACAAAG
Axin2 RT rev	ATCTCCTCAAACACCGCTCCA
hBCL6 RT fwd	AGAGCCCATAAAACGGTCCT
hBCL6 RT rev	TCCCTCAGGGTTGATCTCAG
CD41 RT fwd	AATGGCCCCTGCTGTCGTGC
CD41 RT rev	TGCACGGCCAGCTCTGCTTC
hCTNNB1 RT fwd	GCTTTCAGTTGAGCTGACCA
hCTNNB1 RT rev	CAAGTCCAAGATCAGCAGTCTC
hGAPDH RT fwd	TCTTTTGCCTGCCAGCCGAGC
hGAPDH RT rev	TGACCAGGCGCCCAATACGACC
hKLF1 RT fwd	GTGATAGCCGAGACCGCGCC
hKLF1 RT rev	TTCTCCCCTGTGTGCGTGCG
hLEF1 RT fwd	CGAAGAGGAAGGCGATTTAGCT
hLEF1 RT rev	CTCCTGAGAGGTTTGTGCTTGTC
hPRMT6 RT fwd	TCTGGTTCCAGGTGACCTTC
hPRMT6 RT rev	AGGTAGAGGAGCGCCTGTTT
RUNX1 RT fwd	TCGACTCTCAACGGCACCCGA
RUNX1 RT rev	TGACCGGCGTCGGGGAGTAG
hTAL1 RT fwd	TCGGCAGCGGGTTCTTTGGG
hTAL1 RT rev	CCATCGCTCCCGGCTGTTGG
TCF7 RT fwd	GCAGCTATAACCCAGGCTGG
TCF7 RT rev	CCTCGACCGCCTCTTCTTC

TCF7L1 RT fwd	TTCGTCCTGTAGGTGCTGTG
TCF7L1 RT rev	ACCCACGGTATTGAGCAGAC
TCF7L2 RT fwd	GAAGGAGCGACAGCTTCATA
TCF7L2 RT rev	GGGGGAGGCGAATCTAGTAA

2.1.6 Antibodies

The antibodies used in this study are described in Table 7.

Table 7: Antibodies

ChIP antibodies:

Antibody	Host	Cat.No.	Supplier	ChIP	Concentration
LEF1	rabbit	D6J2W	Cell Signaling	5.0 µg	1.0 mg/ml
PRMT6 (H-2)	mouse	sc-365018	Santa Cruz	5.0 µg	200 µg/ml

Primary antibodies:

Antibody	Host	Cat.No.	Supplier	Dilution	Concentration
LEF1	rabbit	C12A5	Cell Signaling	1:1,000	unspecified
PRMT6 (H-2)	mouse	sc-365018	Santa Cruz	1:250	200 µg/ml
RUNX1 (A-2)	mouse	sc-365644	Santa Cruz	1:250	200 µg/ml
Actin	rabbit	ab1801	Abcam	1: 1,000	1 mg/ml
GAPDH (6C5)	mouse	sc-32233	Santa Cruz	1: 5,000	100 µg/ml

secondary antibodies:

Antibody	Host	Cat.No.	Supplier	Dilution	Concentration
anti-rabbit IRDye 800CW	donkey	926-32213	Li-cor	1: 15,000	1 mg/ml
anti-mouse IRDye 800CW	donkey	926-32212	Li-cor	1: 15,000	1 mg/ml

2.1.7 Equipment

The equipment used in this study is described in Table 8.

Table 8: Equipment

Equipment	Manufacturer
Autoclave, Varioklav 75 S	Thermo Fisher Scientific Inc., Waltham, USA
Basic Power Supply, PowerPac™	Bio Rad Laboratories GmbH, München, Germany
Block incubator, Thermomixer R	Eppendorf AG, Hamburg, Germany
Centrifuge, 2K15	Sigma-Aldrich, München, Germany
Centrifuge, mini, Sprout	Biozym Scientific GmbH, Hessisch Oldendorf, Germany
Centrifuge, Rotina 420	Hettich Zentrifugen AG, Tuttlingen, Germany
Electrophoresis chamber, Compact XS/S	Biometra, Göttingen, Germany
Freezer -20°C, Arctis Öko	AEG AG, Frankfurt am Main, Germany
Freezer -80°C, Ultra-low	Sanyo, Osaka, Japan
Fridge 4°C, Profi line	Liebherr, Kirchdorf, Germany
Heating magnetic stirrer, FB15001	Thermo Fisher Scientific Inc., Waltham, USA
Ice Flaker, SPR-80	Simag, Pogliano Milanese, Italy
Imaging system, Gel Doc XR+	Bio Rad Laboratories GmbH, München, Germany
Imaging System, Odyssey® CLx	Li-cor Biosciences GmbH, Bad Homburg, Germany
Incubator, IF110	Memmert, Schwabach, Germany
Incubators, Steri-Cycle CO2	Thermo Fisher Scientific Inc., Waltham, USA
Laminar flow cabinet Holten Safe 2010	Holten, Thermo Fisher Scientific Inc., Waltham, USA
Microscope, CKX41	Olympus K.K., Shinjuku, Japan
Microwave, MWG 737	Ciatronic, Kempen, Germany
Minishaker, MS2	IKA GmbH & Co. KG, Staufen im Breisgau, Germany
Multi plate reader, Victor X4	Perkin Elmer, Waltham, USA
Orbital shaker, MaxQ™ 4000	Thermo Fisher Scientific Inc., Waltham, USA
PCR Thermocycler, T Professional Basic	Biometra, Göttingen, Germany
Ph meter, HI 2211 pH/ORP	Hanna Instruments, Vöhringen, Germany
Real-Time PCR System, StepOnePlus	Applied Biosciences, Waltham, USA
Scale, LC 2200 S	Sartorius, Göttingen, Germany
Semi-Dry Transfer Cell, Trans-Blot® SD	Bio Rad Laboratories GmbH, München, Germany
Sonication device, Bioruptor® Plus	Diagenode, Seraing, Belgium
Spectrophotometers, Ultrospec 3000	Pharmacia Biotech, Picataway, USA
UV-Vis spectrophotometer, Nanodrop	Thermo Fisher Scientific Inc., Waltham, USA

2.2 Molecular biology techniques

2.2.1 Preparation of Calcium Competent Cells

A frozen glycerol stock of Top10 *E. coli* bacteria was plated onto a LB agar plate without antibiotics and incubated overnight at 37°C. A starter culture was prepared by inoculating 10 mL LB media with bacteria of the LB agar plate. The culture was incubated overnight at 37°C and 250 rpm in a shaking incubator. 500 mL of LB media was inoculated with 5 mL of the starter culture and grown at 37°C and 250 rpm. The cells were incubated until the culture reached an OD₆₀₀ of 0.4. The cell culture was chilled on ice for 30 min. Subsequently the cells were centrifuged at 3,000 g for 15 min at 4°C. The supernatant was removed, and the pellet was resuspended in 200 mL ice cold MgCl₂. The suspension was centrifuged at 2,000 g for 15 min at 4°C. The supernatant was removed, and the pellet was resuspended in 200 mL CaCl₂. The suspension was incubated for 20 minutes on ice and centrifuged. The pellet was resuspended in 25 ml ice cold 85mM CaCl₂, 15% glycerol. The suspension was centrifuged at 1,000 g for 15 min at 4°C. The cells were finally resuspended in 1 mL ice cold 85 mM CaCl₂, 15% glycerol. Aliquots of 50 µL were pipetted into 1.5 mL microcentrifuge tube and snap frozen in liquid nitrogen. Frozen cells were stored at -80°C.

2.2.2 Transformation of Competent Cells

Aliquots of 1.0 µL Top10 *E. coli* bacteria were thawed on ice. 5 µL of Plasmid DNA were mixed with 50 µL of bacteria. The mixture was incubated for 30 min in ice. Heat shock was performed at 42°C for 45 s and the cells were cooled on ice for 5 min. Subsequently the cells were plated on LB agar plates with ampicillin (100 µg/mL). The agar plates were incubated overnight at 37°C.

2.2.3 Mini Plasmid DNA Preparation

Sub-cultured clones were cultivated overnight at 37°C in 4 mL LB-Media with appropriate antibiotics and centrifuged at 8,000 g for 5 min at RT. The plasmids were isolated and purified using the Miniprep kit from Thermo Fisher Scientific (GeneJET Plasmid Miniprep Kit #K0503). DNA was stored at -20°C.

2.2.4 Midi Plasmid DNA Preparation

A starter culture was prepared by inoculating 5 mL LB (ampicillin 100 µg/mL) media with transformed TOP10 cells and grown for 8 h at 37°C and 250 rpm. A 500 mL flask containing 200 mL LB media with ampicillin was inoculated with 200 µL starter culture and incubated overnight at 37°C. The cells were pelleted at 8,000 g for 15 min at 4°C. The plasmids were isolated and purified using the Midiprep kit from Thermo Fisher Scientific (PureLink™ HiPure Plasmid Midiprep Kit # K210005). DNA was stored at -20°C.

2.2.5 Sequencing

The integrity of plasmid DNA was confirmed by Sanger sequencing. The LightRun Tube sequencing protocol from Eurofins Genomics Germany GmbH was used according to the company's instruction.

2.2.6 Agarose Gel Electrophoresis

Fragments of the size from 0.1 to 10 kbp were separated with 0.8 – 2.0% agarose gels. 0.8 – 2.0 g agarose was dissolved under heating in 100 mL TAE buffer. 0.2 – 0.5 µg/mL EtBr was added. Electrophoresis was performed at 120V in a TAE filled chamber for 20 – 40 min. The Gel Doc XR+ System (Bio Rad Laboratories GmbH, München, Germany) was used for analyzing the agarose gel.

TAE buffer 40 mM Tris base; 20 mM acetic acid; 1 mM EDTA sodium salt dihydrate

2.2.7 Polymerase Chain Reaction (PCR)

The polymerase chain reaction (PCR) was used to amplify double stranded DNA and consist of three different reaction steps. First the reaction starts at high temperature to denature the double-stranded DNA. The temperature is decreased in the second step to allow the binding of short oligonucleotides (primers) at specific sites of interest. The third step comprises of the DNA elongation, catalyzed by a heat-stable DNA-polymerase. The primers serve as starting point of the elongation. The Q5[®] High-Fidelity DNA Polymerase from New England Biolabs GmbH was used for the amplification of DNA templates according to the company's instruction. The chemical components of the PCR and the thermocycling conditions are shown in Table 9.

Table 9: Components and thermocycling conditions of the PCR

Component	Volume	Thermocycling Conditions		
5X Q5 Reaction Buffer	10.0 µL	Step	temperature	Time
10 mM dNTPs	1.0 µL	Initial denaturation	98°C	30 s
10 µM Forward Primer	2.5 µL	denaturation	98°C	10 s
10 µM Reverse Primer	2.5 µL	annealing	TA °C	30 s
Template DNA	1.0 µL	elongation	72°C	te s
Q5 High-Fidelity DNA Polymerase	0.5 µL	final extension	72°C	120 s
5X Q5 High GC Enhancer	10.0 µL	hold	4°C	∞
H ₂ O	22.5 µL			

TA = Annealing-temperature; te = Elongation time

The PCR product was purified with the GeneJET PCR Purification Kit (Thermo Scientific, Cat. # K0702)

2.2.8 Cloning of lentiviral plasmids

DNA restriction double digestion was performed on PCR products and plasmid backbones with the Cut Smart System from New England Biolabs GmbH. The used high-fidelity restriction enzymes are shown in Table 4. The plasmid backbones and inserts are shown in Table 5.

Ligation was performed at room temperature overnight. The T4 DNA Ligase (NEB; M0202S) was used according to the company's instruction. The T4 Ligase was inactivated for 10 min at 65°C. Afterwards the DNA was transformed into competent *E. coli* cells.

2.2.9 RNA isolation

To analyze gene expression, total RNA was isolated for the quantification of the mRNA amount of certain genes. $10^5 - 10^6$ fresh cells were pelleted at $400 \times g$ for 5 min at 4°C . The pellet was washed with $500 \mu\text{L}$ PBS to remove residual cell culture media. RNA was isolated using the RNeasy Mini Kit (Qiagen; cat. #74106); according to the company's instruction. The RNA was eluted in $30 \mu\text{L}$ RNase-free water and stored for short term at -80°C .

2.2.10 cDNA synthesis

Complementary DNA (cDNA) was synthesized from the isolated mRNA. The PrimeScript RT Master Mix Perfect Real Time (Takara Bio Europe AB; cat. #RR036A) was used according to the company's instruction. $1,000 \text{ ng}$ RNA were mixed with $4 \mu\text{L}$ Master mix in a total volume of $20 \mu\text{L}$. The reaction mixture was incubated for 15 min at 37°C and heat inactivated for 10 s at 85°C .

2.2.11 Gene Expression analysis / quantitative real-time PCR (qPCR)

Quantitative real-time PCR (qPCR) was used to analyze the expression level of the mRNA of certain genes. The qPCR was performed in a LightCycler 480 (Roche). The chemical components of the qPCR and the thermocycling conditions are shown in Table 10. SYBR Green (Eurogentec) was used as a fluorescent dye which intercalates into double stranded DNA and allows therefore the quantification of the amplified DNA.

Table 10: Components and thermocycling conditions of the quantitative real-time PCR

Component	Volume	Thermocycling Conditions		
		Step	temperature	Time
SYBR Green PCR master mix	$12.5 \mu\text{L}$	Initial denaturation	95°C	600 s
fwd primer ($10 \text{ pmol}/\mu\text{l}$)	$0.5 \mu\text{L}$	denaturation	95°C	10 s
rev primer ($10 \text{ pmol}/\mu\text{l}$)	$0.5 \mu\text{L}$	annealing	58°C	30 s
cDNA	$1.0 \mu\text{L}$	elongation	72°C	30 s
H_2O	$10.5 \mu\text{L}$	measurement	78°C	10 s
		melt curve	$60^\circ\text{C} \rightarrow 95^\circ\text{C}$	

The DNA oligonucleotides used for the qPCR are listed in Table 6. The Glyceraldehyde-3-phosphate dehydrogenase (GAPDH) expression was used for normalization. The data was analyzed with the " $\Delta\Delta\text{Ct}$ " (Livak and Schmittgen, 2001); (Pfaffl, 2001) method by quantifying the threshold cycles (Ct).

ΔCt1 (control) = Ct (gene of interest) – Ct (housekeeping gene)

ΔCt2 (sample) = Ct (gene of interest) – Ct (housekeeping gene)

$\Delta\Delta\text{Ct}$ = ΔCt2 (sample) - ΔCt1 (control)

mRNA expression = $2^{-\Delta\Delta\text{Ct}}$

The mRNA expression values were normalized to the control which is set to 1.0.

2.3 Cell culture methods

2.3.1 Thawing and freezing of cells

Frozen cells stored in liquid nitrogen in the vapor phase were thawed at room temperature and resuspended in 10 mL medium. Cells were pelleted at 400°C for 5 min at room temperature and resuspended in medium and seeded in culture flasks. The cells were incubated at 37°C with 5% CO₂ atmosphere.

Cells were pelleted at 400°C for 5 min at room temperature and washed with 10 mL PBS. The pellet was resuspended in 500 µL Medium (FCS with 10% (v/v) DMSO). The cells were frozen in a freezing container at a cooling rate of 1°C/min at -80°C. The vials were stored in liquid nitrogen in the vapor phase.

2.3.2 Cell quantification with Neubauer counting chamber

Cells were mixed with trypan blue at a ratio of 1:1. The Neubauer counting chamber was loaded with 10 µL of the sample. The unstained viable cells were counted with a light microscope. The number of cells counted in two large squares multiplied by 10.000 corresponds to the number of cells in 1 mL media.

2.3.3 Passaging of the cells

For sub culturing of adherent cells, the medium was aspirated and washed with 10 mL PBS. The cells were detached by adding 2 mL Trypsin for 2 min at 37°C. The digestion was stopped by adding 8 mL DMEM. Cells were pelleted at 400°g for 5 min at room temperature and seeded at a concentration of 3×10^6 cells per 75 cm² cell culture flask. Non-adherent cells were pelleted at 400°g for 5 min at room temperature and split at a 1 to 4 ratio with appropriate medium.

2.3.4 Isolation of primary hCD34⁺ cells

Peripheral blood samples from G-CSF treated healthy donors were collected by apheresis. The samples were provided by the Institute for Transfusion Medicine and Immunohaematology Frankfurt/Main, approved by the ethics committee (permit #329-10). The blood samples were mixed with PBS to a final volume of 35 mL. The samples were laid on 15 mL Ficoll and centrifuged for 40 min at 400x g and RT with lowest deceleration rate. The fraction of white blood cells was collected and mixed with PBS to a final volume of 20 mL. Subsequently the cells were centrifuged at 400 g for 10 min at 4°C. The cells were washed with 10 mL PBS and centrifuged at 400 g for 5 min at 4°C. The pellets were resuspended in PBS at a concentration of 10⁸ cells/500 µL. 100 µL FcR blocking reagent and 100 µL monoclonal mouse anti-human CD34 antibody conjugated magnetic microbeads were added per 300 µL cell suspension (Miltenyi Biotec). Incubation was performed for 30 min at 4°C in the dark. The cells were washed with 10 mL PBS and centrifuged at 400 g for 5 min at 4°C. The cells were resuspended in 1 mL buffer and filtered with a cell strainer (70 µm pore size). LS columns (Miltenyi Biotec) were equilibrated by rinsing them with 5 mL buffer and placed into a magnetic rack. The samples were added to the columns and washed for 3 times with 3 mL buffer. After removal from the magnetic rack, the bead label, CD34⁺ enriched cells were eluted with 5 mL buffer. The enrichment and purity were verified via flow cytometry using anti-Human CD45 FITC/CD34 PE

antibodies. The cells were resuspended in SFEM I media with StemSpan CC100 supplement (Flt3L, SCF, IL-3 and IL-6) and seeded at a density of 5×10^5 cells in 500 μ L medium per well.

2.3.5 Differentiation of primary human CD34⁺ cells

Isolated CD34⁺ cells were expanded for 3 days in SFEM I media with StemSpan CC100 supplement. Megakaryocytic differentiation was induced by resuspending the cells in SFEM II media supplement with StemSpan Megakaryocyte Expansion Supplement (SCF, IL-6, IL-9 and TPO). The expression of the cell surface marker CD41 (Integrin α -IIb) was tested by flow cytometry. StemSpan Erythroid Expansion Supplement (SCF, IL-3, and EPO) was used for erythroid differentiation. Differentiation was verified by expression of the cell surface marker CD71 (Transferrin receptor protein 1)

2.3.6 Transient Transfection

Transient transfection allows the introduction of foreign DNA into a host cell. In contrary to lentiviral transfection, the DNA is not integrated into the host genome. The negatively charged DNA is complexed with a positively charged chemical like polyethyleneimine (PEI). The process of cell membrane passage and transport to the nucleus is still under investigation (Reed et al., 2006).

For Luciferase assays, 9×10^4 HEK293T cells per well were seeded with 1 mL DMEM into 24-well plates. On the next day, 75 μ L DMEM without FCS, 5 μ L PEI and 250 ng of each Plasmid of interest were mixed and incubated for 20 min at RT. 50 μ L of the transfection solution was added to each well. The cells were harvested after 48 hours for luciferase assay.

For Co-Streptavidin Precipitation, 1×10^6 HEK293T cells per well were seeded with 2 mL DMEM into 6-well plates. On the next day, 375 μ L DMEM without FBS, 15 μ L PEI and 500 ng of each plasmid of interest were mixed and incubated for 20 min at RT. 200 μ L of the transfection solution was added to each well. The cells were harvested after 48 hours for Co-streptavidin precipitation.

Lentiviral particles were produced in T175 cell culture flasks, 1.4×10^7 HEK293T cells were seeded in 15 mL DMEM. On the next day, 400 μ L DMEM without FCS, 144 μ L PEI, 10 μ g pMD2.G packaging plasmid, 18 μ g pCMVdelta8.91 packaging plasmid and 25 μ g of the transfer plasmid were mixed and incubated for 20 min at RT. the transfection solution was added directly into the cell culture flasks, the medium was removed after 4 hours and replaced with 30 mL fresh DMEM. The viral particles were harvested after 48 hours and 72 hours.

2.3.7 Concentration of lentiviral particles

48 hours after transfection, the supernatant was centrifuged for 5 min, 400 x g at 4°C to remove cell debris. The supernatant was filtered through a 0,45 μ M filter and transferred into ultracentrifugation tubes. The viral supernatant was underlayered with 20% sucrose solution. The viral particles were concentrated by ultracentrifugation at 20,000 rpm for 2.5 hours at 4°C. The procedure was repeated after 24 hours. The pellet was resuspended in 200 μ L medium and stored at -80°C.

2.3.8 Gene knockdown and overexpression via lentiviral transduction

Human hematopoietic cells were genetically manipulated through lentiviral transduction. The down regulation of gene expression was performed with small hairpin RNAs (shRNAs). Overexpression was

accomplished by the fusion of the gene of interest with the silencing-prone spleen focus forming virus (SFFV) promoter. K562 and CD34⁺ cells were transduced as follows: 1 x 10⁵ cells were cultured with 250 μ L medium containing 5 μ L protamine sulfate (400 μ g/mL). 100 μ L concentrated viral particles were added and the cells were centrifuged for 60 min at 1200 x g at 32°C. The medium was exchanged after 4 hours and the transduction was repeated on the next day. Seven days after transduction the cells were washed two times with 5 mL PBS to remove residual viral particles. Transduction efficiency was determined by flow cytometer as all vectors contained the GFP reporter gene.

2.3.9 Cell cycle analysis

An amount of 500,000 K562 cells was centrifuged at 400 x g for 5 min at room temperature and was washed with 500 μ L PBS. The cells were fixated by resuspension of the cell pellet with 500 μ L ice cold 70% ethanol. The cells were fixated for 30 min at 4°C. The fixated cells were centrifuged at 1.200 x g for 5 min at 4°C and were washed two times in 500 μ L PBS. The cell pellet was resuspended in 500 μ L DAPI staining solution and incubated for 30 min at room temperature in the dark. The cells were centrifuged at 1.200 x g for 5 min at 4°C and were washed with 500 μ L PBS.

2.3.10 Multicolor Flow Cytometry

Multicolor flow cytometry was used to analyze cells regarding their fluorescence, size and granularity. Fluorescent-labeled antibodies were used to distinguish different cell types regarding their expression of cell surface molecules. Transduction efficiency was measured by the expression of GFP proteins encoded on the lentiviral backbones. The cells were measured in the BD LSRFortessa (BD Bioscience). Recorded data was analyzed with the BD FACSDiva software (BD Bioscience).

Fluorescence activated cell sorting (FACS) was used to enrich transduced CD34⁺ hematopoietic stem cells. 7 days after transduction, the cells were washed two times in 10 mL PBS to remove all residual lentiviral particles. After centrifugation at 400 x g for 5 min at 4°C, the cells were resuspended in 1 mL PBS. Successfully transduced CD34⁺ hematopoietic stem cells GFP expressing cells were enriched. Sorting was performed on a FACS Aria (BD Biosciences).

2.4 Protein biochemistry

2.4.1 Luciferase assay

Luciferase assays were used to analyze the activity of promoters of interest. A promoter::luciferase fusion construct was transfected into HEK293T cells. The expressed luciferase enzyme was extracted from the cells and its activity was measured by the light emitting reaction of luciferin, in presence of Mg²⁺ and ATP. The measurement was normalized by measuring the activity of a co-transfected β -Galactosidase. 48 h after transfection, the cells were washed with 1 mL PBS and detached with 90 μ L lysis buffer. The lysates were transferred into new tubes and incubated for 20 min on ice. The tubes were vortexed briefly and centrifuged at 13,000 rpm for 10 min at 4°C. The supernatant was used for the following measurements.

Bioluminescence was detected using a Victor X4 Multiple Plate Reader (PerkinElmer). 5 μ L of the supernatant was pipetted into a white 96-well plate in duplicates. A dispenser was used to add 100 μ L luciferase buffer to each well. The light emission was directly measured with the luminometer. The β -Galactosidase activity was measured to take the transfection efficiency into account. 5 μ L of the supernatant was pipetted into a transparent 96-well plate in duplicates. 100 μ L β -galactosidase buffer was added to the sample and the absorbance at 420 nm was immediately measured.

Lysis buffer	50 mM Tris (pH 7.4); 1% Triton X-100; 50 mM NaCl; Proteinase-Inhibitor
Luciferase buffer	8.65 ml Glycylglycin (25 mM); 500 μ l ATP (20 mM) in H ₂ O, pH 7.5; 100 μ l MgSO ₄ (1M); 750 μ l Luciferin (1 mM)
100 x Mg solution	0.1 M MgCl ₂ , 4.5 M β -mercaptoethanol
1 x ONPG	4 mg/ml ONPG in 0.1 M sodium phosphate
0.1 M sodium phosphate	41 ml 0.2 M Na ₂ HPO ₄ *2H ₂ O; 9 ml 0.2 M NaH ₂ PO ₄ *2H ₂ O; 50 mL H ₂ O
β -galactosidase buffer	105 μ L 100 x Mg solution; 2,310 mL 1 x ONPG; 7,035 mL 0.1 M sodium phosphate (pH 7.5)

2.4.2 Protein labeling

Cells of interest were washed 3 times with PBS to ensure the removal of all remaining RPMI medium. A starter culture of 10⁶ cells was seeded in a six well plate. The control cells were cultivated in light RPMI SILAC medium and the Bio-PRMT6 overexpressing cells were cultivated in heavy RPMI SILAC medium. The light RPMI SILAC medium contained untagged L-arginine (84 mg/L) and L-lysine (146 mg/L) (Sigma). The heavy RPMI SILAC medium contained the tagged ¹³C₆, ¹⁵N₄-L arginine (Arg-10) and ¹³C₆, ¹⁵N₂-L-lysine (Lys-8). The cells were cultivated for at least five cell divisions to ensure that most cells were labelled with the isotopes. After five cell divisions, 10⁸ cells were pelleted at 400 g for 10 min at 4°C. The cells were cooled on ice and the nuclear proteins were isolated (see 2.4.4).

2.4.3 Whole cell lysates

For whole cell lysates, 10⁶ – 10⁷ cells were resuspended in PBS and centrifuged at 400 x g for 10 min at 4°C. The supernatant was discharged, and the pellet was resuspended in 400 μ L RIPA-Buffer. 4 μ L Protease Inhibitor Cocktail (x100) was added and the tube was vortexed briefly. Afterwards the tube was incubated for 20 min at 4°C under rotation. 1 μ L NP-40 was added and the tube was vortexed for 2 min. The cells were centrifuged at 13,000 rpm for 10 min at 4°C. The supernatant was transferred into a new tube and frozen in liquid nitrogen and stored at -80°C.

RIPA-buffer	50 mM TrisHCl pH 8; 0,1 % SDS; 150 mM NaCl; 2 mM EDTA pH8; NP-40; 0,5% sodium deoxycholate
-------------	--------------------------------------------------------------------------------------------

2.4.4 Nuclear extraction

Up to 2.5 x 10⁷ cells were washed with 10 mL PBS and pelleted at 400 g for 10 min at 4°C. The cells were resuspended in 1,000 μ L ice cold buffer A and incubated for 20 min at 4°C under rotation. The tube was centrifuged at 13,000 rpm for 10 min at 4°C. The supernatant containing the cytoplasmic

fraction was transferred into a new tube. 500 μ L buffer C were added to the pellet. The suspension was incubated for 30 min under rotation. The tube was centrifuged at 13,000 rpm for 15 min at 4°C. The supernatant containing the nucleic fraction was transferred into a new tube. Protein samples were frozen in liquid nitrogen and stored at -80°C.

Buffer A	10 mM Tris (pH 7.5); 0,1 mM EDTA (pH 8.0); 0,1 mM EGTA (pH 8.0); 10 mM KCl; 1 mM DTT; Proteinase-Inhibitor
Buffer C	10 mM Tris (pH 7.5); 1 mM EDTA (pH 8.0); 1 mM EGTA (pH 8.0); 0.4 M NaCl; 20% Glycerol; 1 mM DTT; 0.1 % NP-40; Proteinase-Inhibitor

2.4.5 Co-Streptavidin precipitation

48 hours after transient transfection, the HEK293T cells were washed with 500 μ L PBS and detached with 250 μ L lysis buffer. The cells were incubated on ice for 20 min and centrifuged at 13,000 rpm for 10 min at 4°C. And input sample of 25 μ L lysate was removed and frozen at -20°C. The samples of two wells were merged and 250 μ L lysate were mixed with an appropriate amount of Streptavidin Beads (Dynabeads M-280, Life Technologies). The Streptavidin beads were blocked preliminary with Roti Block Blocking Solution (Carl Roth GmbH) and Proteinase-Inhibitor. The solution was incubated overnight at 4°C under rotation. On the next day; the solution was washed six times with lysis buffer. The Streptavidin precipitated proteins were eluted from the beads at 95°C for 5 min with 16 μ L undiluted NuPAGE LDS Sample Buffer and 2 μ L NuPAGE™ Sample Reducing Agent (Cat. # NP0007 and NP0004, Thermo Fisher Scientific). The solution was frozen at -20°C.

Lysis buffer	50 mM Tris (pH 7.4); 1% Triton X-100; 50 mM NaCl; Proteinase-Inhibitor
--------------	------------------------------------------------------------------------

2.4.6 SDS-PAGE and Western blotting

Western blotting is used for the identification and quantification of specific proteins in cell lysates. The protein lysates were diluted with 4X NuPAGE™ Sample Reducing Agent and 10X NuPAGE™ Sample Reducing Agent (Cat. # NP0007 and NP0004, Thermo Fisher Scientific). The solution was incubated for 5 min at 95°C. The proteins were separated by SDS polyacrylamide gel electrophoresis in an SDS-Tris-Glycine buffer system (SDS-PAGE). Electrophoresis was performed at 80 V for 30 min and subsequently for 2 hours at 120 V. PageRuler™ Prestained Protein Ladder (Cat. # 26616, Thermo Fisher Scientific) was used the size measurement. The proteins were transferred to a nitrocellulose membrane (0.45 μ M) with towbin buffer. The Trans-Blot® SD Semi-Dry Transfer Cell (Bio-Rad) was used for transfer for 95 min at 75 mA per membrane. The membrane was blocked with milk solution for 1 hour. Subsequently the membrane was incubated with the primary antibody in milk solution overnight at 4°C. The primary antibodies and dilutions are listed in Table 7. The blots were washed 4 times for 10 min with TBS-T buffer and incubated with the secondary antibody in milk solution (dilution 1:15,000) for 1 hour at room temperature. The secondary antibodies are listed in Table 7. The blots were washed again 4 times with TBS-T. The western blots were analyzed with the Odyssey® CLx Imaging System (LI-COR Biosciences)

SDS buffer	25 mM tris; 192 mM glycine; 0.1% (w/v) SDS
Towbin buffer	25 mM tris; 192 mM glycine; 20% (v/v) methanol, pH 8

Milk solution	5% powdered milk (w/v) in TBS-T buffer
TBS-T buffer	20 mM tris, 150 mM NaCl, 0.1% tween 20, pH 7.6

2.4.7 Chromatin immunoprecipitation (ChIP)

10⁷ cells were resuspended in 10 mL room temperature warm cell culture medium. The proteins were cross-linked by adding 200 µL of 37% formaldehyde to a final concentration of 0.75 %. The cells were incubated for 10 min under rotation at room temperature. 1,250 µL 1 M Glycine was added to a final concentration of 125 mM to stop the cross-linking. The cell suspension was incubated for 10 min under rotation at room temperature and centrifuged at 1,200 x g for 5 min at 4 °C. The pellet was washed for two times with 20 mL cold PBS and centrifuged at 1,200 x g for 5 min at 4 °C. The cells were resuspended in 500 µL ice-cold 1x buffer A and were transferred into a microcentrifuge tube. The cells were incubated on ice for 10 min and mixed every 3 min by inverting. The nuclei were pelleted by centrifugation at 2,000 x g for 5 min at 4°C. The supernatant was removed, and the pellet was resuspended in 500 µL 1x buffer B. The centrifugation was repeated, and the pellet was resuspended in 100 µL 1x buffer B. 0.1 µL Micrococcal Nuclease (Cell Signaling Technology, Cat.: # 10011) was added and the solution was mixed by inverting. The DNA was digested for 20 min at 37°C with frequent mixing, which resulted in a length of approximately 150-900 bp. The digest was stopped by the addition of 10 µL 0.5 M EDTA and cooled for min on ice. The nuclei were pelleted by centrifugation at 16,000 x g for 3 min at 4°C. The supernatant was removed, and the pellet was resuspended in 200 µL ChIP Lysis Buffer. The nuclei were sonicated in a Bioruptor to break the nuclear membrane (sonication high mode, 3x 30s on / 30s off). The lysate was clarified by centrifugation at 9,400 x g for 10 min at 4°C and stored at -80°C.

Protein G beads had to be prepared before usage. 50 µL protein G beads were washed with 300 µL RIPA buffer in low retention tubes. They were incubated in 270 µL RIPA buffer and 30 µL Roti Block solution for 45 min under rotation at 4°C. The blocking solution was removed, and the beads were resuspended in 300 µL RIPA buffer and stored on ice.

The chromatin immunoprecipitation was performed under rotation overnight at 4°C. 30 µL lysate were mixed with 400 µL RIPA buffer and the appropriate amount of antibodies (see Table 7). 20 µL blocked protein G beads and 5 µL proteinase inhibitor were added. On the next day, the beads were washed 3 times with 600 µL low salt buffer and subsequently 3 times with 600 µL high salt buffer. The DNA was eluted from the beads with 120 µL elution buffer at 1000 rpm shaking for 30 min at 30°C. To reverse the cross-link, 5 µL proteinase K (20 mg/mL) was added to the solution and incubated for 4 hours at 700 rpm shaking at 65°C. The DNA was concentrated with the ChIP DNA Clean & Concentrator Kit (Zymo Research). Quantification of the DNA was performed by ChIP qPCR. The used DNA oligonucleotides are listed in Table 6.

1x buffer A	250µl 4x Buffer A (Cell Signaling Technology, Cat.: # 14282S); 750µl H ₂ O; 0.5µl DTT; Proteinase Inhibitor
1x buffer B	300µl 4x Buffer B (Cell Signaling Technology, Cat.: # 14282S); 900µl H ₂ O; 0.6µl DTT

ChIP Lysis buffer	50 mM HEPES-KOH pH 7.5; 140 mM NaCl; 1 mM EDTA pH 8.0; 1 % Triton-X-100, 1 % sodium deoxycholate; 0.1 % SDS
RIPA buffer	50 mM Tris-HCl pH 8; 150 mM NaCl; 2 mM EDTA pH 8,0; 1 % NP-40; 0,5 % sodium deoxycholate; 0.1 % SDS
Low salt buffer	0.1 % SDS; 1 % Triton-X-100; 2 mM EDTA pH 8; 150 mM NaCl; 20 mM Tris-HCl pH 8
High salt buffer	0,1 % SDS; 1 % Triton-X-100; 2 mM EDTA pH 8; 500 mM NaCl; 20 mM Tris-HCl pH 8
Elution buffer	1 % SDS; 100 mM NaHCO ₃

2.4.8 ChIP sequencing analysis

ChIP-seq data from human K562 cells were retrieved from the ENCODE Project (ENCODE Project Consortium, 2012; Davis et al., 2018). The downloaded Model-based Analysis of ChIP-Seq (MACS) peak coordinates (Zhang et al., 2008) were reduced to a 3 columns BED file format and the Bioconductor package ChIPpeakAnno, version 3.10 (Zhu, 2013) was used for the data analysis. The command line arguments for the R script are shown in supplementary Table 14.

The following Downstream ChIP-seq analysis workflow was used for the gene annotation. The 3 columns BED file was converted to Granges. The Ensembl based annotation package (Rainer et al., 2019) EnsDb.Hsapiens.v75 was likewise converted to Granges and used as genome reference. The binding sites were visualized by analyzing the distribution of the distance of the peaks to the nearest transcription start site (TSS). Peak distribution was calculated for promoters, UTRs, Exons, Introns and intergenic regions. The TxDb.Hsapiens.UCSC.hg19.knownGene package was used as annotation reference. The annotated peak data was used for obtaining enriched Gene Ontology (GO) terms. The human GO gene mapping package “org.Hs.eg.db” was used to obtain the GO annotation.

The Integrative Genomics Viewer (IGV) (Robinson et al., 2011) has been used for visualization of the ChIP-sequencing data. The hg19, Genome Reference Consortium Human Build 37 (GRCh37) was used for functional annotation and gene visualization. All genomic coordinates represent the hg19 genome version. The accession numbers of the analyzed sequencing experiments from the ENCODE Project are listed in Table 11.

Table 11: Analyzed ChIP-sequencing experiments with the corresponding encode accession numbers.

Target	Biosample	Accession
LEF1	K562	ENCSR343ELW; ENCSR832OGB
TCF7	K562	ENCSR863KUB
TCF7L2	K562	ENCSR888XZK
TAL1	K562	ENCSR000EHB
GATA2	K562	ENCSR000EWG
LEF1	HEK293T	ENCSR240XWM

2.5 Identification of novel PRMT6 interaction partners

The main work of this project is based on the search for novel interaction partners of the protein arginine N-methyltransferase 6 (PRMT6). This was achieved with combined Co-Streptavidin Precipitation (Co-SP) with subsequent Stable Isotope Labeling with Amino acids in Cell culture (SILAC). This technique was successfully used to identify interacting transcription factors of the peptidyl arginine deiminase IV (PADI4) in erythroleukemic cells (Kolodziej et al., 2014). Co-SP was combined with SILAC in this project to use PRMT6 as bait to identify new hematopoietic transcription factors in erythroleukemic cells. The flow diagram in Figure 18 shows the schematic workflow of the project.

The cDNA of human PRMT6 was amplified by PCR from erythroleukemic K562 cells. The transcript was cloned into the pRRLsAviMCS vector, fusing PRMT6 with the 14 amino acid long AVI (avidin) tag (DSQKMEWRSNAGGS) at its N-terminus. The vector also contains the *E. coli* biotin holoenzyme synthetase (BirA). This enzyme biotinylates the AVI tag of PRMT6, allowing the purification with streptavidin. Further the vector contains an ampicillin resistance for positive selection in *E. coli* and a GFP marker for flow cytometer analysis and positive selection. The hPRMT6-pRRLsAviMCS vector was transiently transfected into HEK293T cells for virus production with the pMD2.G packaging plasmid and the pCMVdelta8.91 packaging plasmid. The lentiviral particles were concentrated via ultracentrifugation. Erythroleukemic K562 cells were transduced with the lentiviral particles and the GFP expression was measured via flow cytometer. The expression of Bio-PRMT6 was analyzed by reverse transcription PCR and Western Blot.

The successfully transduced K562 cells were incubated in RPMI SILAC medium and labeled with $^{13}\text{C}_6$, $^{15}\text{N}_4$ -L arginine (Arg-10) and $^{13}\text{C}_6$, $^{15}\text{N}_2$ -L-lysine (Lys-8). These non-radioactive isotopes allow the later analysis with mass spectrometry. The nuclei of the K562 cells were isolated. PRMT6 is solely present in the nucleus; the cytoplasmatic proteins were excluded in this step. The PRMT6 protein complexes which are located in the nucleus were isolated with biotin-tag affinity purification with streptavidin beads. The concentrated protein complexes were frozen at -80°C and transferred to the work group of Prof. Dr. Thomas Oellerich at the university clinic of Frankfurt. Liquid-Chromatography Mass Spectrometry (LC-MS/MS) analysis was performed and potential interaction partners were identified with MaxQuant protein identification. Proteins with a SILAC ratio >2 were chosen for further analysis. Functional Annotation Clustering of the identified PRMT6 interactome was performed to identify proteins with similar characteristics; The Database for Annotation, Visualization and Integrated Discovery (DAVID) v6.8 was used for Functional Annotation Clustering (Huang et al., 2009a, 2009b). The network analysis protein interaction data was performed with a literature analysis. The newly identified interaction partners of PRMT6 were verified with Co-Streptavidin precipitation in HEK293T cells. The biotin tagged PRMT6 was used as bait and overexpressed via transient transfection. The bait protein was co-transfected. Co-Streptavidin precipitation was performed on whole cell lysates. The interaction was verified via Western Blot. The verified interaction partners were further analyzed for their influence on hematopoiesis together with PRMT6.

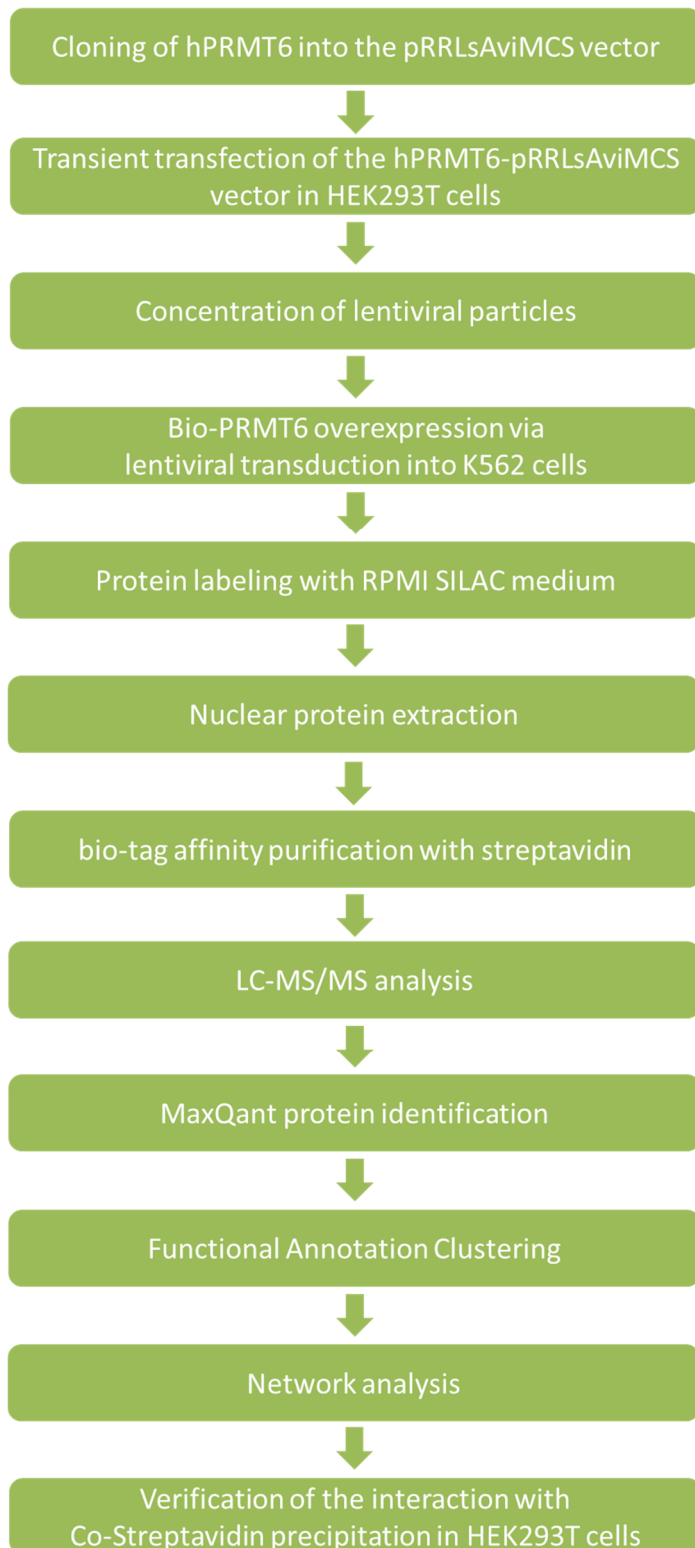


Figure 18: The flow diagram shows the schematic procedure of the identification of novel PRMT6 interaction partners: hPRMT6 was cloned into the pRRLsAviMCS vector and transiently transfected into HEK293T cells. Lentiviral particles were produced and concentrated Bio-PRMT6 was overexpressed via lentiviral transduction in erythroleukemic K562 cells. The proteins were labeled with RPMI SILAC medium and nuclear proteins were extracted. The biotin tagged PRMT6 protein complexes were purified with streptavidin beads. LC-MS/MS analysis was performed and MaxQant protein identification was used to identify the interacting proteins. Functional Annotation Clustering and protein network analysis was utilized to identify protein interaction networks. The newly identified interaction partners were verified Co-Streptavidin precipitation in HEK293T cells.

3 Results

3.1 PRMT6 is important in megakaryocytic and erythroid differentiation

The protein arginine methyltransferase 6 (PRMT6) was identified as a central functional component of an important corepressor complex in hematopoietic progenitor cells (Herglotz et al., 2013). PRMT6 is recruited to promoters of megakaryocytic genes in these progenitor cells and performs asymmetric histone H3 arginine 2 dimethylation (H3R2me2a), resulting in the downregulation of these genes. The importance of PRMT6 was also identified on erythroid genes in hematopoietic progenitor cells (Herkt et al., 2018). Here PRMT6 downregulates the erythroid genes by being recruited to the promoter by transcription factors.

PRMT6 is recruited by the transcription factor RUNX1 to the promoters of the megakaryocytic and erythroid genes in hematopoietic progenitor cells (Herglotz et al., 2013; Herkt et al., 2018). Transcription factors control hematopoietic differentiation in an orchestrated interaction of different factors. A genome-wide analysis identified that GATA1, GATA2, RUNX1, FLI1 and TAL1 simultaneously bind to several promoters of genes controlling the hematopoietic differentiation (Doré and Crispino, 2011; Tijssen et al., 2011).

The protein arginine N-methyltransferase 6 (PRMT6) was used in this project to identify other transcription factors besides RUNX1, which control the hematopoietic differentiation with PRMT6 as a central functional component as corepressor.

3.2 Identification of novel PRMT6 interaction partners

To identify new interaction partners of the protein arginine N-methyltransferase 6 (PRMT6), affinity purification was performed. The full length PRMT6 gene was fused with the 14 amino acid long AVI (avidin)-tag (DSQKMEWRSNAGGS). The *E. coli* biotin holoenzyme synthetase (BirA) (Samols et al., 1988) was used as a biotin ligase recognizing the AVI-tag for biotinylation. Both enzymes were inserted into the genome of the erythroleukemia K562 cell line. The pRRLsAvi-MCS-iGFP-BirA vector was used for the lentiviral transduction. A schematic overview of the combined Co-Streptavidin Precipitation (Co-SP) with the subsequent Stable Isotope Labeling with Amino acids in Cell culture (SILAC) (Ong et al., 2002) is shown in Figure 19. The biotinylated Bio-PRMT6 was purified with streptavidin-coupled Dynabeads. The empty vector without the PRMT6 gene was used as a control.

The Bio-PRMT6 expressing cell line was incubated in RPMI-medium with $^{13}\text{C}_6$, $^{15}\text{N}_4$ -L arginine (Arg-10) and $^{13}\text{C}_6$, $^{15}\text{N}_2$ -L-lysine (Lys-8) and the negative control in medium containing unlabeled L arginine and L-lysine. The non-radioactive isotopic labeled amino acids were incorporated in the cell proteome. Tandem mass spectrometry was performed to identify the differences in the abundance of proteins by higher mass-to-charge ratio (m/z). This allowed identifying PRMT6 interacting proteins after streptavidin pull-down.

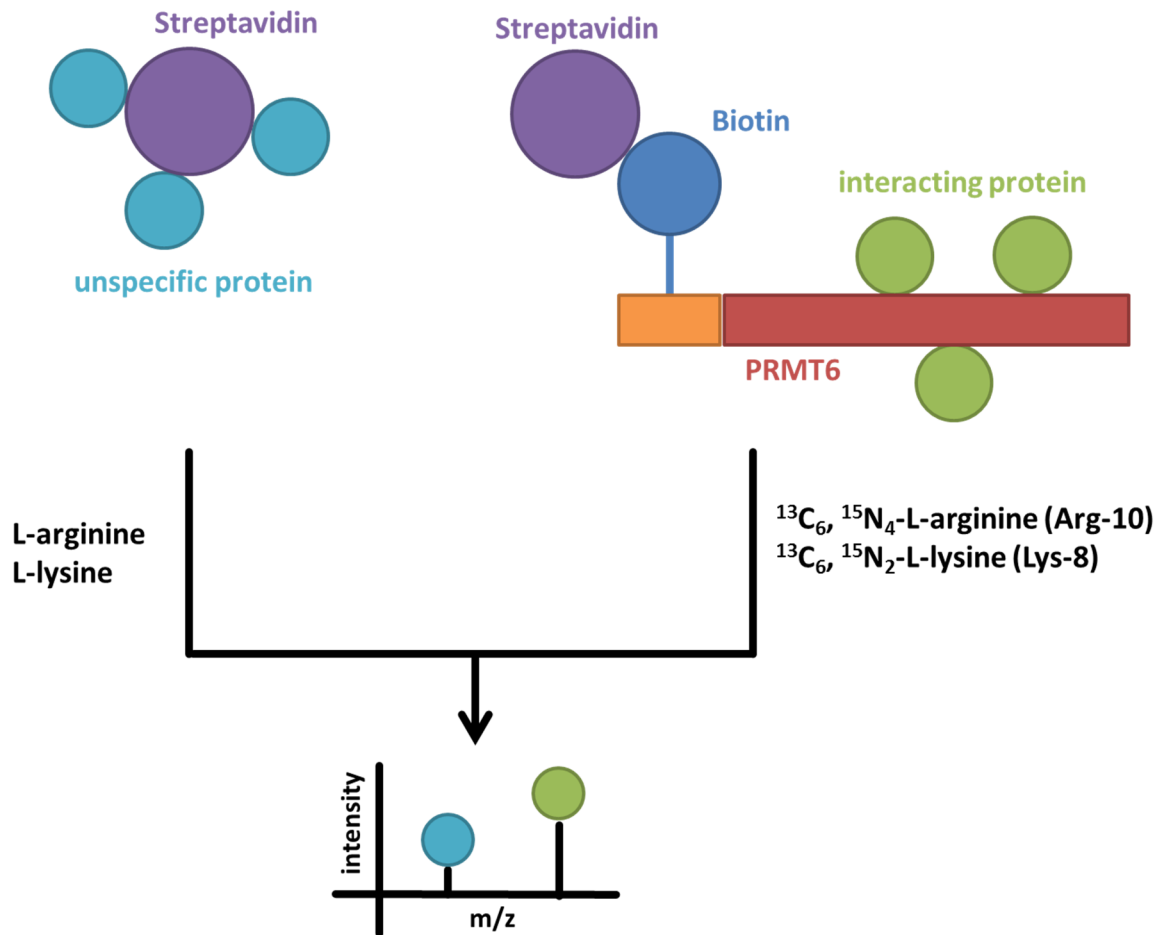


Figure 19: Schematic overview of combined Co-Streptavidin Precipitation (Co-SP) with subsequent Stable Isotope Labeling with Amino acids in Cell culture (SILAC). The full length PRMT6 gene (shown in red, 376 aa) was fused at the amino terminus with an Avi/Biotin tag (shown in orange, 14 aa). The resulting Avi-PRMT6 gene was co-expressed with the BirA ligase, catalyzing the biotinylation of the Avi tag. This allows the purification of Bio-PRMT6 with Stredavidin. Both genes were inserted into the genome of K562 cells through lentiviral transduction with the pRRLsAvi-MCS-iGFP-BirA vector. An empty vector transduction without the PRMT6 insert was used as a negative control which was cultivated in light SILAC RPMI medium with unlabeled L arginine and L lysine. The Bio-PRMT6 overexpressing K562 cell line was cultivated in the heavy SILAC RPMI medium with labeled L arginine (arg-10) and L lysine (lys-8). The labeled Bio-PRMT6 protein was precipitated via streptavidin pull-down and subjected to mass spectrometry. Interacting proteins (shown in green) were identified by higher mass-to-charge ratio (m/z). Unspecific proteins (shown in aquamarine) were excluded by lower m/z. The peak intensity correlates to the protein amount.

In order to identify novel transcription factors which recruit the enzyme PRMT6, several hematopoietic cell lines were analyzed for PRMT6 expression (Figure 20). PRMT6 is expressed in the erythroleukemia cells lines K562, HEL and TF-1. The T-ALL Jurkat cell line and the AML cell lines U937 and Kasumi also show PRMT6 expression. All tested cell lines show PRMT6 expression, supporting the importance of this ubiquitous enzyme.

PRMT6 shows high expression in the erythroleukemia K562 cell line. In K562 cells the enzyme is recruited to target genes of hematopoietic differentiation by the transcription factor RUNX1. This is shown for megakaryocytic genes (Herglotz et al., 2013) and erythroid genes (Kuvardina et al., 2015). These publications demonstrate that PRMT6 shows an immense influence on hematopoietic

differentiation in K562 cells for which this cell line was chosen for further research, also regarding its sufficiently high expression in this cell line.

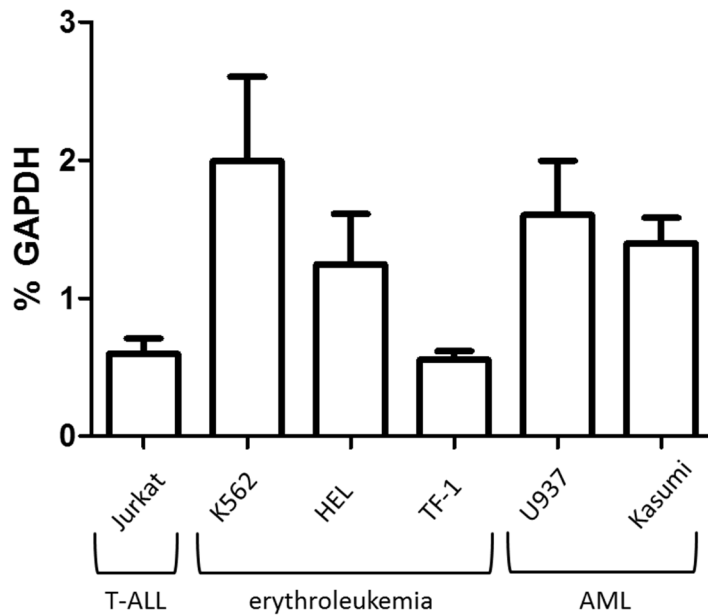


Figure 20: RNA expression of PRMT6 in different hematopoietic cell lines. Jurkat cells are a T-ALL (acute lymphoblastic leukemia) cell line; K562, HEL and TF-1 cells belong to the erythroleukemia cell lines. U937 and Kasumi cell lines belong to the AML (acute myeloid leukemia) cell lines. All show comparable PRMT6 expression, PRMT6 is a ubiquitous enzyme in all tested cell lines. The expression was normalized to the reference gene GAPDH. The error bars represent the standard deviations of at least 3 independent measurements.

The Biotin tagged PRMT6 was introduced into the K562 genome via lentiviral transduction. The overexpression of PRMT6 was confirmed with GFP expression by flow cytometry after 7 days of cultivation. The mRNA and protein measurements are shown in Figure 21. The transduction of Bio-PRMT6 led to 90-fold increased mRNA levels, replacing nearly all untagged enzyme with the tagged enzyme in the nuclei of the K562 cells. The Western blot shows a similar highly increased protein amount of PRMT6. The empty vector transduction did not lead to an increased protein level. Therefore, the empty vector serves as a suitable negative control similar to untransduced cells. The PRMT6 overexpressing K562 cell line was used for the further interactome analysis.

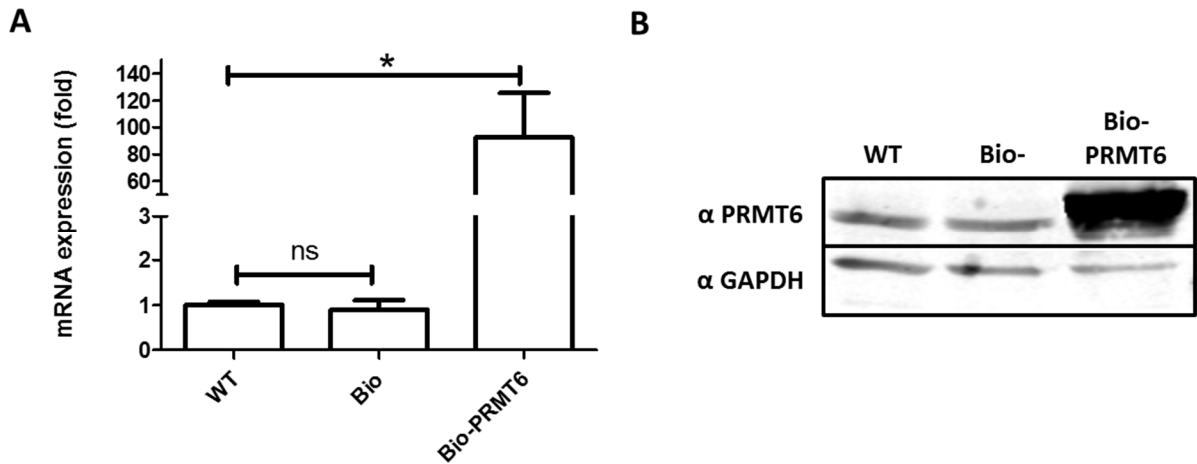


Figure 21: (A) RNA expression of PRMT6 in transduced K562 cells. The empty vector transduction without the PRMT6 insert (Bio-) was used as a negative control and shows comparable PRMT6 expression to the untransduced wild type (WT). The Bio-PRMT6 overexpressing K562 cell line shows over 90-fold PRMT6 expression. The expression was normalized to the reference gene GAPDH. **(B)** Western blot of the transduced K562 cells. Like the RNA expression analysis, the protein amount of PRMT6 is similar in wild type and negative control (Bio-). The Bio-PRMT6 overexpressing K562 cell line shows a high amount of PRMT6 protein. The error bars represent the standard deviations of at least 3 independent measurements. The p-values were calculated using Student's t-test. *p < 0.05, ns: not significant.

In order to use the biotin tagged PRMT6 protein for the identification of novel transcription factors, the streptavidin precipitation needed to be optimized for the PRMT6 protein. The aim of the experiment was to maximize the reduction of the binding of background proteins to the streptavidin beads. On the other hand, it had to be ensured that enough beads were used to extract sufficient amounts of biotin tagged PRMT6 protein. About 1 mg of M-280 streptavidin Dynabeads are able to bind around 200 pMol biotinylated peptide. An increasing amount of 50 µg, 250 µg and 500 µg streptavidin Dynabeads was tested for pulldowns with nuclear lysates from 10⁷ K562 cells each.

The pulldown of biotinylated PRMT6 with 50 µg beads from 10⁷ K562 cells effectively precipitated PRMT6 together with the transcription factor RUNX1 (Figure 22 A). The empty vector control showed no PRMT6 or RUNX1 precipitation, which is shown in the red quadrat. The interaction between PRMT6 and RUNX1 is crucial for the erythroid and megakaryocytic development of K562 cells (Herglotz et al., 2013; Kuvardina et al., 2015); (Herkt et al., 2018). Therefore, the streptavidin biotin pulldown of overexpressed PRMT6 was used to detect endogenously expressed hematopoietic transcription factors.

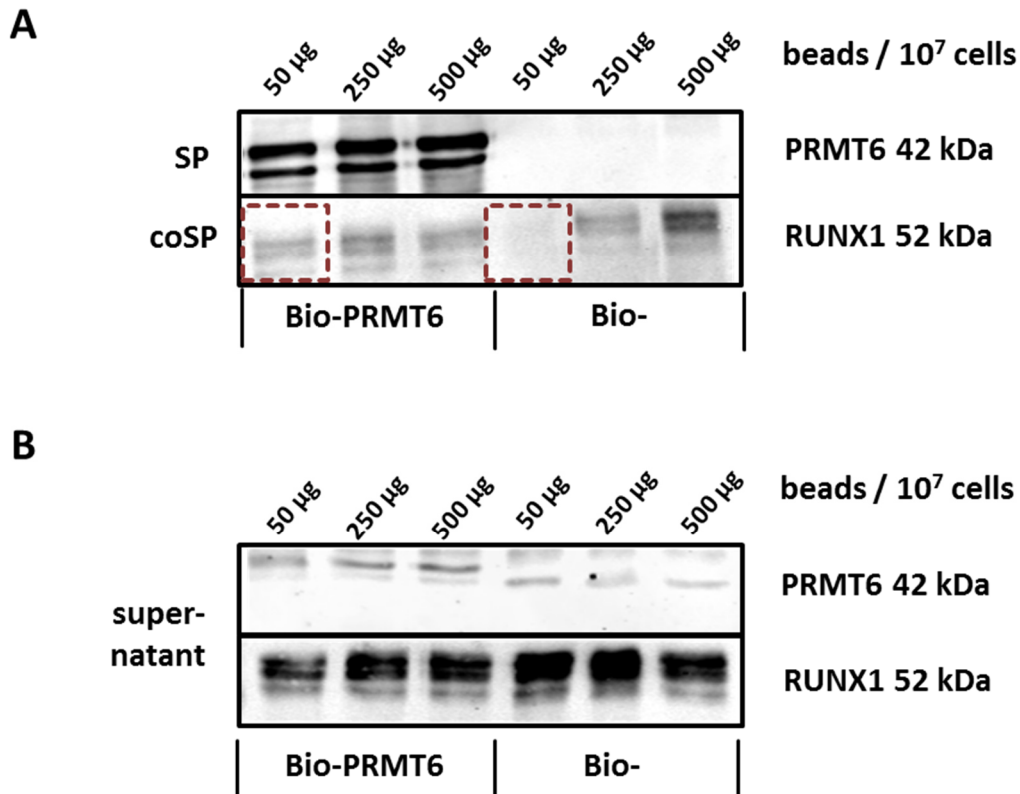


Figure 22: A: Western Blot showing the Co-Streptavidin Precipitation (Co-SP) of biotinylated PRMT6 protein (Bio-PRMT6) from stable transduced K562 cells is shown on the left. The empty vector control is shown on the right (Bio-). An increasing amount of streptavidin beads was used to precipitate the PRMT6 protein from nuclear lysates of 10^7 K562 cells. Increasing the streptavidin beads up to 250 and 500 μg does not lead to increased PRMT6 precipitation. An amount of 50 μg of beads is sufficient for 10^7 K562 cells. The pull down with 50 μg beads allows the Co-Precipitation of endogenous RUNX1 protein, which is not visible in the empty vector control (red quadrat). An increased amount of beads (250 and 500 μg) leads to unspecific binding of RUNX1 in the empty vector control. **B:** The western blot of the supernatant of the precipitation shows that all Bio-PRMT6 protein was pulled from the sample, independent of the bead concentration. All samples show a high concentration of RUNX1 protein.

The experiment showed that the increased amounts of streptavidin Dynabeads did not increase PRMT6 precipitation. Therefore, the amount of 50 μg Dynabeads is sufficient for 10^7 K562 cells. The pulldown of 50 μg Dynabeads showed no PRMT6 residues in the supernatant (Figure 22 B). But increasing the amounts of Dynabeads to 250 and 500 μg led to unspecific binding of RUNX1 to the Dynabeads. Therefore, the amount of Dynabeads should not be increased.

The gained information was used to optimize the ratio between streptavidin Dynabeads, and the biotin tagged PRMT6 overexpressing K562 cells. Finally, PRMT6 was extracted from the nuclear lysates of 10^8 Bio- PRMT6 K562 cells which were mixed with 250 μg beads in five tubes. 10^8 Bio- K562 cells were used as negative control. After the pull down, both samples were collected in a single tube and transferred to the group of Prof. Dr. Thomas Oellerich which performed the quantitative analysis by mass spectrometry.

3.3 PRMT6 interactome functional annotation

The quantitative analysis by mass spectrometry was used to identify unique peptide sequences together with their relative abundance in the nucleus. This information can be used to identify unique proteins which are overrepresented in the analyzed sample. These overrepresented proteins are likely to be interacting proteins of PRMT6, possible cofactors of the enzyme, like transcription factors. The raw data of the PRMT6 interactome were analyzed with the MaxQant software (version 1.5.2.8). 177 interaction partners with a normalized H/L ratio of > 2 were identified as possible members of the PRMT6 interactome. The list of these identified proteins is shown in the supplemental Table 15.

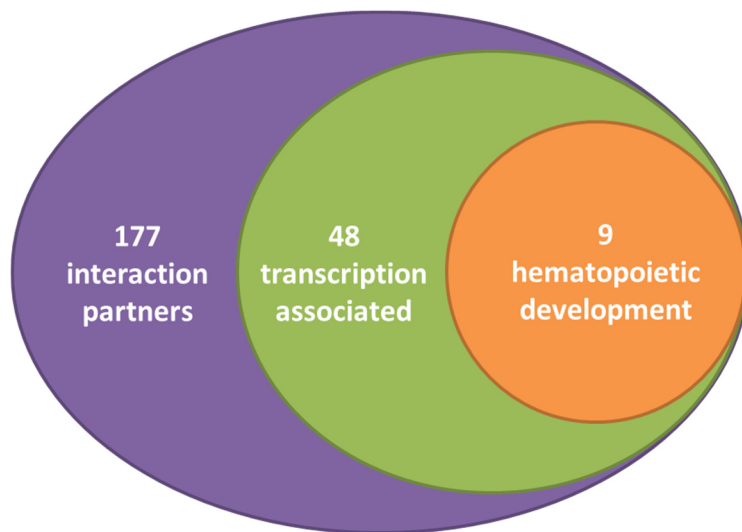


Figure 23: The PRMT6 interactome; The Database for Annotation, Visualization and Integrated Discovery (DAVID) v6.8 was used for Functional Annotation Clustering (Huang et al., 2009a, 2009b). From 177 possible interaction partners, 48 proteins are annotated to be associated with transcription, 9 of these proteins are annotated to be involved in hematopoietic or lymphoid organ development.

Functional Annotation Clustering was performed with the Database for Annotation, Visualization and Integrated Discovery (DAVID) v6.8 (Huang et al., 2009a, 2009b). The analysis confirmed that the subcellular distribution of PRMT6 is in the nucleus (Herrmann et al., 2009); three-fourths (132 of 177) of its interacting proteins were annotated with function and localization in the nucleus, PRMT6 is therefore mostly located in the nuclei of K562 cells. One third of these proteins (48 hits) are associated with transcription, like transcription factors or histone modifying enzymes, supporting the epigenetic role of PRMT6 in histone modification. 9 of these proteins are annotated to be involved in hematopoietic or lymphoid organ development. The Euler diagram of these relations is shown in Figure 23.

The 9 transcription associated proteins which are involved in hematopoietic or lymphoid organ development are shown in Figure 24 and Table 12. The p-value of the enriched GO-term is 1.20E-03. The identified transcription factors which interact with PRMT6 are GATA2, SOX6, RUNX1, KLF1. All of these transcription factors are crucial for the erythroid and megakaryocytic differentiation (Perkins et al., 1995; Cantù et al., 2011; Doré and Crispino, 2011; Tijssen et al., 2011). PRMT6 plays an important role in the megakaryocytic-erythroid bifurcation, facilitated by the transcription factor RUNX1

(Herglotz et al., 2013; Kuvardina et al., 2015; Herkt et al., 2018). This interaction was verified with the mass spectrometry interactome analysis of PRMT6 in K562 cells. Further the histone methyltransferase PRMT1 is a known interaction partner of PRMT6 (Thomas et al., 2010) which is also important for erythroid and megakaryocytic differentiation (Hua et al., 2013).

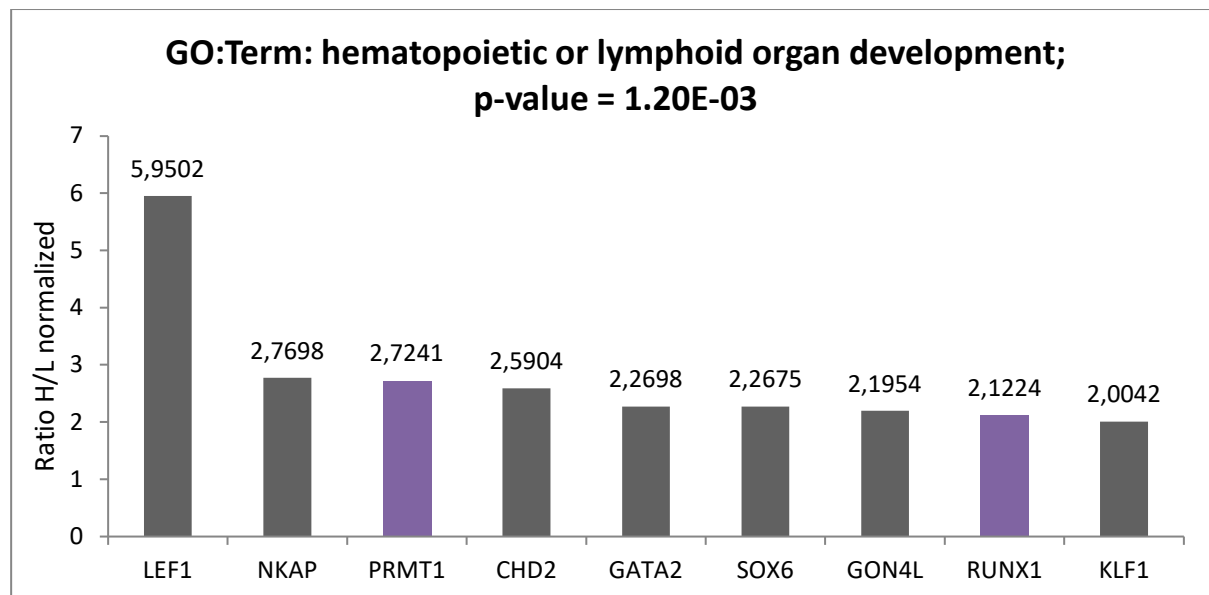


Figure 24: Functional Annotation Clustering of the PRMT6 interactome identified 9 proteins with functionality in transcription and hematopoietic or lymphoid organ development. The already published interaction partners of PRMT6 are shown in purple; PRMT1 (Thomas et al., 2010) and RUNX1 (Herglotz et al., 2013).

The transcription factor LEF1 shows the highest normalized enrichment with an H/L ratio of 5.9502. This factor has a crucial role in lymphopoiesis, essential in T-and B-cell differentiation. Pre-B and T lymphocytes of adult mice express the transcription factor (van Genderen et al., 1994). LEF1 regulates T cell differentiation (Okamura et al., 1998) and B lymphocyte proliferation (Reya et al., 2000). The influence of this factor to erythroid and megakaryocytic differentiation is not known and therefore LEF1 was chosen for further research.

Table 12: List of the 9 proteins with annotation in hematopoietic or lymphoid organ development

Gene symbol	Ratio H/L normalized	Name
LEF1	5,9502	lymphoid enhancer binding factor 1
NKAP	2,7698	NF-kappa-B-activating protein
PRMT1	2,7241	Protein arginine methyltransferase 1
CHD2	2,5904	chromodomain helicase DNA binding protein 2
GATA2	2,2698	GATA binding protein 2
SOX6	2,2675	SRY-box transcription factor 6
GON4L	2,1954	gon-4 like
RUNX1	2,1224	RUNX family transcription factor 1
KLF1	2,0042	Kruppel like factor 1

3.4 Network analysis of protein interaction data

A protein interaction analysis revealed that the newly identified factors are embedded into an interaction network which is shown in Figure 25. The possible interaction of LEF1, SOX6 and GATA2 with PRMT6 has been revealed in this work, shown with red edges. The interaction of PRMT1 and PRMT6 is suggested in (Thomas et al., 2010) and the interaction of RUNX1 with PRMT6 was revealed in (Herglotz et al., 2013), shown with purple edges. Further RUNX1 shows to be centered in this interaction network by interacting also with GATA2 (Pippa et al., 2017) and with PRMT1 (Zhao et al., 2008).

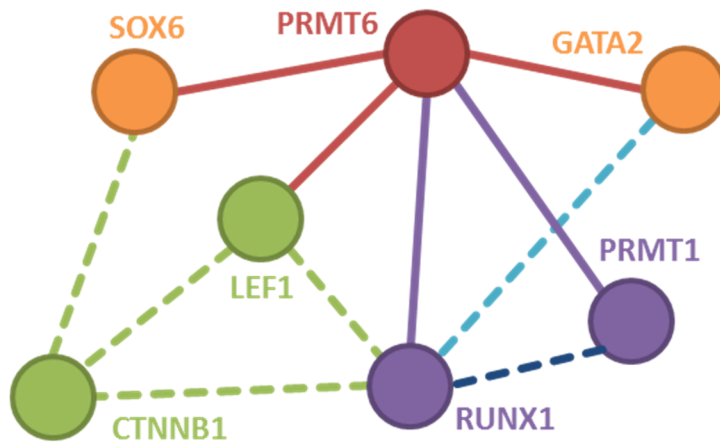


Figure 25: Analysis of PRMT6 protein network. The red conjunctions show newly identified interacting proteins: LEF1, SOX6 and GATA2. The interaction of PRMT6 with PRMT1 (Thomas et al., 2010) and RUNX1 (Herglotz et al., 2013) has been verified. The transcription factors SOX6, LEF1 and RUNX1 share β -catenin as interacting protein, shown in green (Iguchi et al., 2007), (Huber et al., 1996), (Li et al., 2019). The protein network is further supported by LEF1-RUNX1 interaction (Kahler and Westendorf, 2003), (Levanon et al., 1998); PRMT1-RUNX1 interaction (Zhao et al., 2008) and RUNX1-GATA2 interaction (Pippa et al., 2017).

The Wnt signaling factor LEF1 interacts with RUNX1 (Levanon et al., 1998; Kahler and Westendorf, 2003). The Wnt factor β -catenin on the other hand interacts with three different PRMT6 associated transcription factors: It interacts with LEF1 (Huber et al., 1996), SOX6 (Iguchi et al., 2007) and RUNX1 (Li et al., 2019). LEF1 is a central node in this network and was chosen for further analysis and protein interaction verification. LEF1 is important in lymphopoiesis and essential in T-and B-cell differentiation factor (van Genderen et al., 1994).

3.5 Verification of the LEF1-PRMT6 protein interaction with Co-Streptavidin Precipitation

To verify the newly identified interaction between PRMT6 and LEF1, Co-Streptavidin precipitation (Co-SP) was performed in HEK293T cells. A plasmid containing the human cDNA of the prey protein was co-transfected with a plasmid containing the human cDNA of the bio-tagged bait. Whole cell lysates were produced after 48 h of incubation after transfection. Additionally, to the overexpression of Bio-PRMT6 in K562 cells, the tagged enzyme was overexpressed together with the LEF1. The streptavidin pulldown revealed a strong binding of LEF1 with PRMT6, confirming the mass spectrometry experiment. The western blot of the pull down is shown in Figure 26 A.

Several nodes of the identified LEF1 PRMT6 protein network (see Figure 25) were confirmed with Co-SP. Of special interest was the verification of the RUNX1 interactions. RUNX1 recruits PRMT6 to hematopoietic promoters and represses gene expression at that loci (Herglotz et al., 2013). Bio-PRMT6 and RUNX1 were co-transfected in HEK293T cells. RUNX1 was co-precipitated after PRMT6 pull down (Figure 26 B).

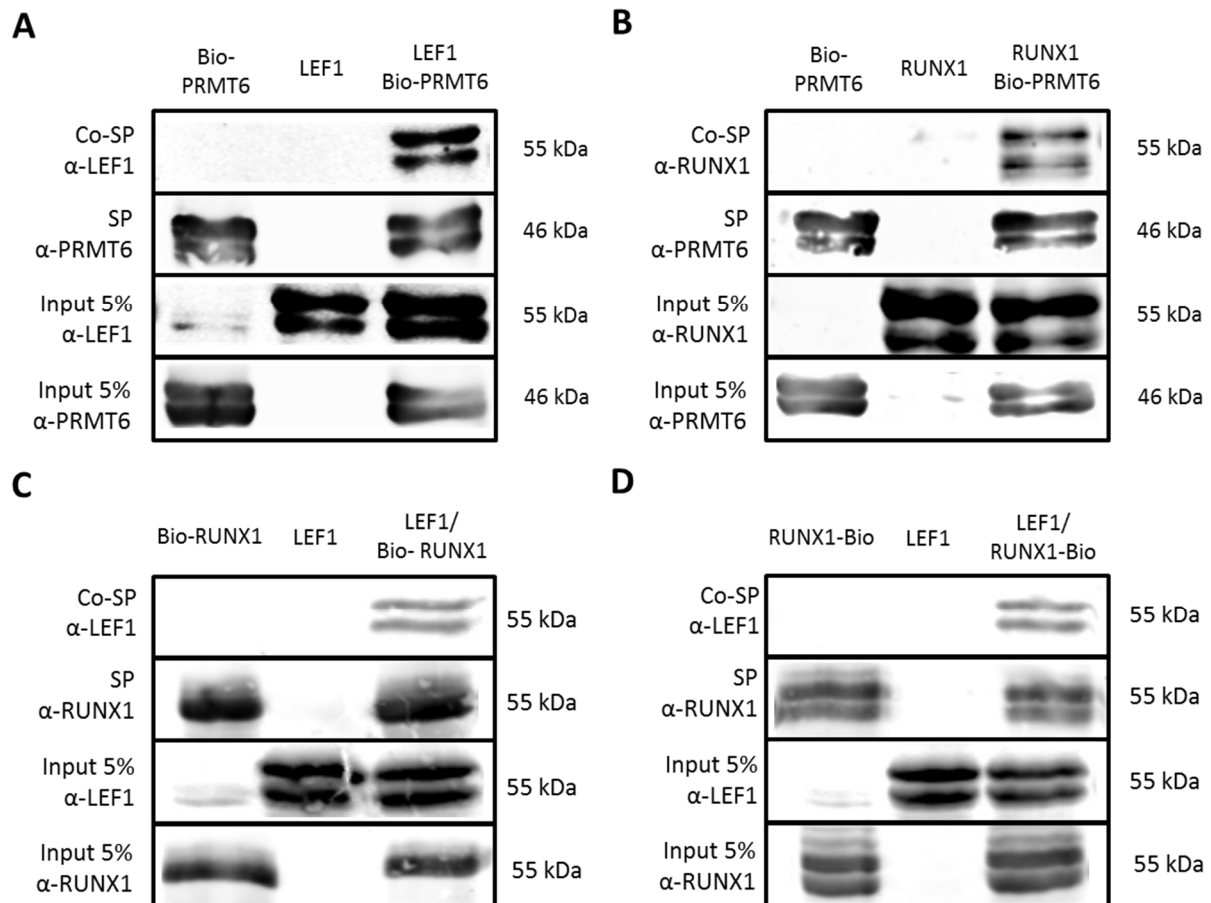


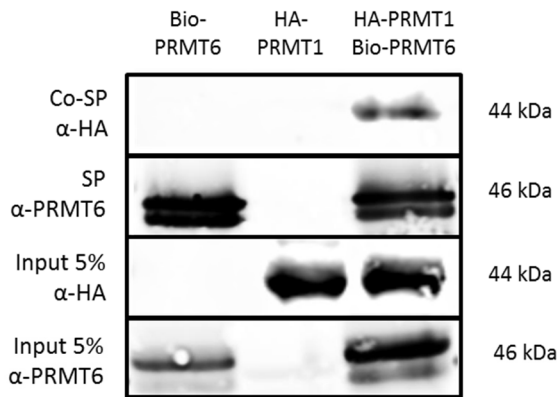
Figure 26: Protein interactions of the identified protein network were verified with Co-Streptavidin Precipitation (Co-SP). Bio-tagged bait-protein was co-transfected with unmodified prey-protein expression vector into HEK293T cells. (A) Co-SP of PRMT6 and LEF1. PRMT6 was pulled out from extracts with streptavidin beads (SP). Co-precipitation of LEF1 was detected with an anti-LEF1 antibody (upper lane, Co-SP). (B) Co-SP of PRMT6 and RUNX1. PRMT6 was pulled out from extracts with streptavidin beads (SP). Co-precipitation of RUNX1 was detected with an anti-RUNX1 antibody (upper lane, Co-SP). (C and D) Co-SP of RUNX1 and LEF1. RUNX1 was pulled out from extracts with streptavidin beads (SP). Co-precipitation of LEF1 was detected with anti-LEF1 antibody (upper lane, Co-SP).

The interaction of RUNX1 and LEF1 (Kahler and Westendorf, 2003) was reevaluated in this experiment. In order to analyze the interaction between LEF1 and RUNX1, biotinylated RUNX1 protein was used. Similar to PRMT6, the full length RUNX1 gene was fused with the 14 amino acid long AVI-tag to allow its biotinylation by the BirA ligase. The AVI-tag was fused N-terminal (Bio-RUNX1) and C-terminal (RUNX1-Bio). The Streptavidin pulldown let in both cases to the co-precipitation of overexpressed LEF1 protein (Figure 26C and D). C or N-terminal fusion of the AVI-tag peptide does not affect cofactor binding.

The PRMT6 interactome analysis showed that PRMT1 is an interaction partner of PRMT6. Both proteins are histone modifying enzymes, PRMT1 methylates H4R3, activating gene expression and PRMT6 methylates H3R2, repressing gene expression (Litt et al., 2009; Yang and Bedford, 2013). PRMT6 and PRMT1 are similar in size (375 aa and 316 aa, respectively). Both share the same conserved catalytic domains (Figure 5); (Yang and Bedford, 2013). PRMT6 itself is known to homodimerize and performs automethylation at arginine R35 at its homodimerization partner (Singhroy et al., 2013). This modification enhances the protein stability. Förster resonance energy transfer measurements showed a possible heterodimerization between PRMT1 and PRMT6 (Thomas et al., 2010).

The PRMT6 and PRMT1 interaction was verified by co-transfection of Bio-PRMT6 and HA-PRMT1 in HEK293T cells. HA-PRMT1 was co-precipitated after the PRMT6 pull down (Figure 27 A). This experiment shows that overexpressed PRMT6 is able to heterodimerize with other overexpressed PRMTs. The similarity of PRMT1 and PRMT6 was analyzed with a protein alignment. PRMT6 itself homodimerizes, this opens the possibility that it also performs heterodimerization with homologs by the binding of similar protein domains. The alignment of PRMT6 and PRMT1 shows a percentage identity of 31.94 %, with conserved catalytic domains (Figure 27 B).

A



B

```

PRMT6  MSQPKK-----RKLESGGGGEGEGTEEEEDGAEREAAALRPRRTKRERDQLYYECYSDV  54
PRMT1  MAAAEAANCIMENFVATLANGMSLQPPLLEEVSCGQAESSEKPNaedMTSKDYFDSYAHF  60
      * :      . : : . * . :      * * . . : : * : * . . : : * : * . .
      Motif I                               Motif post I

PRMT6  SVHEEMIADRVRTDAYRLGILRNWAALRGKTVLDVGAGTGILSIFCAQAGARRVYAVEAS  114
PRMT1  GIHEEMLKDEVRTLTYRNSMFHNRHLFKDKVLDVGS GTGILCMFAAKAGARKVIGIECS  120
      . : * * * * : * * * * : * * . : : * : * * * * * * * * * * * * * * *
      Motif II double E motif

PRMT6  AIWQQAREVVRFNGLIEDRVHVLPGPVETVELPE-QVDAIVSEWMGYLLHESMLSSVLHA  173
PRMT1  SISDYAVKIVKANKLDHVVTIIGKGV EVELPVEKVDIIISEWMGYCLFYESMLNTVLYA  180
      . * : * : * : * : * : * * * * * * * * * * * * * * * * * * * * *
      Motif III

PRMT6  RTKWLKEGGLLPASAELFIAPISDQ-MLEWRLGFWSQVKQHYGVDMSCLEGFATRCLMG  232
PRMT1  RDKWLAPDGLIFPDRATLYVTAIEDRQYKDYKIHWWEN---VYGFDMSCIKDVAIKEPLV  237
      * * * * * * * * * * * * * * * * * * * * * * * * * * * * * * *
      THW loop

PRMT6  QVTFPGGESEKPLVLSTSPFHPATHWKQALLYLNEPVQVEQD TDVSGEITLLPSRDNPRR  352
PRMT1  NIEFTRC--HKRTGFSTSPESPYTHWKQTVFYMEDYLTVKTGEEIFGTIGMRPNAKNNRD  346
      : : *      . * : * * * * * * * * * * * * * * * * * * * * * * *
      * * * * * * * * * * * * * * * * * * * * * * * * * * * * * * *

PRMT6  LRVLLRYKVG DQEE---KTKDFAMED  375
PRMT1  LDFIDLDFKGLCELSCSTDYRMR-  371
      * . : . . *      . : * : *
  
```

Figure 27: (A) Protein interactions of the identified protein network were verified with Co-Streptavidin Precipitation (Co-SP). Avi-tagged bait-protein was co-transfected with HA-tagged prey expression vector into HEK293T cells. Co-SP of PRMT6 and PRMT1: PRMT6 was pulled out from extracts with Streptavidin beads (SP). Co precipitation of PRMT1 was detected with an anti HA antibody (upper lane, Co-SP). (B) The Clustal Omega protein alignment of PRMT1 and PRMT6 is shown. The UniProt IDs are: Q96LA8 (PRMT6) and Q99873 (PRMT1). The percentage identity of the amino acid alignment is 31.94 %. The conserved catalytic domains are shown in red; modified from (Yang et al., 2015).

3.6 PRMT6 TOP-flash assay

The previous experiment confirmed the interaction of LEF1 and PRMT6. Luciferase reporter assays were performed to further study the binding of the histone modifier PRMT6 to the DNA binding LEF1 transcription factor. Together both factors were analyzed if they affect promoters with LEF1 DNA binding motives.

The TOP-flash assay is a widely used method to measure Wnt signaling *in vivo* and *in vitro* (Molenaar et al., 1996). The TCF/LEF1 consensus site was cloned in front of the *luciferase* gene in order to measure Wnt signaling by luciferase assay. The M50 Super 8x TOPFlash (Veeman et al., 2003) vector was used for the experiment; the mutated M51 Super 8x FOPFlash was used as a negative control (see Figure 28 A). This artificial promoter consists of 7 times the TCF/LEF1 consensus site AGATCAAAGG. The negative control consists of 6 times the mutated consensus site AGGCCAAAGG. LEF1 and constantly active β -catenin were co-transfected to activate the reporter gene. This system was used to identify the impact of PRMT6 on LEF1.

The TOP/FOP ratio of the empty transduction without any factors was 1.28, showing weak endogenous induction of Wnt-Signaling in the HEK293T cell culture system. The TOP/FOP ratio with over expressed LEF1 was 2.20; with constantly active β -catenin it was 2.26 and with PRMT6 it was 1.88. Overexpression of LEF1 and constantly active β -catenin led to the highest TOP/FOP ratio of 8.69. In this case LEF1 and β -catenin are not degraded and recruit epigenetic activators to the promoter resulting in the highest activation of the TOP-flash reporter.

The impact of PRMT6 was analyzed by the addition of an increased amount of PRMT6 vector to the LEF1/ β -catenin overexpression. The co-transfection of 250 ng PRMT6 vector led to a reduction of the TOP/FOP ratio to 7.00. Amounts of 500 ng and 1.000 ng PRMT6 vector led to ratios of 2.73 and 2.02 respectively. The TOP/FOP luciferase assay showed that PRMT6 is directly binding to the transcription factor LEF1. An increased amount of PRMT6 protein directly displaces the constantly active β -catenin from the LEF1 transcription factor and thereby represses the gene expression of the luciferase reporter. The displacement of β -catenin by PRMT6 occurs in a dose-dependent manner.

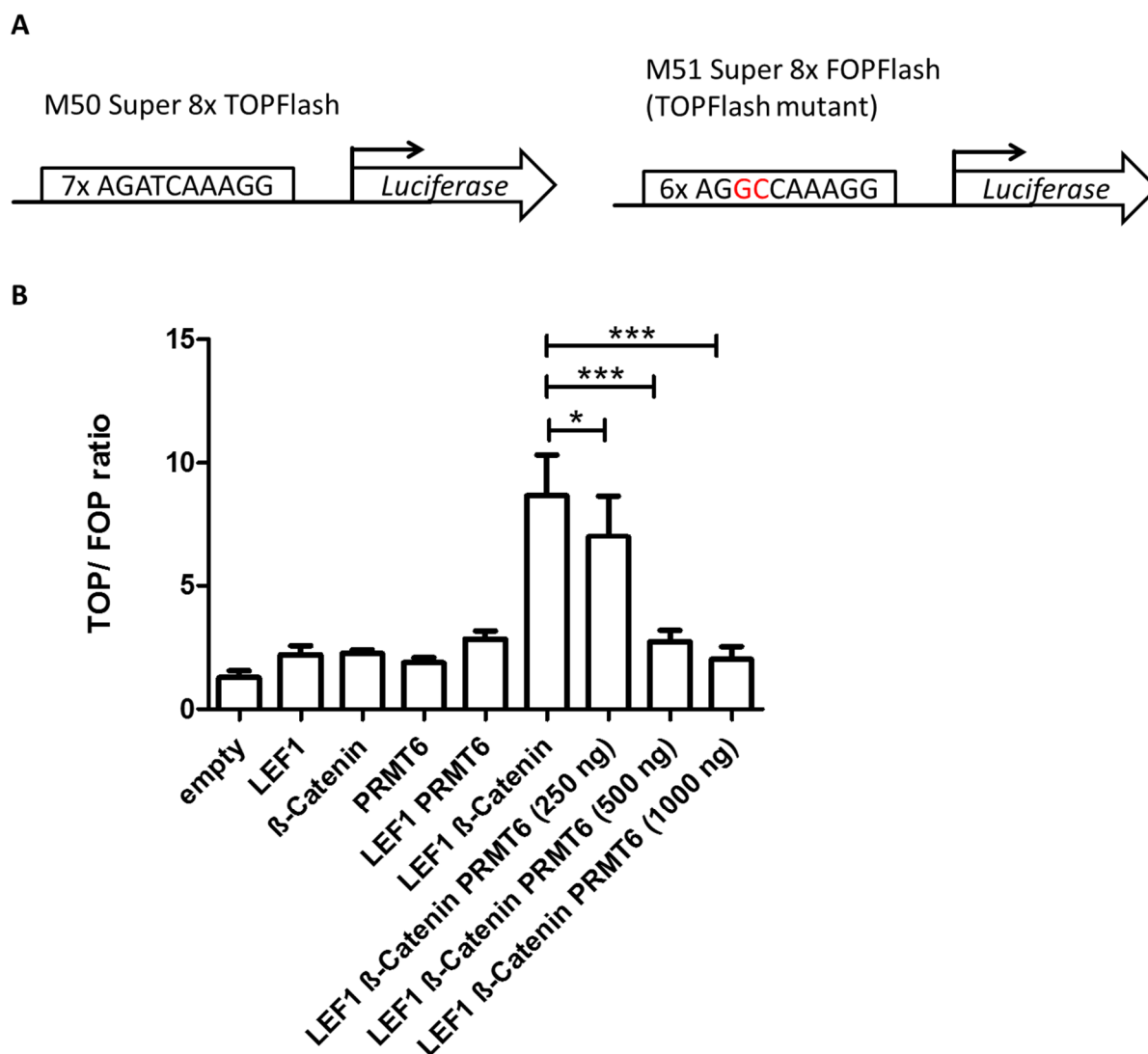


Figure 28: PRMT6 TOP-flash assay; (A) Schematic representation of the M50 Super 8x TOPFlash promoter. 7 TCF/LEF binding motives (AGATCAAAGG) were cloned with a minimal promoter in front of the *luciferase* gene. The M51 Super 8x FOPFlash promoter was used as a control. 6 mutated TCF/LEF binding motives were cloned instead. The two point mutations are shown in red. (B) HEK293T cells were transfected with the TOPFlash system shown in A. Co-expression of LEF1 and β -Catenin shows the highest luciferase activation. An increasing PRMT6 co-expression disrupts this activation. The values of the luciferase expression were normalized to the activity of the co-transfected β -Galactosidase. The normalized TOPFlash promoter values were normalized to the normalized FOPFlash promoter values. The bars represent the mean with standard deviation of four independent experiments, each measured in technical duplicates. The p-values were calculated using Student's t-test; *p < 0.05, **p < 0.01, ***p < 0.001.

3.7 LEF1 expression in different leukemia cell lines

LEF1 is an important transcription factor in lymphopoiesis and is essential in the development of T- and B-cells (van Genderen et al., 1994). The described PRMT6 interactome identified by mass spectroscopy showed that the endogenously expressed LEF1 is a novel PRMT6 interaction partner in K562 erythroleukemic cells. In order to analyze the role of LEF1 in the erythroid/megakaryocytic development, the expression of LEF1 was tested in several different hematopoietic cell lines on RNA and protein level (Figure 29). The focus of this experiment was the analysis of the LEF1 expression in different myeloid cells lines.

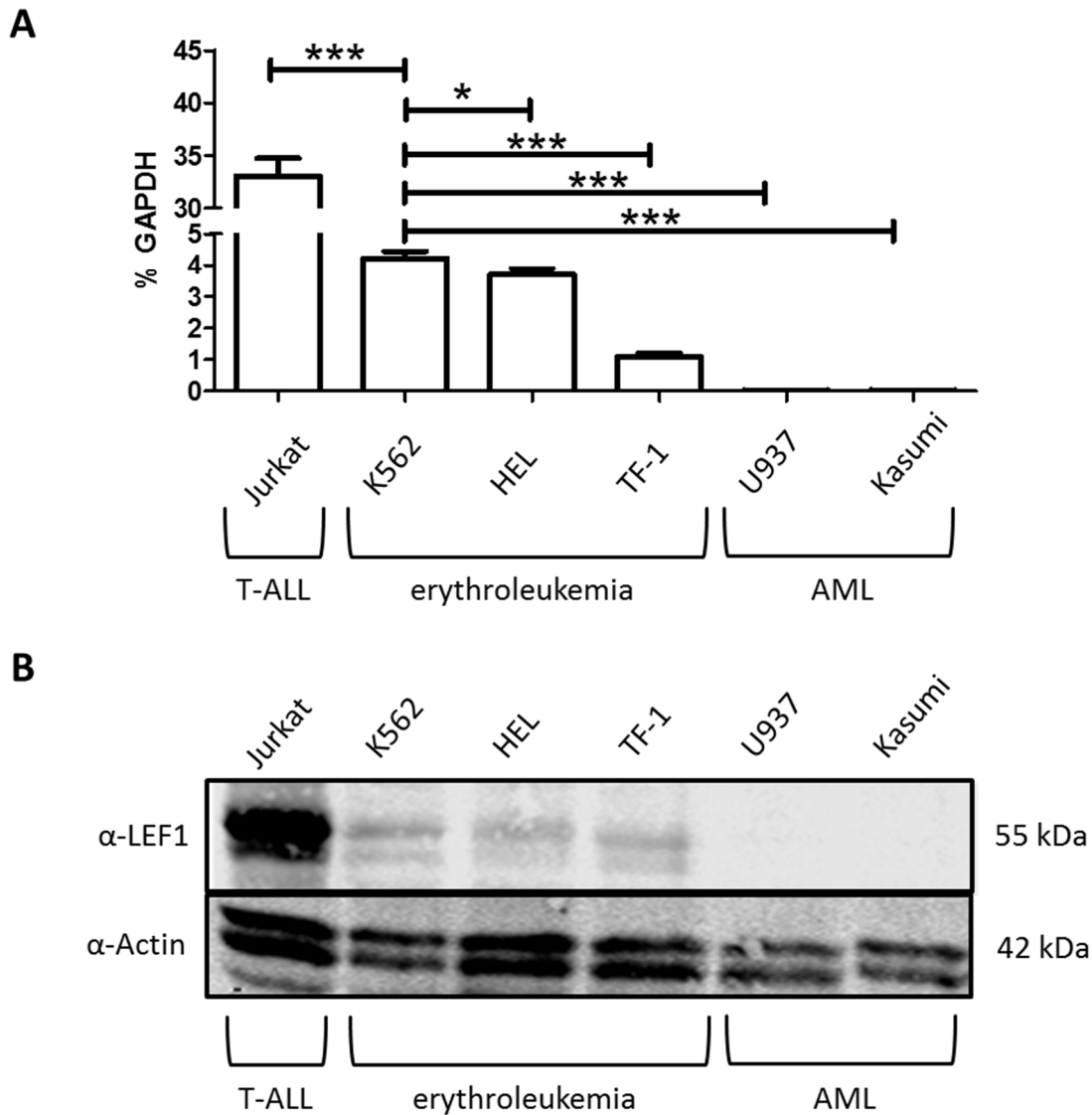


Figure 29: (A) RNA expression of *LEF1* in different hematopoietic cell lines. Jurkat cells belonging to the T-ALL cell line showed the highest expression values. K562, HEL and TF-1 cells belong to the erythroleukemia cell lines. These cells show a weaker but detectable *LEF1* expression. U937 and Kasumi cell lines belong to the AML cell lines and show no *LEF1* expression. The expression was normalized to the reference gene *GAPDH*. The error bars represent the standard deviations of at least three independent measurements. The p-values were calculated using Student's t-test; *p < 0.05, **p < 0.01, ***p < 0.001. **(B)** Western blot of different hematopoietic cell lines. Similar to the RNA expression analysis, the protein amount of LEF1 is the highest in the T-ALL Jurkat cell line. The erythroleukemia cell lines K562, HEL and TF-1 all contain detectable LEF1 protein amounts. LEF1 protein is not detectable in the AML cell lines U937 and Kasumi.

RNA expression and whole cell protein analysis showed comparable results. The T-ALL Jurkat cell line serves as positive control and shows the highest expression of *LEF1*, as it was identified as an important factor in the lymphoid development (van Genderen et al., 1994). The erythroleukemia cell lines K562, HEL and TF-1 all show detectable *LEF1* expression. In contrast, the AML cell lines U937 and Kasumi do not show any detectable *LEF1* RNA expression or protein. This experiment shows that LEF1 is abundant in a subset of myeloid cells, particular in the erythroid/megakaryocytic lineage. This finding was further investigated by the identification of target genes through ChIP-Seq data analysis of the transcription factor.

3.8 LEF1 ChIP-Seq analysis in K562 cells

In order to decipher the role of LEF1 in the erythroid/megakaryocytic development, ChIP-Seq data of the erythroleukemia cell line K562 was analyzed. ChIP-Seq data from the ENCODE Project was used; a sequencing project which gathered 1.1 million ChIP-Seq peaks from 318 transcription factors in K562 cells (ENCODE Project Consortium, 2012; Davis et al., 2018). 16,748 LEF1 peaks were extracted and annotated to the human genome.

The quality control of the MACS peaks shows that the majority of the peaks locate around the transcriptional start sites of genes (Figure 30 A). Nearly one fourth (24.2%) of the peaks are located in potential promoter regions (1,000 bp upstream sequence of UCSC RefSeq genes). These potential promoter regions comprise less than 1.0% of the human genome. The rest of the peaks are located in UTRs 5.7%, Exons 2.8%, Introns 34.4% and intergenic regions 32.9% (Figure 30 B). This information shows that LEF1 directly targets promoters in the genome of erythroleukemic K562 cells. Therefore, it plays an active role in the control of transcription by recruiting partners like PRMT6 and RUNX1 to the transcription start sites.

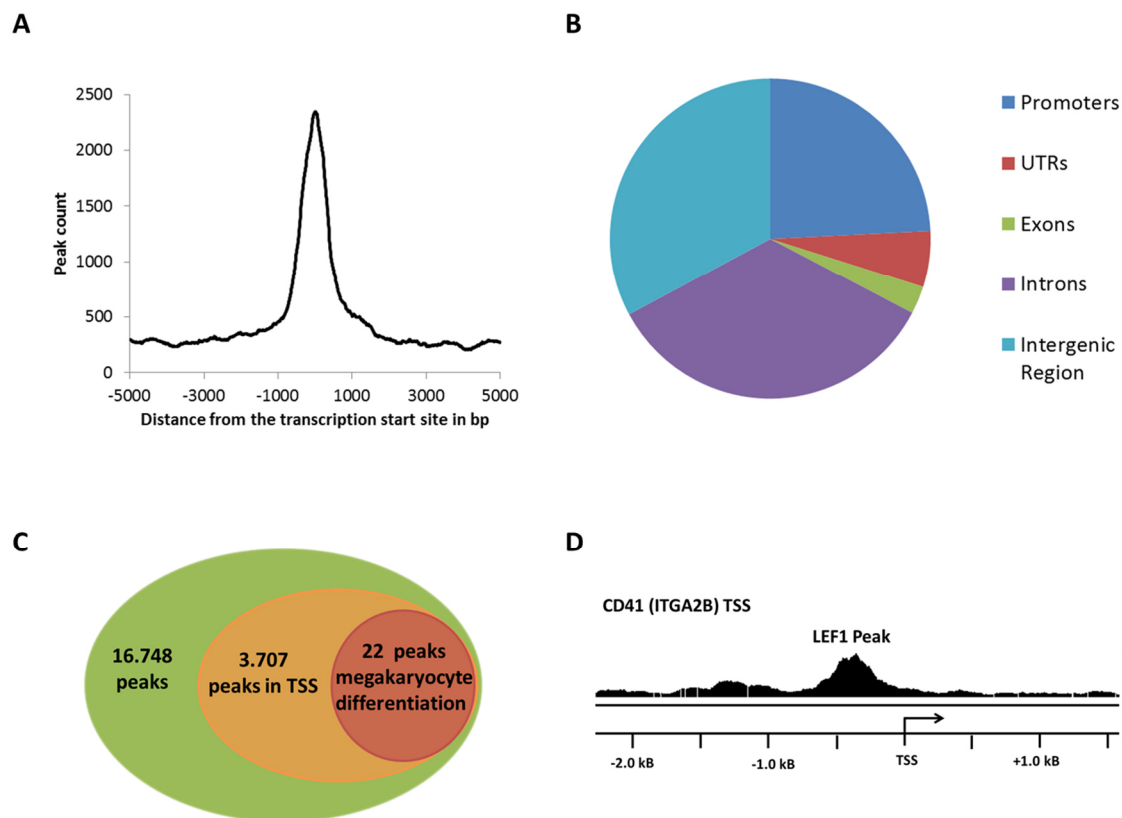


Figure 30: LEF1 ChIP-Seq analysis in K562 cells; (A) Distribution of the aggregated peak numbers around the transcription start site. The distance from the TSS is shown in bp. The peak count shows that most LEF1 peaks are located near a transcription start site. (B) Peak distribution over different genomic features: 24.2% of the peaks are located in promoter regions or introns. 32.9% are located in intergenic regions and 42.9% in UTRs and Introns. (C) The annotation shows that out of 16,748 peaks, 3,707 peaks are located +/- 500 bp around a transcription start site. The GO-term GO:0030219 (megakaryocyte differentiation) is enriched in the dataset with a p-value of 9,38E-04, with 22 LEF1 peaks in the TSS of megakaryocytic genes. (D) The CD41 (ITGA2B) promoter is shown as an example (hg19; chr17: 42,469,201-42,465,500). The LEF1 peak is located around -400 bp of the TSS.

3.707 LEF1 peaks (22.1 %) are located near the transcription start site (+/- 500 bp). A Gene ontology analysis showed that the term megakaryocyte differentiation (GO:0030219) was enriched with a p-value of 9.38E-04 (Figure 30 C). This identifies LEF1 as a potential regulator of megakaryopoiesis. The analysis showed that LEF1 binds to 22 genes controlling megakaryocytic differentiation; the genes are listed in Table 13. CD41 (*ITGA2B*) and *NFE2* are direct targets of LEF1. Both genes were also identified as direct RUNX1/PRMT6 targets (Herglotz et al., 2013). In addition, the gene of the megakaryocytic growth factor thrombopoietin (*TPO*) is also a direct target of LEF1. Several histone modifying enzymes are identified as targets: *KMT2A*, *KMT2E*, *RBBP5* and *ASH2L*. Further, histone variants of histone 3 and histone 4 are targets of LEF1.

Table 13: List of LEF1 peaks in GO:0030219 (megakaryocyte differentiation)

Gene symbol	Name
ITGA2B	Integrin Subunit Alpha 2b (CD41)
THPO	Thrombopoietin
TAL1	TAL BHLH Transcription Factor 1
NFE2	Nuclear Factor, Erythroid 2
CBFB	Core-binding factor subunit beta (master-regulator of RUNX1)
KMT2A	Lysine Methyltransferase 2A
KMT2E	Lysine Methyltransferase 2E
RBBP5	RB Binding Protein 5, Histone Lysine Methyltransferase Complex Subunit
ASH2L	ASH2 Like, Histone Lysine Methyltransferase Complex Subunit
H3F3A	H3.3 Histone A
HIST1H3D	H3 Clustered Histone 4
HIST1H3J	H3 Clustered Histone 12
HIST1H4J	H4 Clustered Histone 11
HIST1H4C	H4 Clustered Histone 3
HIST1H4H	H4 Clustered Histone 8
MOV10	Mov10 RISC Complex RNA Helicase
TNRC6B	Trinucleotide Repeat Containing Adaptor 6B
AGO1	Argonaute RISC Component 1
RBM15	RNA Binding Motif Protein 15
WASF2	WASP Family Member 2
CNOT4	CCR4-NOT Transcription Complex Subunit 4
MED1	Mediator Complex Subunit 1

This ChIP seq analysis shows that LEF1 targets megakaryocytic genes in the erythroleukemia cell line K562. This explains its presence in the myeloid cell lines (Figure 29). The impact of LEF1 on

differentiation is mostly described in cells of lymphoid differentiation (van Genderen et al., 1994). This newly identified impact on megakaryopoiesis will be further analyzed.

The analysis of CHIP seq peaks in erythroleukemic K562 cells showed that LEF1 targets megakaryocytic genes. In order to analyze if this is a cell type specific effect, the CHIP-seq peaks of different cell lines were compared. The LEF1 CHIP seq data of HEK293T cells were used as a control; HEK293T cells originated from embryonic kidney cells. The dataset was retrieved from the ENCODE Project.

The promoter region of the *Axin2* gene was used as a positive control. The Wnt/ β -catenin signaling pathway directly induces the transcription of *Axin2*, which takes part in a possible negative feedback loop (Jho et al., 2002). LEF1 targets the promoter of *Axin2* in HEK293T cells and K562 cells, independent of its cell type (Figure 31 A).

The LEF1 transcription factor binds to promoters of genes which are involved in megakaryocyte differentiation (GO:0030219). LEF1 is enriched at the promoter of *ITGA2b* (CD41) but shows no enrichment in HEK293T cells (Figure 31 B). Also, the promoter region of *THPO* shows LEF1 enrichment in K562 cells but not in HEK293T cells (Figure 31 C).

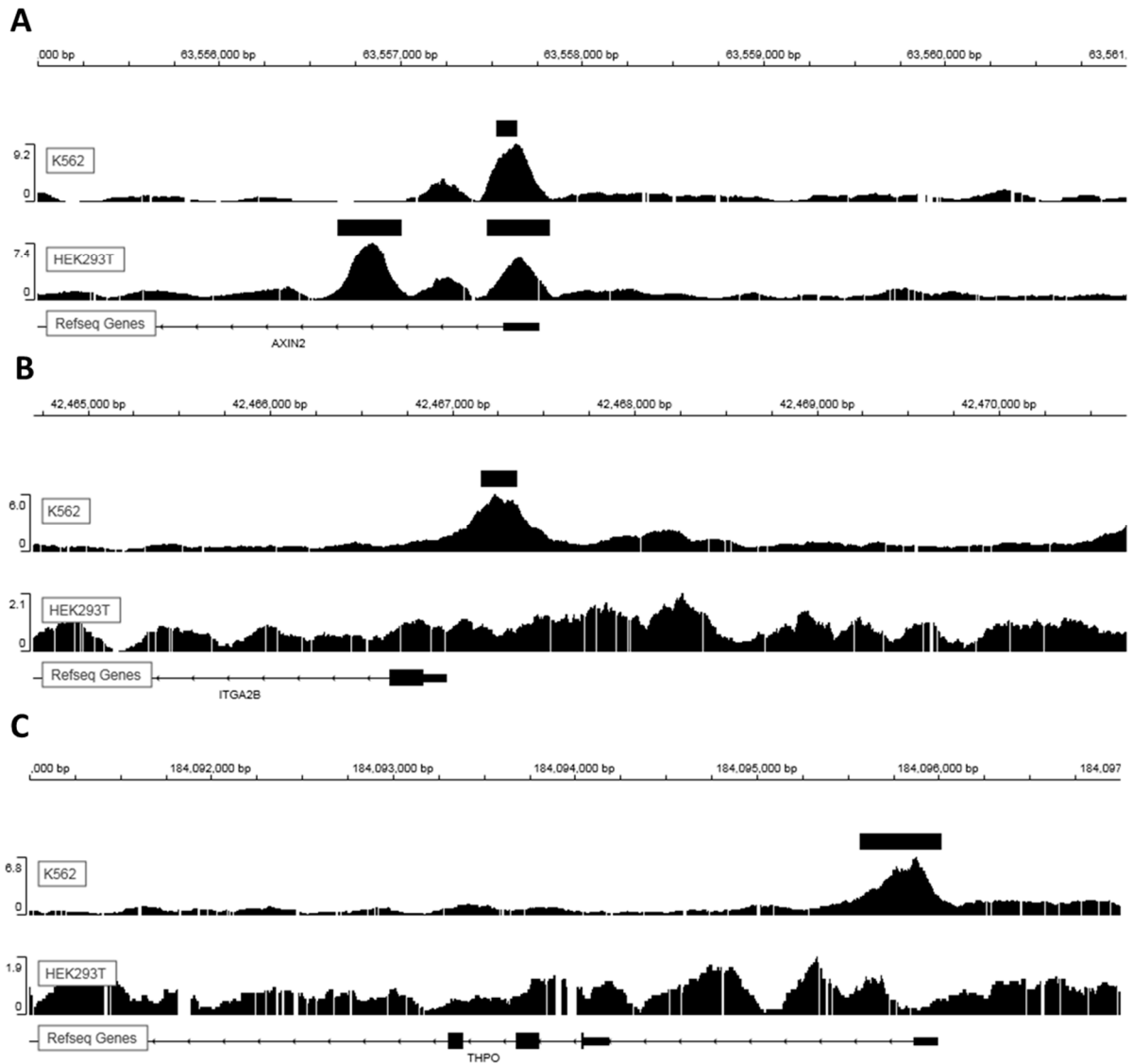


Figure 31: Comparison of LEF1 peaks in different cell lines. The gene models of hg19 refseq were used. The Y-Axis shows the enrichment over IgG control. (A) TSS of *Axin2* (chr17:63,555,001-63,561,000) (B) TSS of *ITGA2B* (chr17:42,464,701-42,470,700) (C) TSS of *THPO* (chr3:184,091,001-184,097,000).

Common targets of the Wnt/ β -catenin signaling pathway like *Axin2* show LEF1 enrichment in all cell types. Megakaryocytic target genes show LEF1 binding only in erythroleukemic K562 cells. Binding of LEF1 to promoters of *ITGA2b* (CD41) and *THPO* is cell type specific.

The TCF/LEF family consists of four transcription factors: LEF1; TCF7; TCF7L1 and TCF7L2. All factors target the same consensus sequence WWCAAAG in promoter regions. In order to identify if megakaryocytic genes are targeted by different factors of the TCF/LEF family, ChIP-seq data from TCF7 and TCF7L2 were compared with LEF1. The datasets of TCF7 and TCF7L2 were retrieved from the ENCODE Project.

The promoter region of the *Axin2* gene was used as a positive control. The analysis revealed that the common target *Axin2* is occupied by the factors LEF1, TCF7 and TCF7L2 in K562 cells. Furthermore, the important erythroid/megakaryocytic differentiation factor TAL1 is binding to the *Axin2* promoter but not to the factor GATA2 (Figure 32 A).

The megakaryocytic gene *ITGA2B* (CD41) is targeted by LEF1 and the erythroid/megakaryocytic transcription factors GATA2 and TAL1. The factors TCF7 and TCF7L2 on the other hand are not binding to the *ITGA2B* promoter (Figure 32 B). The Wnt/ β -catenin signaling pathway targets *ITGA2B* directly through the transcription factor LEF1, but not TCF7 and TCF7L2.

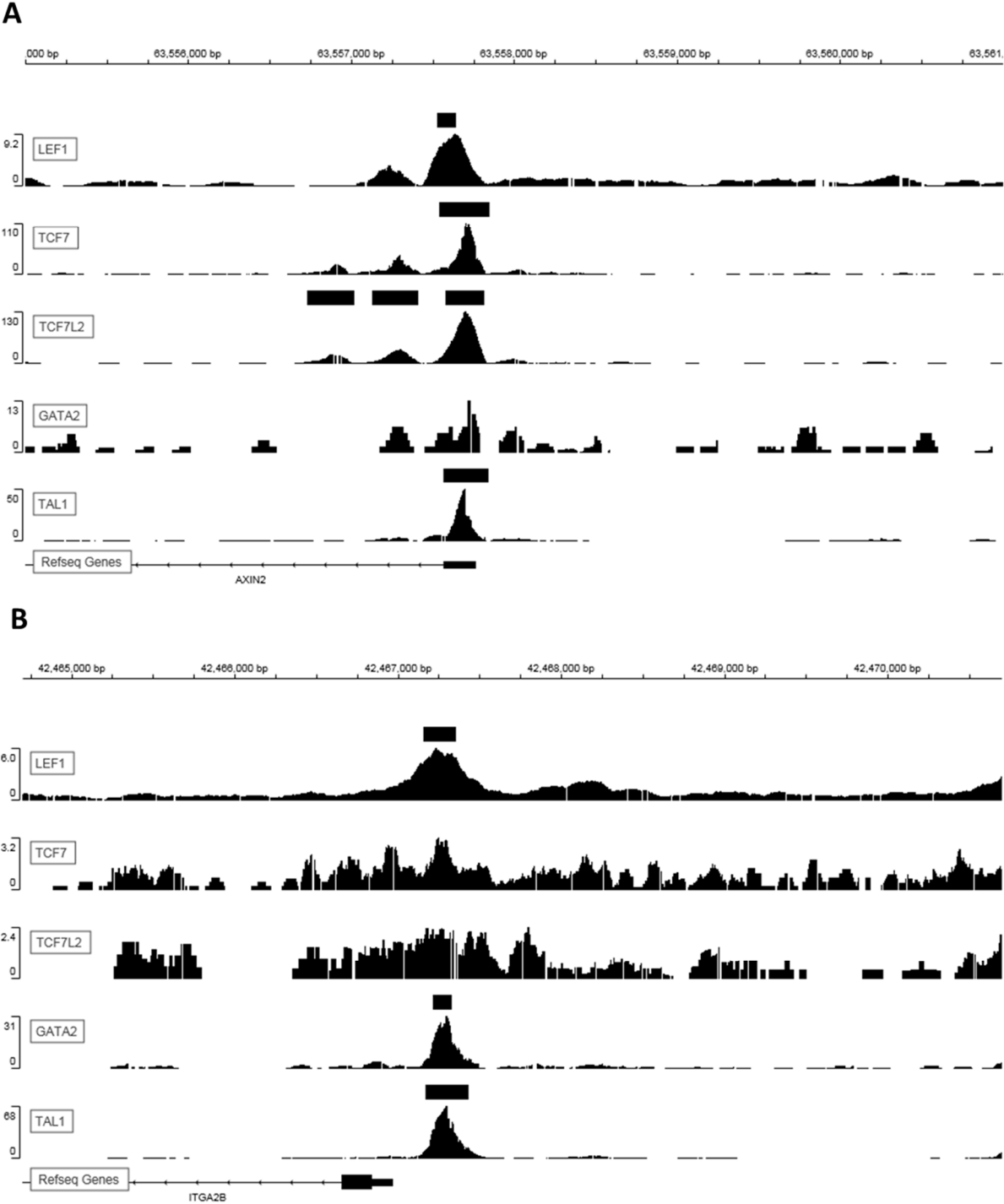


Figure 32: Comparison of different TCF/LEF peaks in K562 cells. The gene models of hg19 refseq were used. The Y-Axis shows the enrichment over IgG control. (A) TSS of *Axin2* (chr17:63,555,001-63,561,000) (B) TSS of *ITGA2B* (chr17:42,464,701-42,470,700).

3.9 Verification of the identified LEF1 peaks

The analysis of ChIP-Seq data from the ENCODE Project identified several LEF1 peaks in the promoter regions of megakaryocytic target genes in K562 cells. These findings of the sequencing analysis were verified with chromatin immunoprecipitation (ChIP). K562 cells were transduced with the LeGO-LEF1 overexpression vector. The empty LeGO overexpression vector was used as a control. The LeGO vector contains a GFP reporter gene which was used to verify the transduction efficiency.

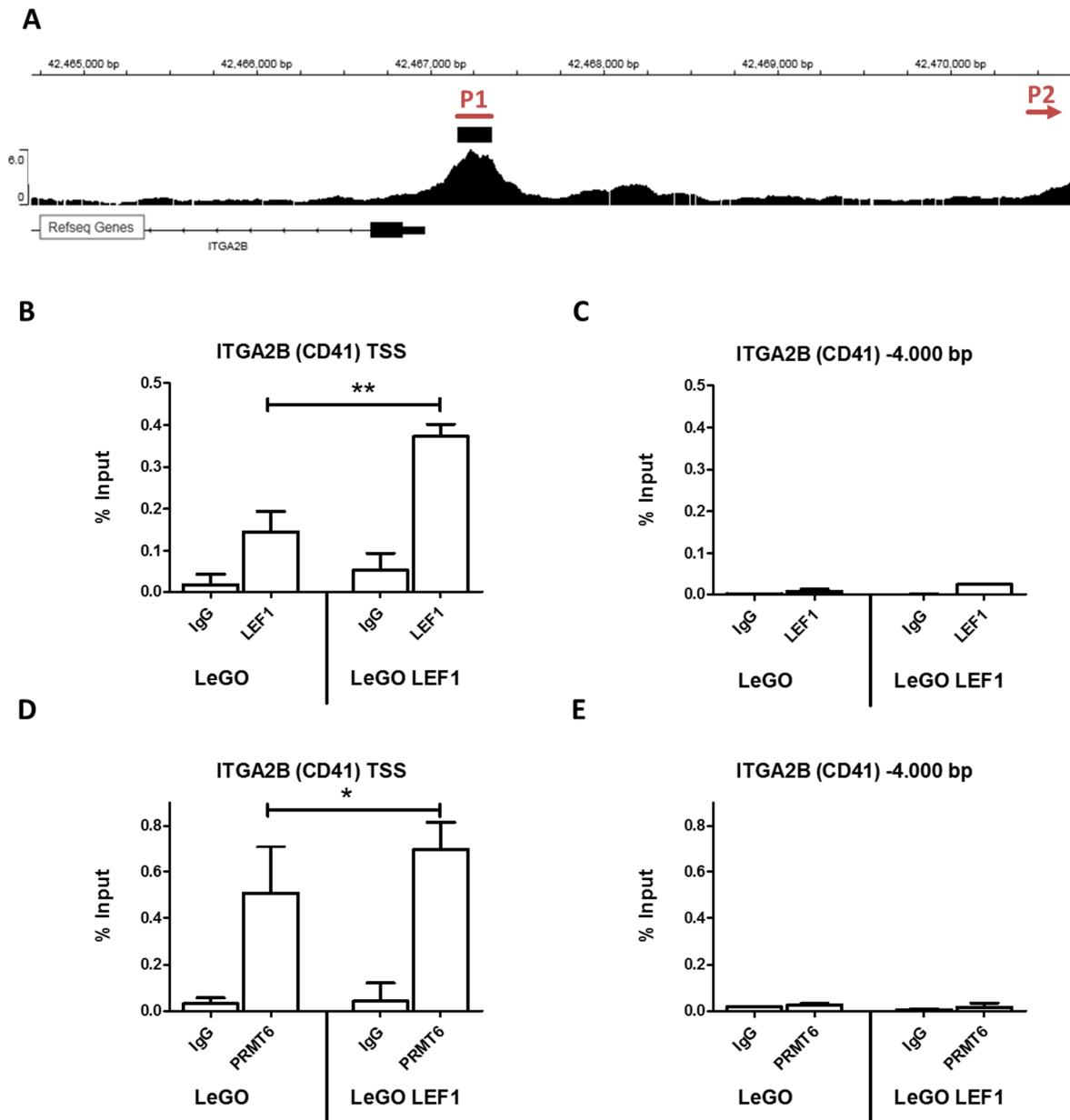


Figure 33: Verification of the identified LEF1 peak at the *ITGA2B* promoter; (A) TSS of *ITGA2B* (chr17:42,464,701-42,470,700). The gene models of hg19 refseq were used. The Y-Axis shows the enrichment over IgG control. P1 is the location of the primer pair at the TSS and P2 is a primer pair 4.000 bp upstream of the TSS. (B and C) Verification of the identified LEF1 peak; (D and E) PRMT6 binding at the promoter; The ChIP experiments were performed with lentiviral transduced K562 cells, overexpressing LEF1. The empty vector was used as negative control. ChIPs were performed with an anti-LEF1 and anti-PRMT6 antibody. Isotype-matched IgG antibodies were used as negative control. Bars represent the mean results, with SD derived from triplicates. The p-values were calculated using Student's t-test. *p < 0.05, **p < 0.01, ***p < 0.001.

The LEF1 peak at the *ITGA2B* promoter was verified with ChIP-qPCR. The ChIP seq data is visualized in (Figure 33 A) The primer pair P1 is located at the transcription start site. The primer pair P2 serves as negative control -4.000 bp away from the LEF1 peak.

The LEF1 overexpressing K562 cells show a positive input enrichment of 0.39 %. The empty vector control shows a lower enrichment of 0.15 % (Figure 33 B). The negative control is located 4.000 bp upstream of the TSS and shows only reduced enrichment of 0.03 % (Figure 33 C). This experiment verifies that the transcription factor LEF1 directly targets the promoter of the megakaryocytic gene *ITGA2B* (CD41).

The LEF1 overexpressing K562 cells showed enriched PRMT6 binding of 0.69 % at the LEF1 peak. The empty vector control shows enrichment of 0.51 % (Figure 33 D). The negative control shows reduced enrichment of 0.03 % (Figure 33 E). PRMT6 and LEF1 both occupy the TSS at the *ITGA2B* promoter. LEF1 recruits PRMT6 to the *ITGA2B* promoter.

The megakaryocytic transcription factor RUNX1 is transcribed from two promoters resulting in different isoforms of the protein. The *RUNX1* locus spans 260 kb; the two promoters are 160 kb apart from each other (Levanon et al., 2001). A putative enhancer site was identified 20 kb upstream of one of the promoters. The ChIP-seq analysis revealed that LEF1 binds to that enhancer site (Figure 34 A). Furthermore, the putative enhancer is occupied by the hematopoietic factors RUNX1, TAL1 and GATA2. The primer pair P1 is located at the enhancer site. The primer pair P2 serves as negative control +800 bp away from the LEF1 peak.

The LEF1 overexpressing K562 cells show a positive input enrichment of 1.14 %. The empty vector leads to an enrichment of 0.22 % (Figure 34 B). The negative control is located 800 bp downstream and shows reduced enrichment of 0.19 % and 0.05 % (Figure 34 C).

The LEF1 overexpressing K562 cells showed enriched PRMT6 binding of 0.97 % at the peak. The empty vector control shows enrichment of 0.59 % (Figure 34 D). The negative control shows reduced enrichment of 0.13 % (Figure 34 E). PRMT6 and LEF1 both occupy the enhancer site at the *RUNX1* promoter. LEF1 recruits PRMT6 to the *RUNX1* promoter.

CCND1 was identified as Wnt/ β -catenin signaling target by direct binding of LEF1 to its promoter (Tetsu and McCormick, 1999) and was therefore used as a positive control. A potential LEF1 binding site was identified at the TSS of *CCDN1* (Figure 35 A) The primer pair P1 is located at the transcription start site. The primer pair P2 serves as negative control -4.000 bp away from the LEF1 peak.

The LEF1 overexpressing K562 cells give a positive input enrichment of 0.44 %; the empty vector an enrichment of 0.12 % (Figure 35 B) The negative control is located 4.000 bp upstream and shows reduced enrichment with 0.06 % (Figure 35C). PRMT6 binding is enriched after LEF1 overexpression with 0.55 % at the peak. The empty vector control shows enrichment of 0.32 % (Figure 35D). The negative control shows reduced enrichment of 0.09 % (Figure 35E). PRMT6 and LEF1 both occupy the TSS at the *CCND1* promoter. LEF1 recruits PRMT6 to the *CCND1* promoter.

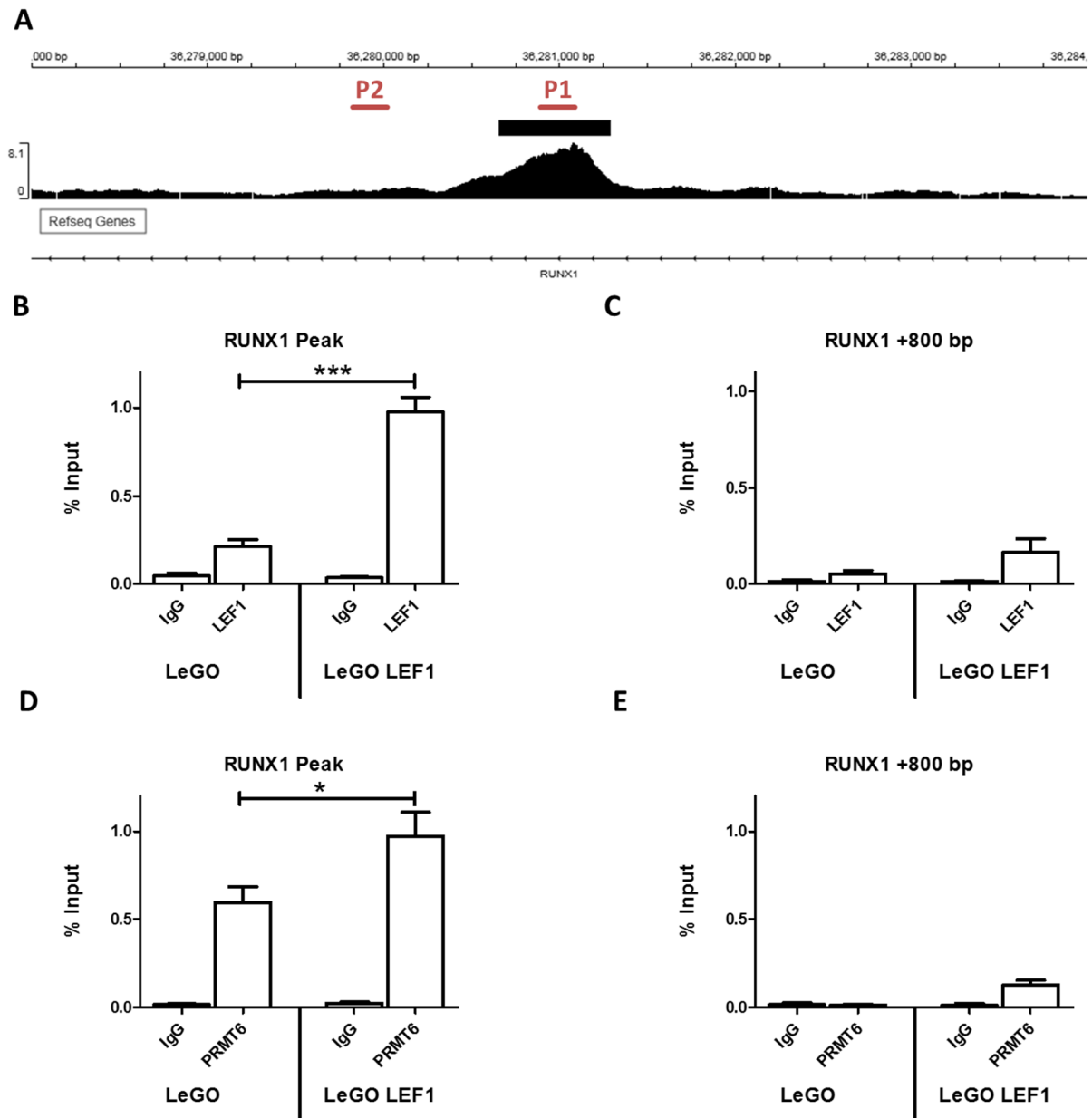


Figure 34: Verification of the identified LEF1 peak at the *RUNX1* enhancer (A) Enhancer site of *RUNX1* (chr21:36,278,001-36,284,000); located 20 kb upstream of the TSS. P1 is the location of the primer pair at the Enhancer and P2 is a primer pair 800 bp downstream of the enhancer. The gene models of hg19 refseq were used. The Y-Axis shows the enrichment over IgG control. (B and C) Verification of the identified LEF1 peak at the *RUNX1* locus (D and E) PRMT6 binding at the enhancer; The ChIP experiments were performed with lentiviral transduced K562 cells, over expressing LEF1. The empty vector was used as negative control. ChIPs were performed with an anti-LEF1 and anti-PRMT6 antibody. Isotype-matched IgG antibodies were used as negative control. Bars represent the mean results, with SD derived from triplicates. The p-values were calculated using Student's t-test. *p < 0.05, **p < 0.01, *p < 0.001.**

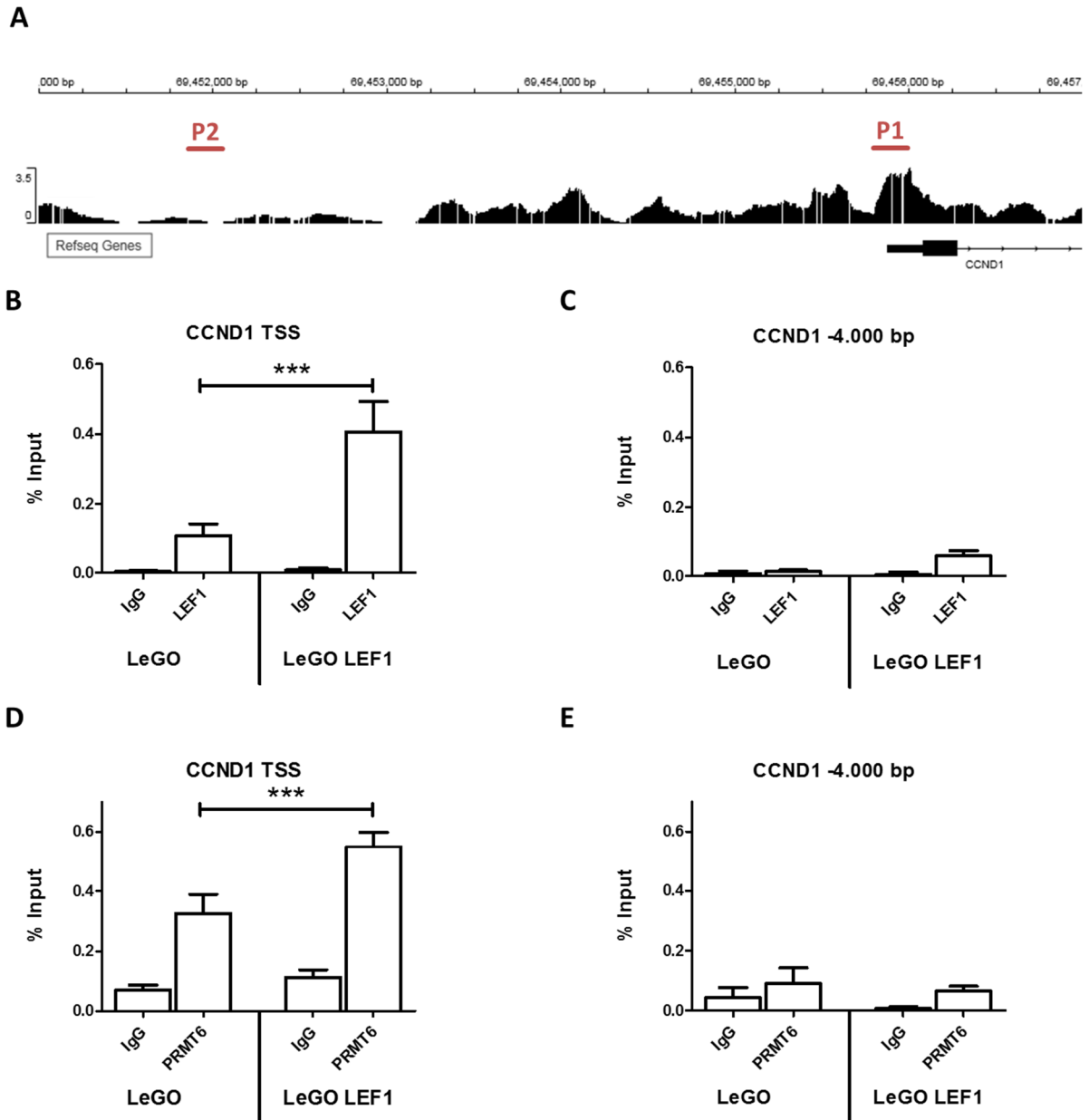


Figure 35: Verification of the putative LEF1 peak at the *CCND1* promoter; (A) TSS of *CCND1* (chr11:69,451,001-69,457,000). P1 is the location of the primer pair at the TSS and P2 is a primer pair 4.000 bp upstream of the TSS. The gene models of hg19 refseq were used. The Y-Axis shows the enrichment over IgG control. (B and C) Verification of the identified LEF1 peak at the *CCND1* locus; (D and E) PRMT6 binding at the promoter; The ChIP experiments were performed with lentiviral transduced K562 cells, over expressing LEF1. The empty vector was used as negative control. ChIPs were performed with an anti-LEF1 antibody. Isotype-matched IgG antibodies were used as negative control. Bars represent the mean results, with SD derived from triplicates. The p-values were calculated using Student's t-test. * $p < 0.05$, ** $p < 0.01$, * $p < 0.001$.**

3.10 LEF1 knockdown in K562 cells

The previous CHIP-qPCR experiments showed that the promoter of *ITGA2B* (CD41) is directly targeted by the transcription factor LEF1. The erythroleukemic K562 cells were lentivirally transduced with pGIPZ shRNA vectors for the specific knockdown of selected target genes. The cells were transduced with two different shLEF1 RNAs and the shLacZ RNA as negative control. Two different shLEF1 RNAs were used to exclude unspecific influence of the pGIPZ vector backbone. The RNA expression was measured after 7 days of incubation. The pGIPZ vectors contains a GFP marker which allowed for positive selection with FACS measurements.

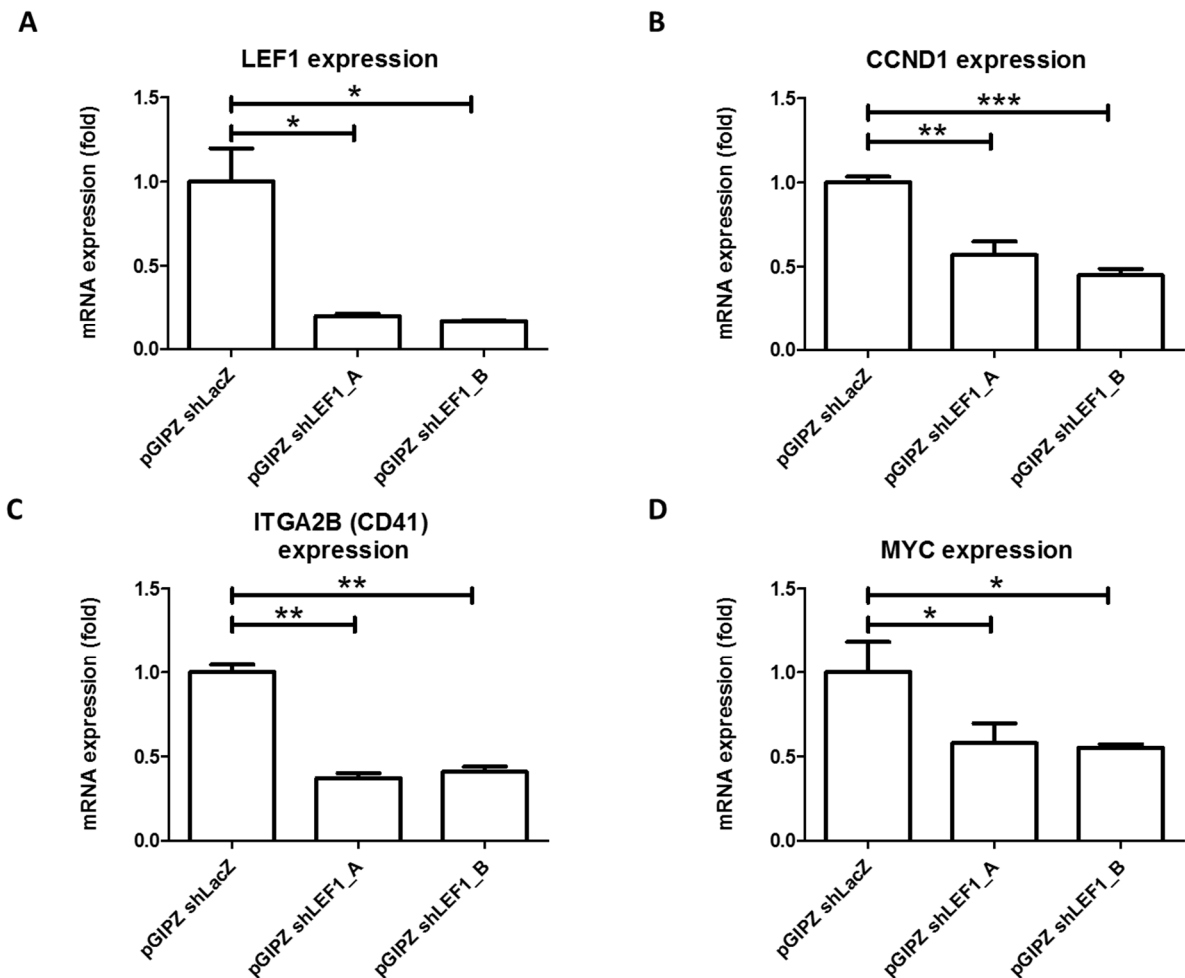


Figure 36: RNA expression of two separate pGIPZ shLEF1 knockdown vectors in erythroleukemic K562 cells, 7 days after transduction. The expression was normalized to the reference gene *GAPDH*. (A) After the shRNA knockdown, the *LEF1* expression is reduced to less than 20 %. (B) The *LEF1* target gene *CCND1* (Tetsu and McCormick, 1999) is reduced in both *LEF1* knockdowns. (C) *ITGA2B* expression is reduced to less than 50 %. (D) The *LEF1* target gene *MYC* (He et al., 1998) is also reduced in both *LEF1* knockdowns. The error bars represent the standard deviations of at least two independent measurements. The p-values were calculated using Student's t-test. *p < 0.05, **p < 0.01, ***p < 0.001, ns: not significant.

Both knockdowns of the two different shRNAs reduced the *LEF1* expression to less than 20 % compared to the shLacZ control (Figure 30 A). The *LEF1* expression is in both cases intensively reduced. The *CCND1* gene is a direct target of the *LEF1*/Wnt/ β -catenin signaling (Tetsu and McCormick, 1999). The expression was reduced to less than 60 % by the *LEF1* knockdown (Figure

30 B). The *ITGA2B* (CD41) gene was identified as new direct LEF1 target in erythroleukemic K562 cells. The knockdown of LEF1 led to a reduced expression of 37 % by shLEF1_A and 41 % by shLEF1_B (Figure 30 B). The *MYC* gene is a direct target of the LEF1/Wnt/ β -catenin signaling (He et al., 1998). The expression was reduced to less than 60 % by both LEF1 knockdowns (Figure 30 D). The Knockdown experiment confirms that the identified genes are directly targeted by LEF1.

The knockdown of LEF1 was validated on protein expression level. The Western blot analysis of the shLEF1 knockdowns confirms the RNA expression analysis. Whole cell lysates were produced 7 days after transduction. The western blot shows, that both LEF1 shRNAs lead to reduced LEF1 protein levels (Figure 37 A). The cell proliferation was not inhibited after the knockdown of the LEF1 transcription factor. The cells were counted 7 days after transfection and no difference was determined (Figure 37 B).

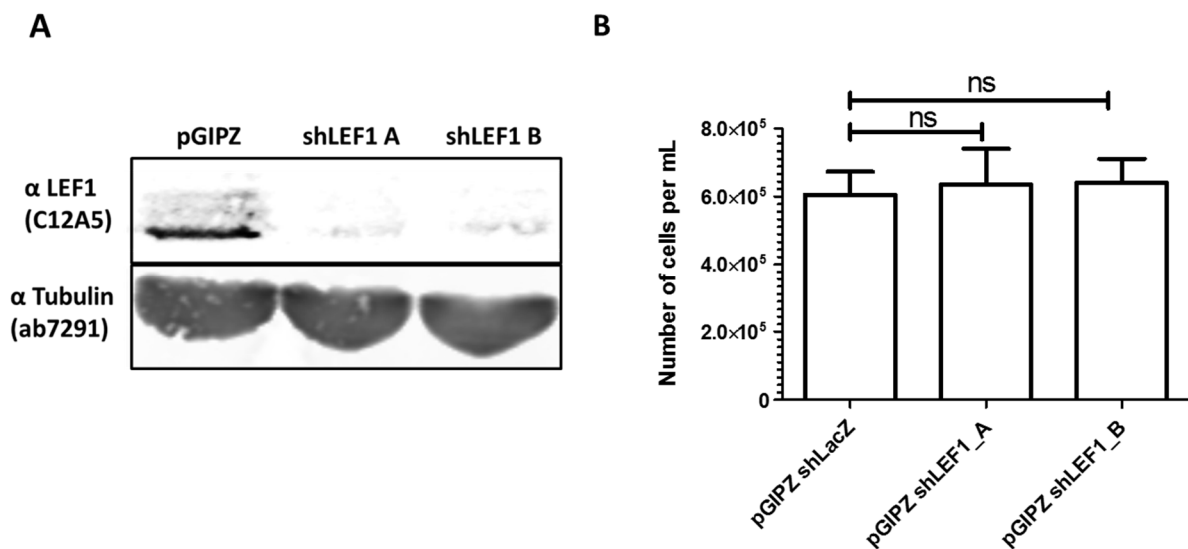


Figure 37: (A) Western blot of the two separate pGIPZ shLEF1 knockdown vectors in erythroleukemic K562 cells, 7 days after transduction. Similar to the RNA expression analysis, the protein amount of LEF1 is reduced in the shRNA knockdowns. An antibody against tubulin was used as loading control. (B) The severe LEF1 knockdown from the shRNAs does not lead to reduced number of cells, 7 days after transfection. The error bars represent the standard deviations of at least four independent measurements. The p-values were calculated using Student's t-test. * $p < 0.05$, ** $p < 0.01$, *** $p < 0.001$, ns: not significant.

The knockdown of LEF1 confirmed that the transcription factor targets the promoters of megakaryocytic genes like *CCND1* and *ITGA2B* (CD41) in K562 cells. Next this effect was analyzed by overexpression of LEF1.

3.11 LEF1 overexpression in K562 cells

The previous shLEF1 knockdown experiments and the LEF1 ChIP seq analysis showed that the promoters of *CCND1* and *ITGA2B* (CD41) are direct targets of the transcription factor. LEF1 cDNA was cloned into the lentiviral overexpression LeGO vector. The cDNA of the full length LEF1 and the dominant negative LEF1 (dnLEF1) protein (see Figure 9) were used for the experiment. The vectors were transduced via lentiviral transduction into K562 cells. The LeGO vector contains a GFP selection marker which allowed the positive selection via FACS.

RNA measurements were performed seven days after transduction. The transduction efficiency is shown in Figure 38 A. The full length *LEF1* produced 31.6-fold increased mRNA levels and the dnLEF1 produced 19.3-fold increased mRNA levels. LEF1 overexpression enhances the *CCND1* expression to 1.8-fold. Also, the dominant negative *LEF1* overexpression, which is missing the β -catenin binding motif, enhances the *CCND1* expression to 1.6-fold (Figure 38 B). LEF1 binds to the promoter of *CCND1* and activates its expression, independent of the recruitment of the cofactor β -catenin.

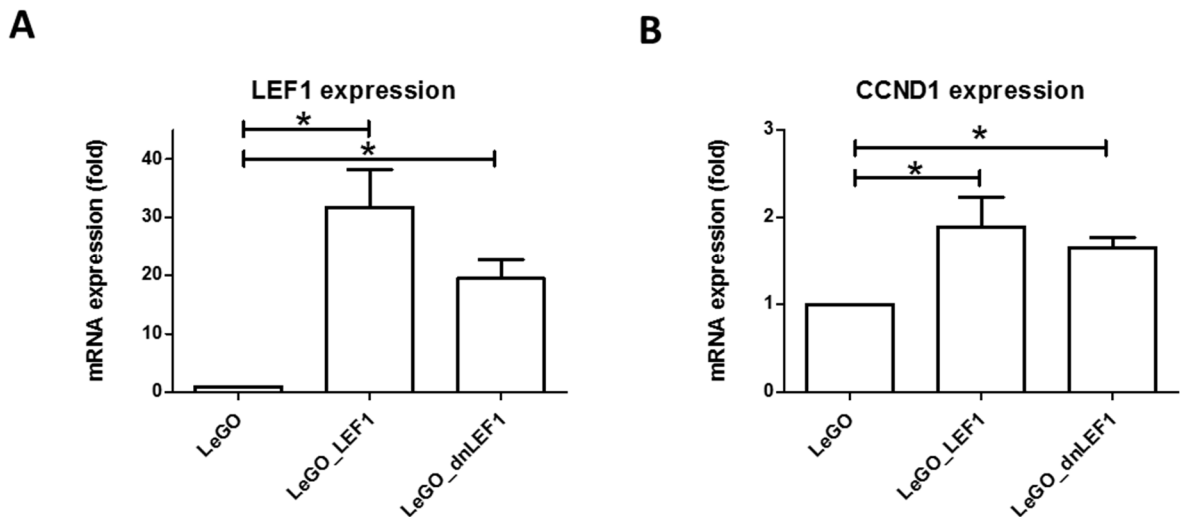


Figure 38: RNA expression of two LEF1 overexpression vectors in erythroleukemic K562 cells, 7 days after transduction. The full length *LEF1* and the truncated dominant negative *LEF1* constructs were overexpressed. The expression was normalized to the reference gene *GAPDH*. (A) Both over expression vectors lead to an increased *LEF1* expression. (B) The LEF1 target gene *CCND1* shows increased expression after LEF1 overexpression. The error bars represent the standard deviations of at least three independent measurements and two independent transductions. The p-values were calculated using Student's t-test. *p < 0.05, **p < 0.01, *p < 0.001, ns: not significant.**

The promoter of *ITGA2B* (CD41) and the enhancer of *RUNX1* were identified as direct LEF1 targets. *ITGA2B* is downregulated after shLEF1 knockdown. Both genes show no difference in expression after LEF1 overexpression (Figure 39 A and B). *PRMT6* and β -catenin were used as control. Similarly, both show no increased expression after the LEF1 overexpression (Figure 39 C and D).

The overexpression analysis shows that the transcription factor LEF1 itself is able to activate the transcription of the cell cycle regulator *CCND1* in K562 cells but not the target genes *ITGA2B* (CD41) and *RUNX1*.

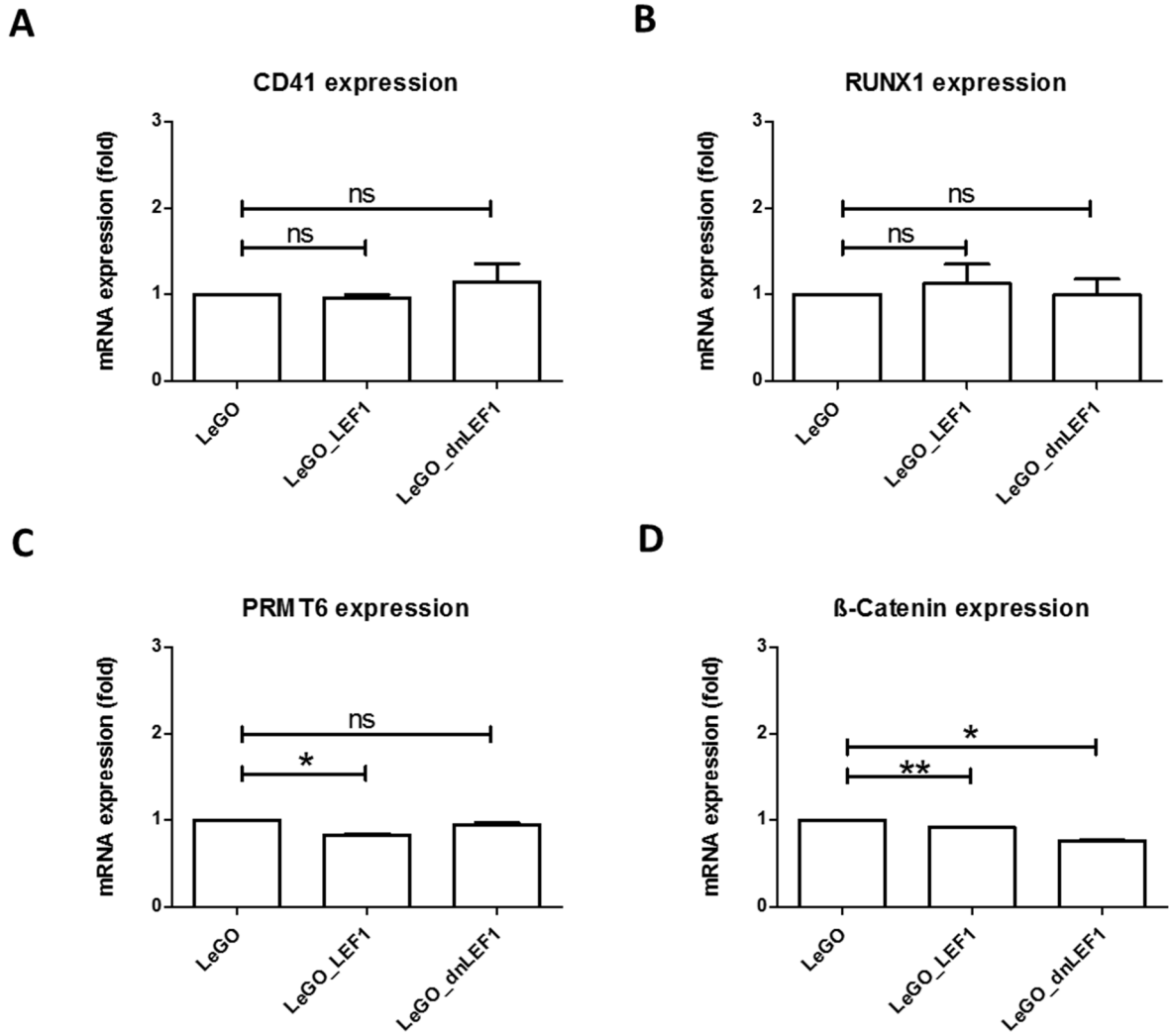


Figure 39: RNA expression of two LEF1 overexpression vectors in erythroleukemic K562 cells, 7 days after transduction. The full length LEF1 and the truncated dominant negative LEF1 construct were overexpressed. The expression was normalized to the reference gene *GAPDH*. (A and B) The LEF1 target genes *ITGA2B* and *RUNX1* show no difference in expression after LEF1 overexpression. (C and D) *PRMT6* and *β-catenin* shows no increased expression after LEF1 overexpression. The error bars represent the standard deviations of at least three independent measurements and two independent transductions. The p-values were calculated using Student's t-test. *p < 0.05, **p < 0.01, *p < 0.001, ns: not significant.**

The overexpression of LEF1 was validated on protein expression level. The Western blot analysis of the LEF1 overexpression confirms the RNA expression analysis. Whole cell lysates were produced 7 days after lentiviral transduction. The Western Blot is shown in (Figure 40). The LeGO_LEF1 vector leads to increased LEF1 protein levels.

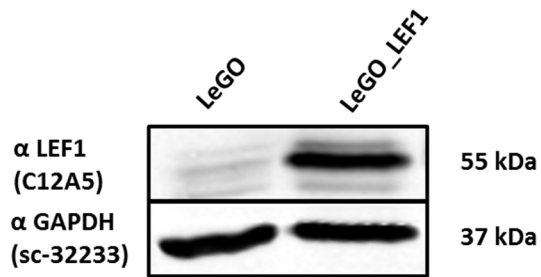


Figure 40:Western blot of the LEF1 over-expressing erythroleukemic K562 cells, 7 days after transduction. An antibody against GAPDH was used as loading control. Similar to the RNA expression analysis the LeGO_LEF1 expressing K562 cells show a strong LEF1 expression.

The manipulation of the LEF1 expression with shRNAs resulted in the reduced expression of the putative LEF1 target genes *ITGA2B* (CD41) and *RUNX1*. The manipulation of LEF1 abundance by overexpression instead lead to no altered expression levels of the two putative target genes. The next experiment shows the overexpression of the LEF1 activator β -catenin in K562 cells in order to analyze the discrepancy of the LEF1 experiments.

3.12 β -catenin overexpression in K562 cells

β -catenin is a cofactor which is recruited by the TCF/LEF1 transcription factor family to target promoters. The protein is associated with increased expression of the target genes (MacDonald et al., 2009). The β -catenin cDNA was cloned into the lentiviral overexpression LeGO vector. cDNA of the truncated Δ N89 β -catenin which lacks the GSK-3 β phosphorylation site (see Figure 11) was used for the experiment (Kolligs et al., 1999). The truncated protein acts as dominant active coactivator, which is not targeted for proteasomal degradation. The β -catenin vector was transferred via lentiviral transduction into K562 cells. The GFP selection marker of the LeGO vector was used for the positive selection via FACS. The RNA measurements were performed seven days after transduction.

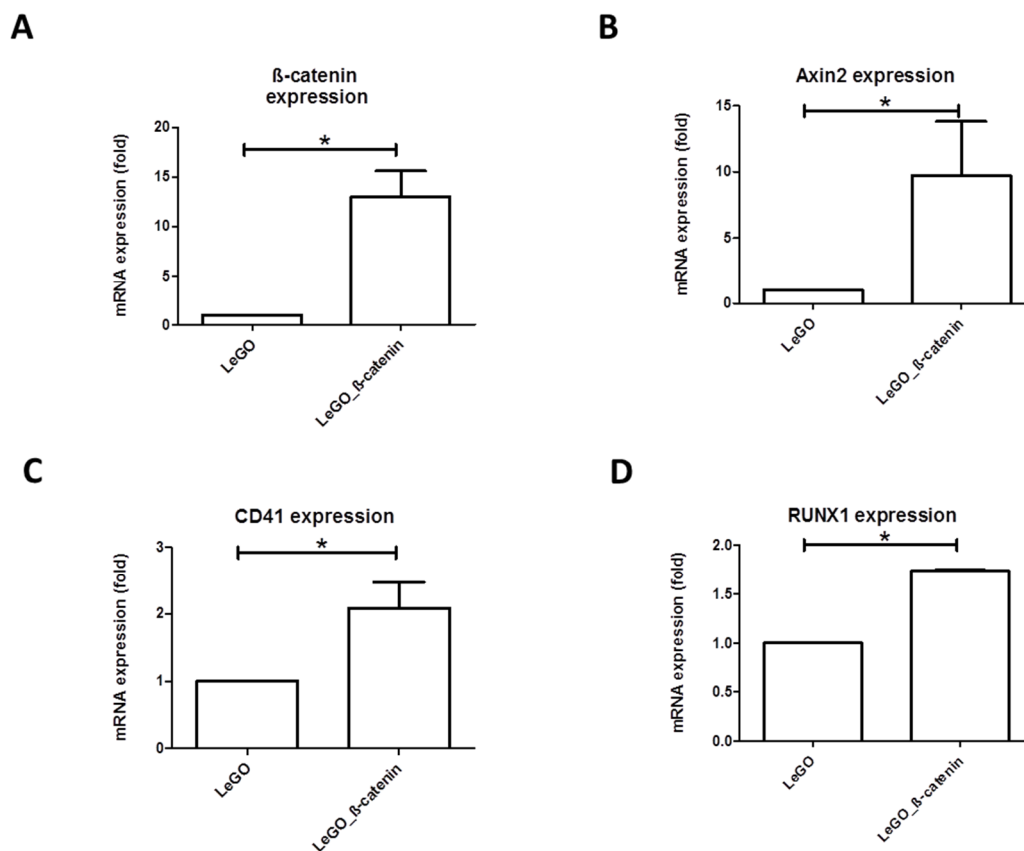


Figure 41: RNA expression of β -catenin overexpression vectors in erythroleukemic K562 cells, 7 days after transduction. The constantly active deltaN89- β -catenin was overexpressed, megakaryocytic genes show higher expression. The expression was normalized to the reference gene *GAPDH*. (A) A strong β -catenin overexpression was measured. (B) The Wnt/ β -catenin target *Axin2* (Jho et al., 2002) shows increased expression after β -catenin overexpression (C and D) *CD41* (ITGA2B) and *RUNX1* show increased expression as well. The error bars represent the standard deviations of at least three independent measurements and two independent transductions. The p-values were calculated using Student's t-test. *p < 0.05, **p < 0.01, *p < 0.001, ns: not significant.**

The overexpression shows 12-fold increased β -catenin levels (Figure 41 A) confirming a successful transduction of the coactivator. The Δ N89 β -catenin protein lacks the GSK-3 β phosphorylation site, and therefore accumulates in the nucleus. The *Axin2* gene shows increased expression after the β -catenin overexpression (Figure 41 B). *Axin2* is activated in a negative feedback loop, counteracting

increased β -catenin levels (Jho et al., 2002). The Axin2 expression confirms that the overexpressed truncated Δ N89 β -catenin is functional and activates the genes of the Wnt pathway.

The putative LEF1 target *ITGA2B* (CD41) is activated by β -catenin. The expression is 2-fold increased (Figure 41 C). Similarly, the expression of the megakaryocytic transcription factor *RUNX1* is activated by 1.6-fold (Figure 41 D). Megakaryocytic gene expression is controlled by the Wnt signaling pathway.

The TCF/LEF transcription factors family (Arce et al., 2006) consists of four members (see Figure 9). In the next experiment it was tested, which transcription factor is activated in K562 cells after Wnt activation. The β -catenin overexpression leads to a 2.5-fold increased expression of *LEF1* (Figure 42 A). The other three family members *TCF7*, *TCF7L1* and *TCF7L2* shows only slightly increased expression in K562 cells (Figure 42 B to D).

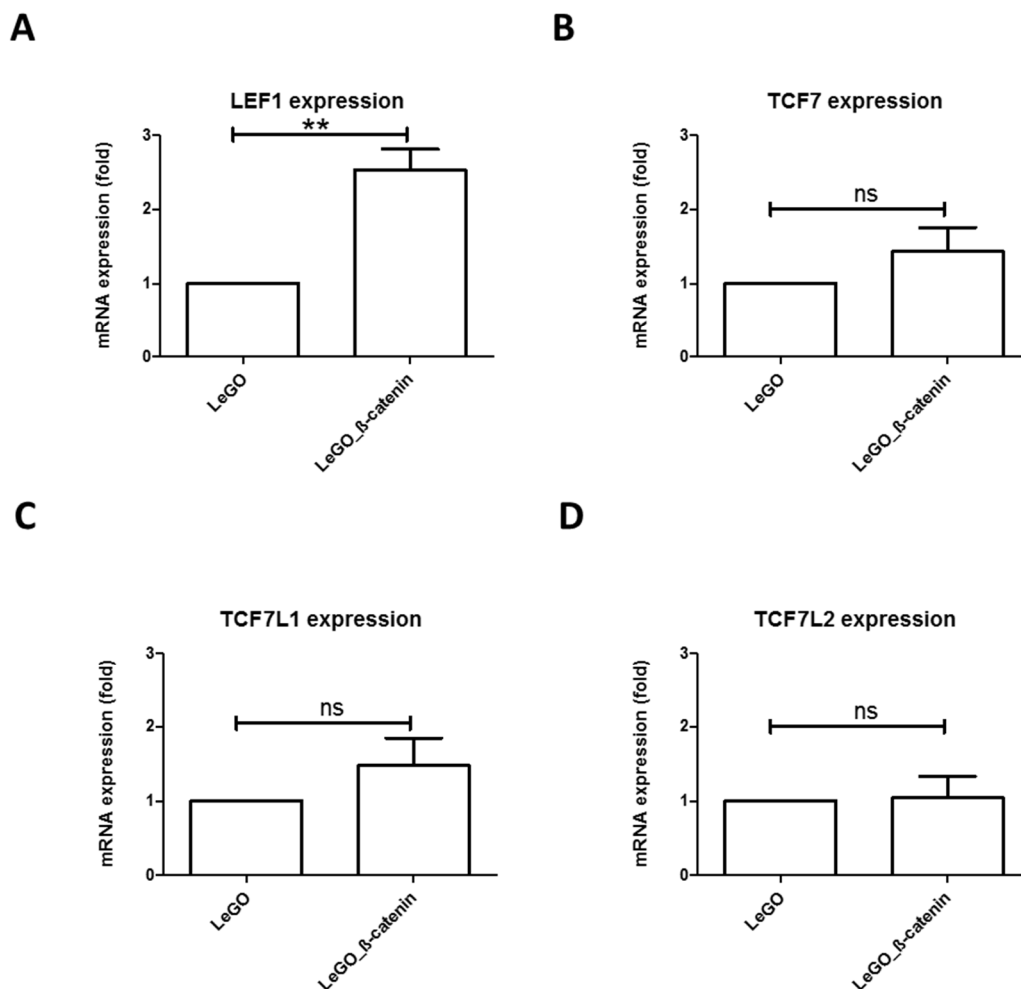


Figure 42: RNA expression of β -catenin over-expression vectors in erythroleukemic K562 cells, 7 days after transduction. The constantly active deltaN89- β -catenin was overexpressed. The expression was normalized to the reference gene *GAPDH* (A) *LEF1* expression is significantly increased after β -catenin overexpression. (B- D) *TCF7*, *TCF7L1* and *TCF7L2* do not show an increased expression after β -catenin overexpression. The error bars represent the standard deviations of at least three independent measurements and two independent transductions. The p-values were calculated using Student's t-test. *p < 0.05, **p < 0.01, ***p < 0.001, ns: not significant.

The ChIP seq analysis (Figure 30) revealed 3,707 possible LEF1 peaks. Amongst others, the erythroid transcription factors *TAL1*, *KLF1* and *BCL6* harbor putative LEF1 binding sites in their promoter regions as well. The RNA expression analysis shows that overexpression of β -catenin only leads to slightly different expression values of these erythroid transcription factors (Figure 43 A to C). The enzyme *PRMT6* which directly interacts with LEF1 also shows no differential expression after β -catenin overexpression (Figure 43 D).

The overexpression of β -catenin shows that LEF1 is an important activator of the Wnt signaling pathway in erythroleukemic K562 cells. Megakaryocytic target genes are directly activated by this pathway. Erythroid genes on the other hand are unaffected. The *PRMT6* expression is unaltered by this pathway.

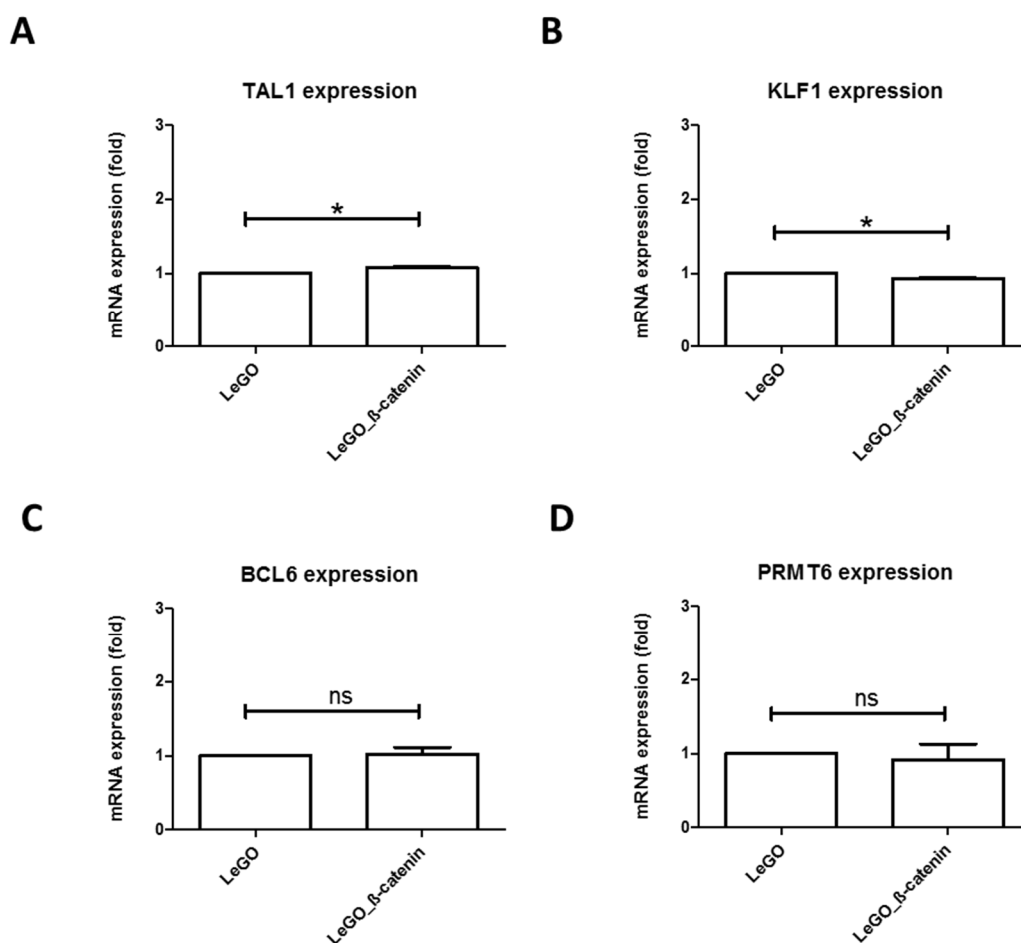


Figure 43: RNA expression of β -catenin over-expression vectors in erythroleukemic K562 cells, 7 days after transduction. The constantly active deltaN89- β -catenin was overexpressed. The expression was normalized to the reference gene *GAPDH* (A-D) *TAL1*, *KLF1*, *BCL6* and *PRMT6* do not show an increased expression after β -catenin overexpression. The error bars represent the standard deviations of at least 3 independent measurements and two independent transductions. The p-values were calculated using Student's t-test. *p < 0.05, **p < 0.01, *p < 0.001, ns: not significant.**

3.13 Verification of LEF1 binding sites in megakaryocytic cells

The previously described experiments were mostly performed in K562 cells, which show erythroleukemic characteristics like being CD235a positive. Also, the cells are able to spontaneously differentiate into megakaryocytic cells with TPA treatment, resulting in CD41 upregulation. Tetradecanoylphorbol acetate (TPA) is a protein kinase C (PKC) activator, which leads to the unspecific activation of several pathways.

A more specific approach is the use of TPO differentiation primary human CD34⁺ cells, in order to analyze if LEF1 takes an important role in megakaryocytic differentiation. The primary human CD34⁺ cells were differentiated with TPO for 10 days and the endogenous expression of LEF1 was analyzed in megakaryocytic cells. Whole cell lysates were produced after every 2 to 3 days of differentiation. Figure 44 shows the Western Blot analysis. LEF1 is constantly expressed in the first 10 days of megakaryocytic differentiation.

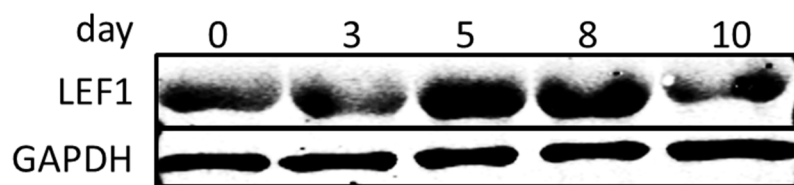


Figure 44: Western blot of the LEF1 expression in TPO differentiated CD34⁺ cells. Cell lysates were produced every 2 to 3 days. LEF1 is constantly expressed during the megakaryocytic differentiation. An antibody against GAPDH was used as loading control.

The previous experiment showed that the LEF1 protein is abundant in megakaryocytic cells. Chromatin precipitation was performed to analyze if the LEF1 is functional and able to bind to a megakaryocytic promoter. Figure 45 A shows the identified LEF1 peak at the *ITGA2B* (CD41) promoter from the analyzed ChIP-seq data.

Figure 45 B confirms that LEF1 directly binds to the *ITGA2B* (CD41) promoter of megakaryocytic differentiated cells. CD34⁺ cells which were expanded to hematopoietic cells show no binding of LEF1. The negative control shows no binding of LEF1 in both conditions (Figure 45 C).

PRMT6 binds to the promoter of *ITGA2B* in differentiated hematopoietic cells (Figure 45 D). It has been shown, that PRMT6 is recruited to the *ITGA2B* promoter in order to repress its expression (Herglotz et al., 2013). The binding of PRMT6 to the *ITGA2B* (CD41) promoter increases in megakaryocytic cells. PRMT6 is recruited by LEF1 to the promoter. The negative control (Figure 45 E) shows no enrichment of PRMT6 in both treatments.

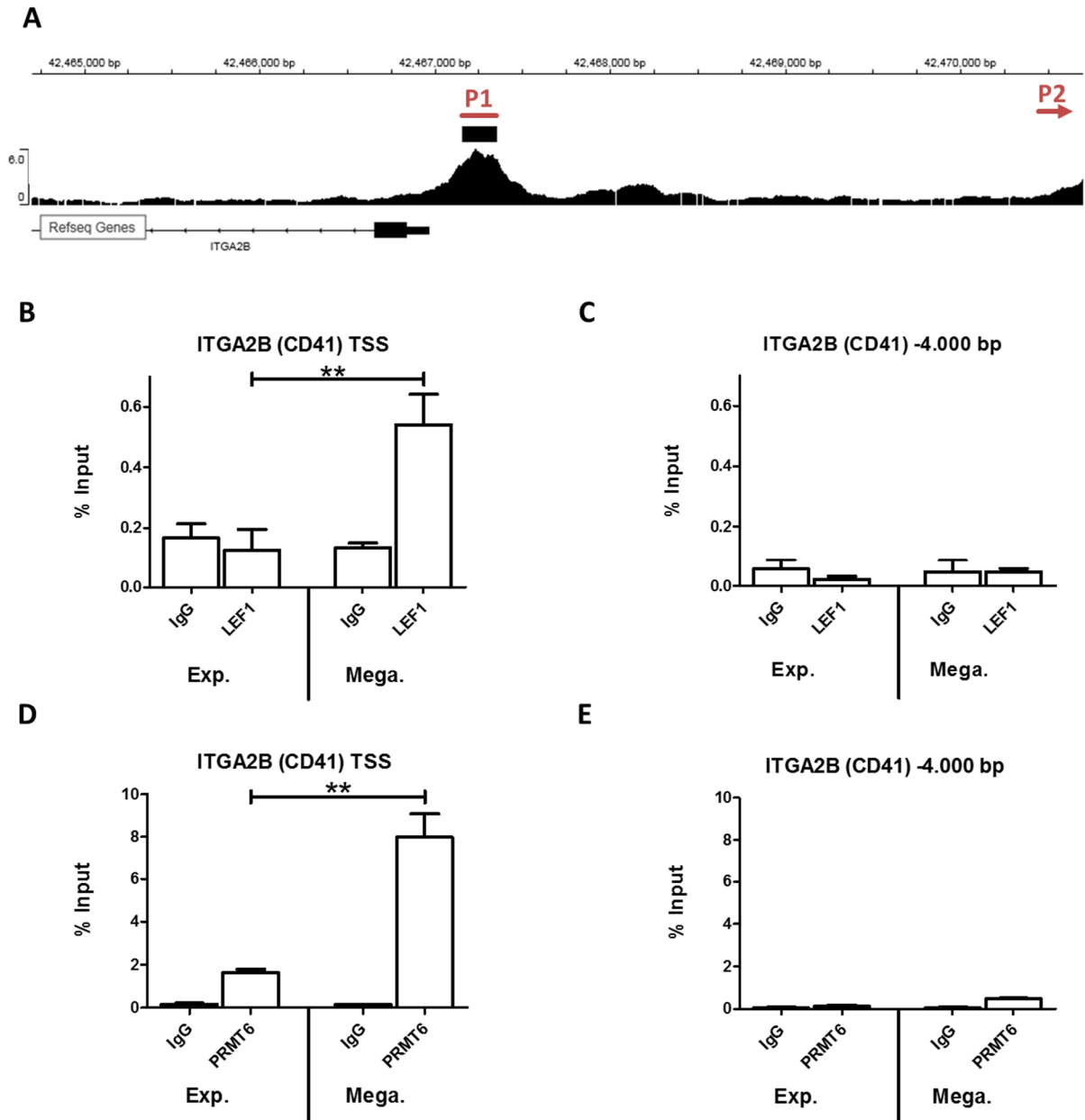


Figure 45: LEF1 binding during megakaryocytic differentiation. Verification of the identified LEF1 peak. The ChIP experiments were performed with CD34⁺ cells differentiated for 9 days in expansion medium and CD34⁺ cells differentiated for 9 days to megakaryocytes with TPO. (A) TSS of *ITGA2B* (chr17:42,464,701-42,470,700) in K562 cells. The gene models of hg19 refseq were used. The Y-Axis shows the enrichment over IgG control. P1 is the location of the primer pair at the TSS and P2 is a primer pair 4.000 bp upstream of the TSS (B) A strong LEF1 signal over background can be seen in TPO differentiated CD34 cells at the transcription start site. (C) -4000 bp upstream of the promoter, no LEF1 signal was detected. (D and E) PRMT6 binding at the promoter. ChIPs were performed with an anti-LEF1 antibody. Isotype-matched IgG antibodies were used as negative control. Bars represent the mean results, with SD derived from triplicates. The p-values were calculated using Student's t-test. *p < 0.05, **p < 0.01, *p < 0.001, ns: not significant.**

3.14 β -catenin overexpression in megakaryocytic cells

The previous experiment confirmed that PRMT6 and LEF1 are binding to the *ITGA2B* promoter in primary megakaryocytic differentiated cells. The next experiment was performed to analyze the effect of the activated Wnt signaling in megakaryocytes. Therefore, constantly active Δ N89 β -catenin was overexpressed in primary cells.

The β -catenin cDNA was cloned into the lentiviral overexpression LeGO vector. The undifferentiated human CD34⁺ cells were transduced with the Δ N89- β -catenin overexpression vector. The CD34⁺ cells were differentiated for 7 days to megakaryocytes with TPO. The GFP expression of the LeGO vector was used for positive selection via FACS and the RNA expression was measured 7 days after transduction.

β -catenin expression was highly increased by 8.2-fold compared to the control (Figure 46 A), confirming a successful transduction. The *PRMT6* expression was not affected by the overexpression (Figure 46 B), PRMT6 is not directly controlled by the Wnt signaling pathway. *LEF1* is activated by β -catenin overexpression in megakaryocytes. The expression is significantly increased by 1.7-fold (Figure 46 C). The megakaryocytic genes *RUNX1* and *ITGA2B* (CD41) are targets of β -catenin, the expression is increased 2.0-fold (Figure 46 D and E).

The analysis of the Wnt signaling pathway in the primary human CD34⁺ cells confirmed the findings of the analysis in the erythroleuemic K562 cells. The megakaryocytic transcription factor *RUNX1* and the megakaryocytic differentiation marker *ITGA2B* (CD41) are direct targets of LEF1, which recruits cofactors like PRMT6 and β -catenin to the promoter.

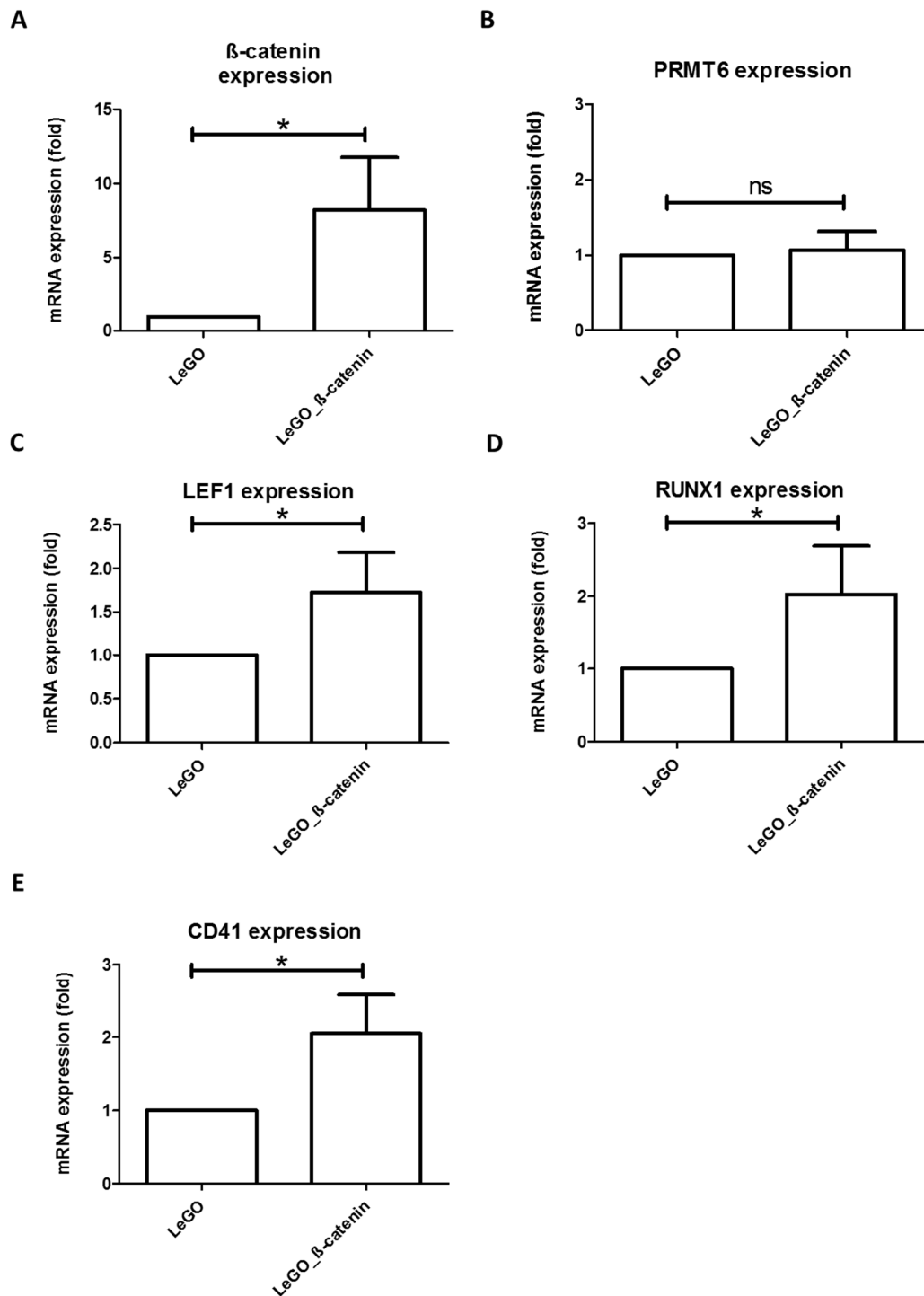


Figure 46: RNA expression of β -catenin overexpression vectors in TPO treated CD34⁺ cells, 7 days after transduction. The constantly active deltaN89- β -catenin was overexpressed. The expression was normalized to the reference gene GAPDH (A) The cells show increased β -catenin expression. (B) The *PRMT6* expression was not affected by the β -catenin overexpression. (C) The *LEF1* expression increased after β -catenin overexpression. (D-E) The megakaryocytic genes *RUNX1* and *ITGA2B* (CD41) showed increased expression. The error bars represent the standard deviations of at least three independent measurements and three independent transductions. The p-values were calculated using Student's t-test. *p < 0.05, **p < 0.01, ***p < 0.001, ns: not significant.

3.15 Expression analysis of erythroid and megakaryocytic cells

The experiments in this work showed that LEF1, PRMT6 and β -catenin target the promoters of several important megakaryocytic genes. The endogenous expression of these genes was analyzed in primary human CD34⁺ cells which were differentiated with EPO to erythroid cells for 9 days and differentiated with TPO to megakaryocytic cells for 9 days. Primary human CD34⁺ cells were expanded for two days and used as a control.

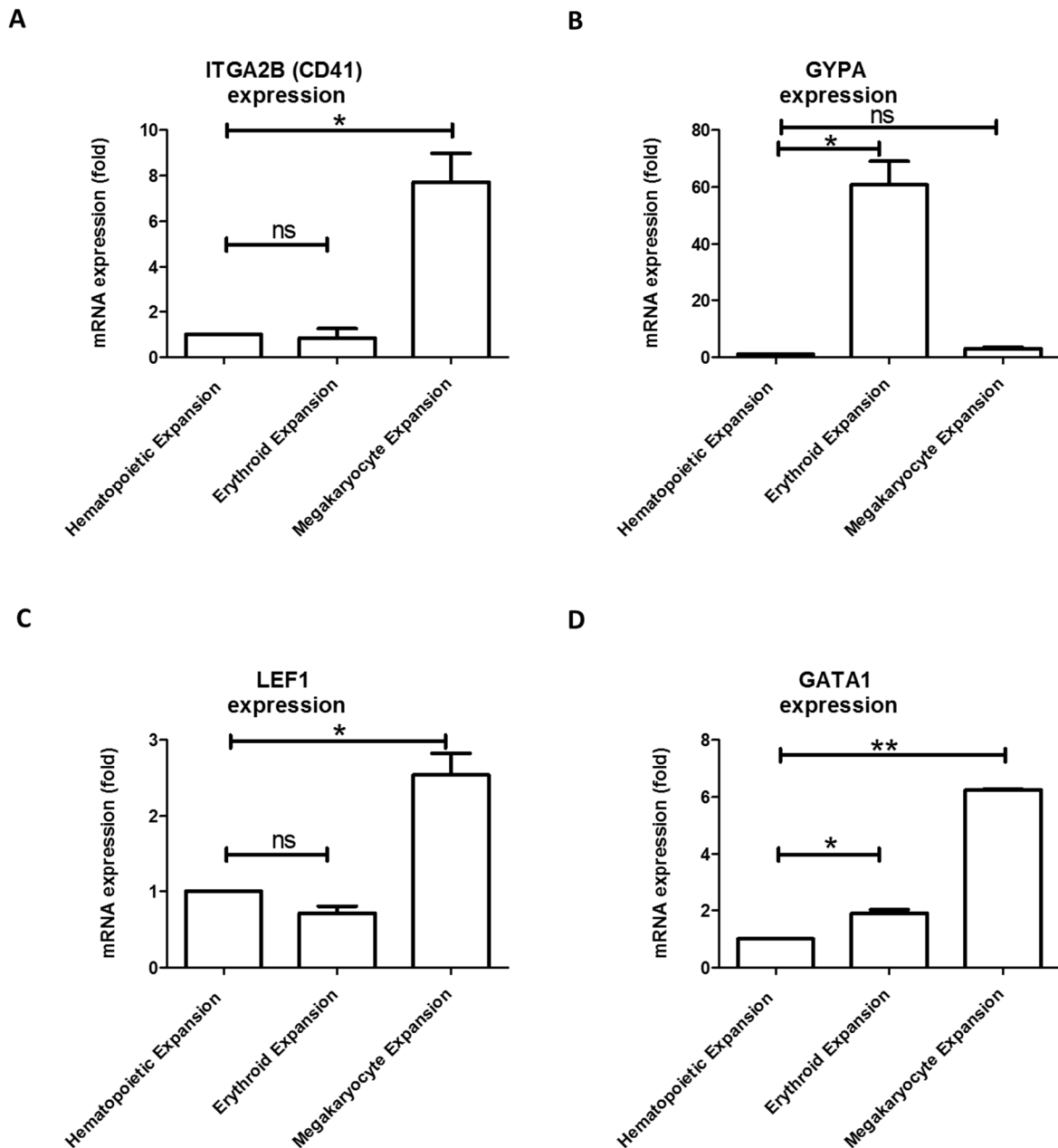


Figure 47: RNA expression of differentiated hematopoietic cells. CD34⁺ cells were differentiated for 2 days in expansion medium and CD34⁺ cells differentiated for 9 days to erythroid cells with EPO and to megakaryocytes with TPO. The expression was normalized to the reference gene *GAPDH*. (A) The *ITGA2B* expression was increased in megakaryocytes. (B) The *GYPA* expression was increased in erythroid cells. (C) *LEF1* expression was increased in megakaryocytes (D) *GATA1* expression was increased in erythroid cells and megakaryocytes. The error bars represent the standard deviations of at least three independent measurements and two independent experiments. The p-values were calculated using Student's t-test. *p < 0.05, **p < 0.01, ***p < 0.001, ns: not significant.

The efficiency of the differentiation process was measured by the analysis of expression markers. The expression of the LEF1 target gene *ITGA2B* (CD41) increased 7.7-fold in megakaryocytes and *GYP A* (CD235a) expression increased 60.7-fold in erythroid cells (Figure 47 A and B), confirming the successful differentiation of the cells.

The *LEF1* expression was increased after TPO treatment in megakaryocytes 2.5-fold (Figure 47 C). The expression was not increased after EPO treatment. This confirms that LEF1 is an important transcription factor of megakaryopoiesis. *GATA1* expression was increased 2-fold in erythroid cells and 6.2-fold in megakaryocytes (Figure 47 D). *GATA1* is an important transcription factor in erythroid and megakaryocytic differentiation (Fujiwara et al., 1996; Shivdasani et al., 1997).

The expression of the LEF1 target gene *RUNX1* was increased 1.5-fold in erythroid cells and 2.4-fold in megakaryocytes (Figure 47 A). *RUNX1* is an important regulator of the erythroid and megakaryocytic differentiation. (Herglotz et al., 2013; Herkt et al., 2018). *CCND1* was upregulated 4-fold in megakaryocytes (Figure 47 B). The protein promotes polyploidization in megakaryocytes and is necessary for thrombocyte production (Muntean et al., 2007). It is a direct target of LEF1. Similar to the *LEF1* expression, the *β -catenin* expression was increased in megakaryocytes and erythrocytes but is not significant. (Figure 47 C), where it selectively activates Wnt target genes like *LEF1*, *ITGA2B* and *RUNX1*. The *PRMT6* expression was slightly increased in erythroid cells and megakaryocytes (Figure 47 D). *PRMT6* controls the differentiation process of both the EPO and the TPO differentiation (Herglotz et al., 2013; Herkt et al., 2018).

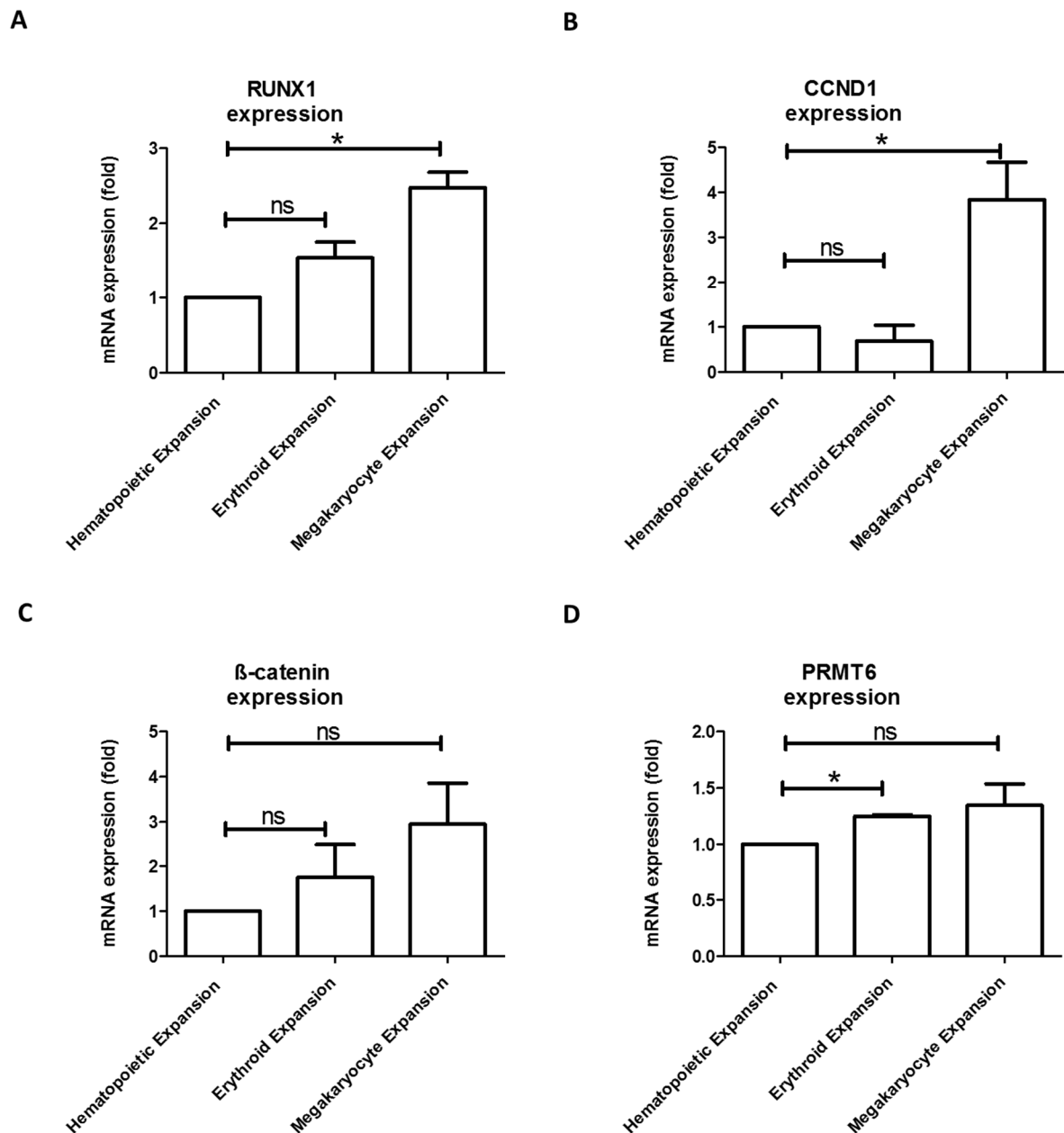


Figure 48: RNA expression of differentiated hematopoietic cells. CD34⁺ cells were differentiated for 2 days in expansion medium and CD34⁺ cells differentiated for 9 days to erythroid cells with EPO and to megakaryocytes with TPO. The expression was normalized to the reference gene *GAPDH*. (A) The *RUNX1* expression was increased in erythroid cells and megakaryocytes. (B) The *CCND1* expression was increased in megakaryocytes. (C) *β-catenin* expression was increased in erythroid cells and megakaryocytes (D) *PRMT6* expression was slightly increased in erythroid cells and megakaryocytes. The error bars represent the standard deviations of at least three independent measurements and two independent experiments. The p-values were calculated using Student's t-test. *p < 0.05, **p < 0.01, ***p < 0.001, ns: not significant.

The TCF/LEF1 family (Arce et al., 2006) consists of four member (Figure 9). The previous experiments showed, that the activation of the Wnt signaling pathway in K562 cells specially activates the expression of *LEF1* but not *TCF7*; *TCF7L1* and *TCF7L2*. *LEF1* activates the Wnt targets in K562 cells. The expression of *LEF1* was increased in TPO treated primary human CD34⁺ cells (Figure 47 C) similar to the increased expression in Wnt activated K562 cells. The transcription factors *TCF7*; *TCF7L1* and *TCF7L2* show no increased the expression after treatment with EPO or TPO (Figure 49). Only the transcription factor *LEF1* is activated during differentiation.

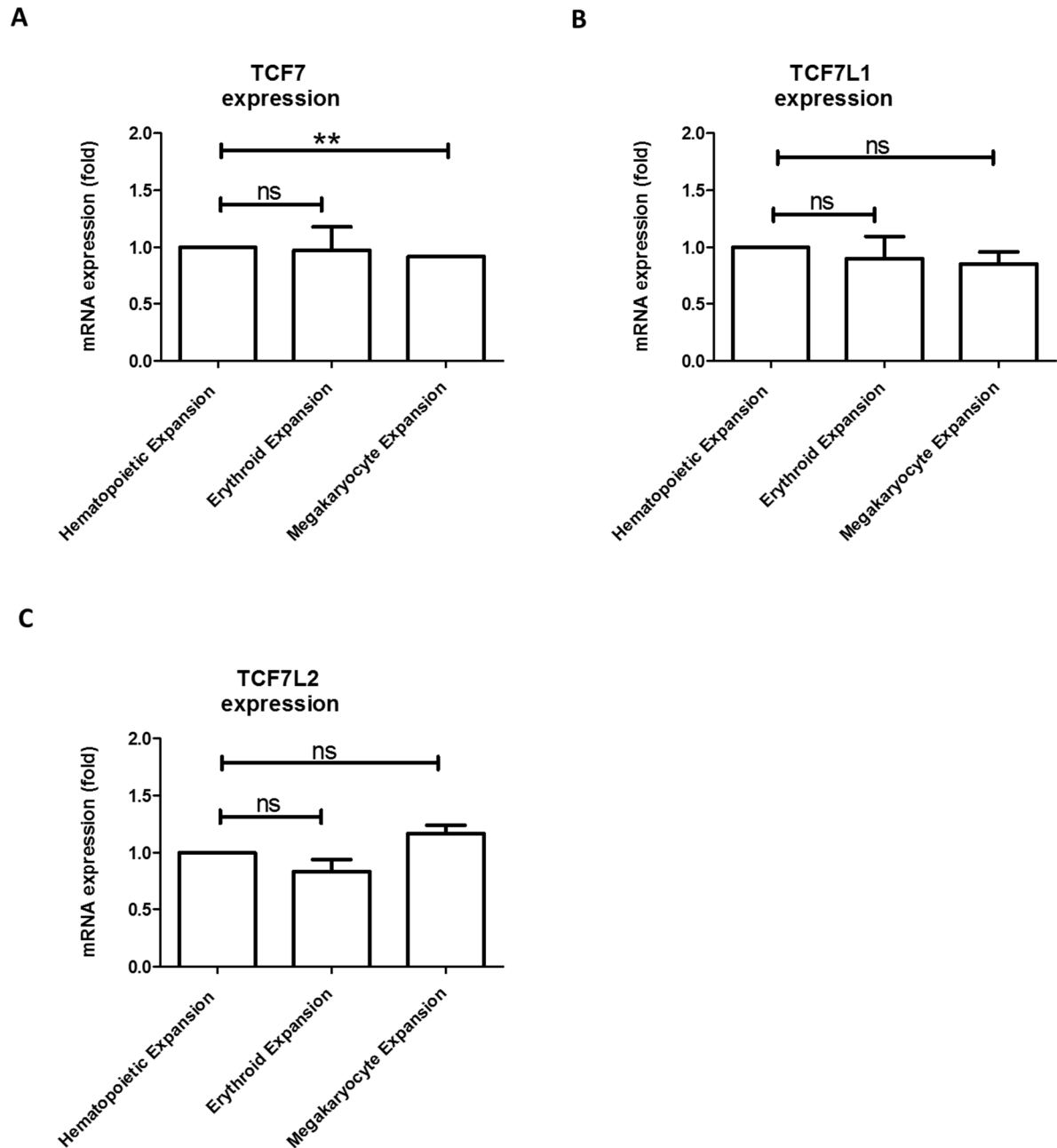


Figure 49: RNA expression of differentiated hematopoietic cells. CD34⁺ cells were differentiated for 2 days in expansion medium and CD34⁺ cells differentiated for 9 days to erythroid cells with EPO and to megakaryocytes with TPO. The expression was normalized to the reference gene *GAPDH*. (A - C) The controls *TCF7*; *TCF7L1* and *TCF7L2* show no increased expression after differentiation to erythroid cells and megakaryocytes. The error bars represent the standard deviations of at least three independent measurements and two independent experiments. The p-values were calculated using Student's t-test. *p < 0.05, **p < 0.01, ***p < 0.001, ns: not significant.

The experiments in human primary CD34⁺ cells confirmed that the PRMT6 interacting transcription factor LEF1 directly activates important megakaryocytic target genes like *ITGA2B* (CD41), *RUNX1* and *CCND1*. This activation is facilitated through an interaction with PRMT6 and Wnt pathway proteins like β -catenin. PRMT6 itself was identified as an important megakaryocytic regulator (Herglotz et al., 2013).

3.16 PRMT6 Knockdown shows a direct influence on the cell cycle

The previous experiments showed that the promoter of CCND1 is a direct target of the transcription factor LEF1. The overexpression and knockdown of LEF1 revealed that the transcription factor directly activates the expression of CCND1. Furthermore, the ChIP experiments showed that LEF1 recruits PRMT6 to the promoter region. The following experiments were performed to evaluate the impact of PRMT6 on CCND1. The erythroleukemic K562 cells were lentivirally transduced with pGIPZ shPRMT6 vectors for the specific knockdown of the PRMT6 gene. The cells were transduced with two different shPRMT6 RNAs to exclude unspecific influence of the pGIPZ vector backbone and the shLacZ RNA as negative control. The RNA expression was measured after 7 days of incubation. The pGIPZ vector contains a GFP marker which allowed for the positive selection of transduced cells with FACS measurements.

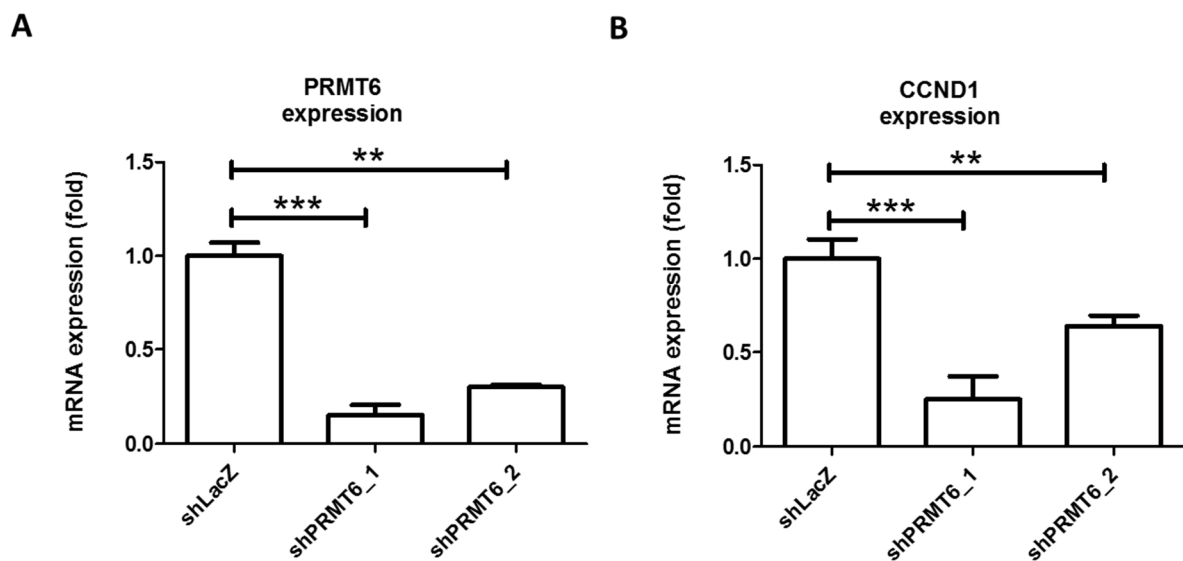


Figure 50: RNA expression of two separate pGIPZ shPRMT6 knockdown vectors in erythroleukemic K562 cells, 7 days after transduction. The expression was normalized to the reference gene GAPDH. (A) After the shRNA knockdown, the PRMT6 expression is reduced to less than 40 %. (B) The LEF1/PRMT6 target gene CCND1 (Tetsu and McCormick, 1999) is reduced in both PRMT6 knockdowns. The error bars represent the standard deviations of at least three independent measurements. The p-values were calculated using Student's t-test. *p < 0.05, **p < 0.01, *p < 0.001, ns: not significant.**

Both knockdowns of the two different shRNAs reduced the expression of PRMT6 to less than 30 % compared to the shLacZ control (Figure 50 A). The PRMT6 expression is in both cases significantly reduced. The CCND1 gene is a direct target of the LEF1 (Tetsu and McCormick, 1999). The expression was reduced to 27 % and 65 % by the PRMT6 knockdown (Figure 50 B).

CCND1 is an important regulator of the mitotic cell cycle and is required for the G1 phase progression. The protein accumulates during the G1 phase in the nucleus and degrades in the S phase of the mitotic cell cycle. Therefore, a cell cycle analysis was performed with DAPI staining. The transduced K562 cells were fixated with 70 % ethanol and measured in the Pacific Blue channel of the flow cytometer.

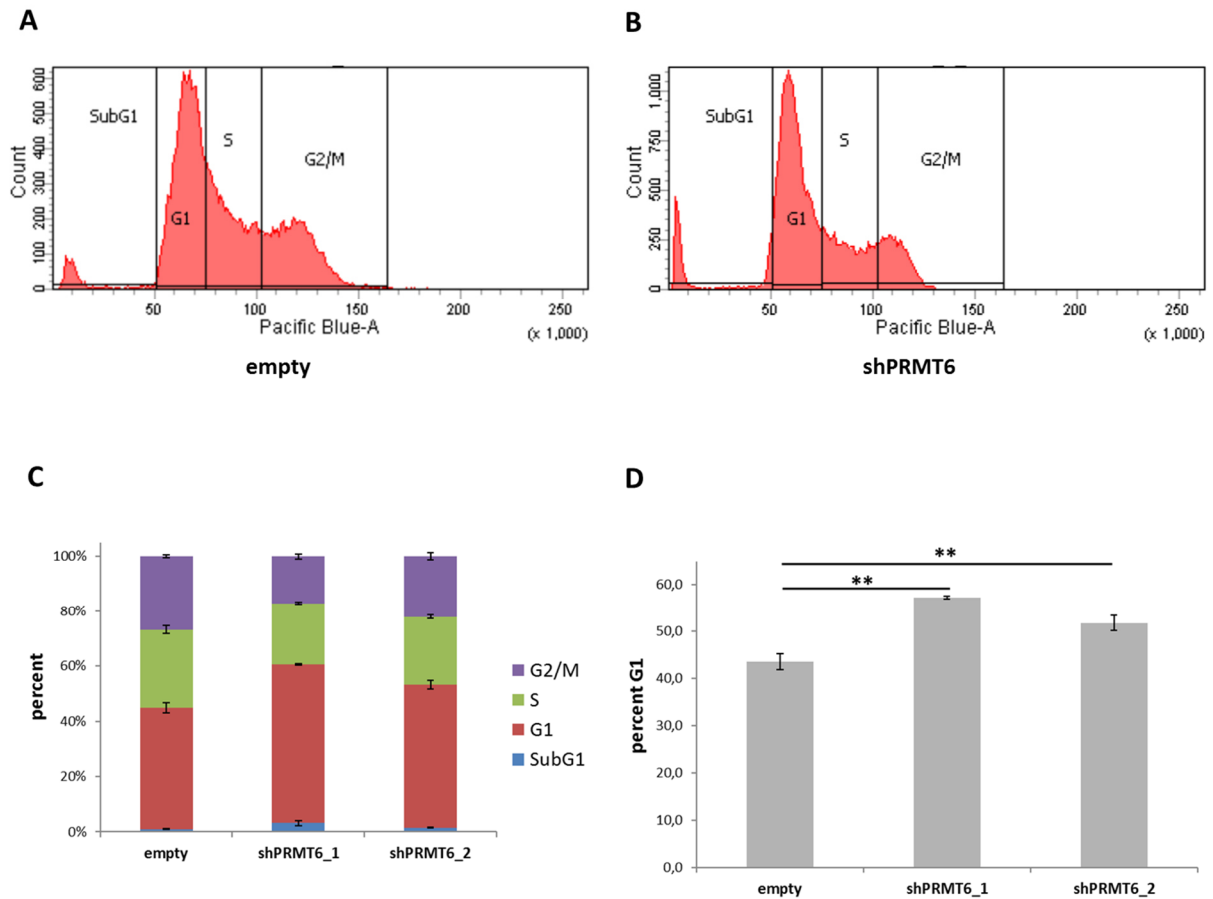


Figure 51: Cell cycle analysis of transduced K562 cells. The cells were fixated with 70 % ethanol, the double stranded DNA was DAPI stained. (A) Normal cell cycle progression of K562 cells transduced with the empty vector control. (B) Aberrant cell cycle progression of K562 cells transduced with shPRMT6. (C - D) The cell cycle analysis revealed an increased number of cells in the G1 phase after PRMT6 knockdown; G1 (Gap 1); S (Synthesis); G2 (Gap 2); M (mitosis). The error bars represent the standard deviations of at least three independent measurements. The p-values were calculated using Student's t-test ****p < 0.01**.

The cell cycle analysis upon PRMT6 knockdown revealed that the enzyme influences the mitotic cell cycle progression. The knockdown of PRMT6 downregulated *CCND1* expression and increased the number of cells which reside in the G1 phase of the mitotic cell cycle. Therefore, the fraction of the S phase and the G2/M was reduced after knockdown. The data shows that PRMT6 partly acts through the LEF1 target *CCND1* to regulate the cell cycle.

4 Discussion

The protein arginine methylase PRMT6 is an important regulator in the development of hematopoietic cells. Several publications have shown that PRMT6 directly targets the megakaryocytic-erythroid bifurcation. This particular branching point was intensely studied, and it has been shown that the transcription factor RUNX1 recruits PRMT6 to promoters of target genes to form a repression complex. Megakaryocytic targets are CD41, *miR27a*, CD42b, *TSP-1*, *PU.1* and *NF-E2* (Herglotz et al., 2013). Similarly, erythroid targets like KLF1 and GYPA are regulated by the RUNX1/PRMT6 repression complex (Kuvardina et al., 2015; Herkt et al., 2018). Therefore, this complex directly controls the production of erythrocytes and platelets.

Depending on the cellular background, PRMT6 is able to form other regulatory complexes. In a lung cancer model, PRMT6 interacts with the interleukin-enhancer binding protein 2 (ILF2), where it potentiates the tumor progression (Avasarala et al., 2020). In primary mouse embryonic fibroblasts (MEFs), the NF-kappa-B (RELA) transcription factor binds to PRMT6 and facilitates interleukin 6 expression (Di Lorenzo et al., 2014). A mass spectrometric analysis of the PRMT6 interactome in the pluripotent human embryonal carcinoma cell line NTERA-2 showed the transcription factors ILF2 and ILF3 as possible interaction partners (Stein, 2011). A ChIP-seq study in the NTERA-2 cell line revealed that PRMT6 is highly enriched at the binding motifs of transcription factors like GATA1, HBP1, RARA, V-ERBA, CEBPA and YY1, which are important in the myeloid and megakaryocytic-erythroid differentiation (Nötzold, 2015).

Due to its importance in the megakaryocytic-erythroid bifurcation and the ability to interact with many different transcription factors, PRMT6 has been chosen to be used to identify new factors controlling this branching point. For this purpose, the well-studied erythroleukemia cell line K562 was used for the interaction studies as it also shows a high endogenous expression of PRMT6. Stable Isotope Labeling with Amino acids in Cell culture (SILAC) with birA-biotin tag affinity purification and the subsequent quantitative mass spectrometry showed to be suitable to decipher the interaction between transcription factors and cofactors (Kolodziej et al., 2014). PRMT6 complexes were successfully isolated with the method and the hematopoietic interactome was analyzed.

4.1 PRMT6 interactome

The successful quantitative mass spectrometry revealed a PRMT6 interactome of 177 potential interaction partners. 74.5 % of these proteins were annotated to be subcellular distributed in the nucleus, supporting the finding that PRMT6 is entirely located in the nucleus (Herrmann et al., 2009). 48 of these proteins are transcription factors or epigenetic cofactors, proving that PRMT6 is involved in highly complex transcriptional processes. Nine of these proteins are already known factors of hematopoietic development. The interaction of PRMT6 with two of these identified factors were already published: PRMT1 and RUNX1, serving as a positive control.

Förster resonance energy transfer measurements showed that PRMT6 is not only able to homodimerize, but is also able to build heterodimers with PRMT1 (Thomas et al., 2010). This finding opens the question to the nature of this interaction, as PRMT1 is targeting H4R3, which has an

activating role in transcription. PRMT6 itself is targeting H3R2 which results in the repression of transcription. (Yang and Bedford, 2013). This contrast can be explained by the fact, that both PRMTs have a 31.94 % sequence identity of the amino acid alignment, sharing the same conserved catalytic domains. This suggests that PRMT1 and PRMT6 are able to heterodimerize because of similarity and not functionality. A quantitative mass spectrometry analysis of a non-overexpression system is necessary to decipher this question.

PRMT1 itself has been identified as an important factor of erythroid differentiation (Hua et al., 2013). The study revealed that the overexpression of PRMT1 promotes erythroid differentiation in erythroleukemic K562 cells and primary human CD34⁺ cells. PRMT1 upregulates erythroid factors like *GATA1*, *KLF1*, hemoglobin and the surface marker glycoprotein A (*GYPA*). Also the interaction of PRMT6 and RUNX1 could be verified again, which was intensively studied as a central functional component in the megakaryocytic-erythroid bifurcation, there it directly represses the expression of key factors of differentiation (Herglotz et al., 2013; Kuvardina et al., 2015; Herkt et al., 2018). The pulldown assay of biotinylated PRMT6 in K562 cells precipitated endogenous RUNX1, confirming the previous studies.

Beside PRMT1 and RUNX1, a list of previously unknown PRMT6 interacting factors was identified. The factors GATA2, SOX6 and KLF1 are all extensively studied in their role in erythroid differentiation. GATA2 is expressed in early erythroid progenitors, probably representing the state of hematopoietic development in which the erythroleukemic K562 cells reside. Here it serves to regulate HSC maintenance and proliferation. During the erythroid development GATA2 is repressed and the levels of GATA1 increase (Ferreira et al., 2005). GATA1 itself control the production of erythrocytes by activating the heme biosynthesis (Orkin, 1992) and the production of alpha- and beta globin (Evans et al., 1988).

SOX6 shows some similarities to LEF1 as it contains a conserved high mobility group (HMG) DNA-binding domain. Interestingly SOX6 is able to downregulate the CCND1 expression and interacts directly with beta catenin (Iguchi et al., 2007). Overexpression of SOX6 in erythroleukemic K562 cells and primary human cord blood CD34⁺ cells induced erythroid differentiation and hemoglobinization in both models (Cantù et al., 2011). KLF1 is a transcription factor which controls a wide range of the terminal erythroid differentiation and directly targets genes like alpha- and beta- globin and the heme biosynthesis (Tallack et al., 2010).

Interestingly, a network analysis of protein interaction data showed a relationship of the nine identified hematopoietic transcription associated proteins. The described transcription factors SOX6, GATA2, RUNX1 and LEF1 constitute an interaction network with the co-factors and histone modifiers PRMT1, PRMT6 and β -catenin. The LEF1 transcription factor is significant in this network, as it is able to interact with RUNX1, β -catenin and PRMT6. The impact of RUNX1 and PRMT6 on the megakaryocytic-erythroid bifurcation is well studied (Herglotz et al., 2013; Kuvardina et al., 2015; Herkt et al., 2018). But due to the fact that the role of the LEF1/ β -catenin interaction was not explored in this bifurcation, LEF1 was chosen for further investigation.

The three remaining factors which do not cluster in the protein network are GON4L, CHD2 and NKAP. All of them are part of the hematopoietic differentiation. Studies in zebrafish and mice showed, that GON4L (Gon-4 Like) is essential during hematopoietic development. The Protein interacts with the transcription factor YY1 (Yin Yang 1) and the transcriptional co-repressors Sin3a and HDAC (Lu et al., 2011). The chromodomain helicase DNA binding protein 2 (CHD2) affects hematopoietic stem cell differentiation. Chd2 knockout experiments in mice indicated a different hematopoietic cell distribution. Mutants showed a deficiency in erythroid differentiation and an increase in the number of megakaryocytes (Nagarajan et al., 2009). NFKB Activating Protein (NKAP) is a transcriptional repressor which regulates the Notch signaling pathway. It associates with HDAC3 and is required for T cell development (Pajerowski et al., 2009).

4.2 LEF1 is a new interaction partner of PRMT6

Several nodes of the newly identified protein interaction network were confirmed with Co-Streptavidin Precipitation in HEK293T cells. The biotin tagged bait was co-transfected with the prey protein. After 48 hours of incubation, whole cell lysates were analyzed by western blot. The interaction of RUNX1 and PRMT6 was verified again, confirming the previous findings of (Herglotz et al., 2013). Likewise, the interaction of PRMT1 and PRMT6 is reproducible in the HEK293T cells.

The newly identified interaction partner LEF1 was verified in the co-transfection experiment. Direct protein-protein interaction between LEF1 and PRMT6 was shown in K562 cells and was not an artefact of the quantitative SILAC mass spectrometry. Furthermore, the verified interaction between LEF1 and RUNX1 supports the model that an orchestra of different transcription factors recruits PRMT6 to promoter regions. This was also shown for several parts of the Wnt signaling pathway. The interaction of RUNX1 with LEF1 leads to the repression of the T cell receptor (TCR) enhancers alpha and beta (Levanon et al., 1998). The repression is performed by the recruitment of TLE/Groucho corepressors by the transcription factors. ChIP-seq analysis in CD4⁺CD8⁺ thymocytes confirms the interaction between RUNX1 and LEF1 (Emmanuel et al., 2018). The DNA binding sites of LEF/TCF1 overlap with RUNX1 in this cell type suggesting a complex orchestration. Target genes of these complex were DNA polymerase subunit gamma (POLG) and TCF1.

The TOP-flash assay was utilized to verify the impact of the LEF1 and PRMT6 interaction on promoter level. These TCF/LEF1 consensus site containing luciferase vectors are widely used in Wnt signaling research (Molenaar et al., 1996). The assay showed that PRMT6 has a dose-dependent effect on the transcriptional activity of LEF1. Co-transfection of LEF1 with constantly active β -catenin led to a severely increased TOP/FOP ratio. This effect was reduced by the co-transfection of increased amounts of PRMT6. The TOP-flash assay showed that PRMT6 directly displaces β -catenin from promoter regions, facilitated by the binding of LEF1.

4.3 LEF1 and PRMT6 in myeloid cells

RNA and protein expression analysis of LEF1 in myeloid cells revealed that this transcription factor is present in the erythroleukemic cell lines K562, HEL and TF-1. The myeloid cell lines U937 and Kasumi do not show a detectable amount of LEF1. Similar results were shown in a study of the β -catenin

nuclear localization in myeloid cells (Morgan et al., 2019). LEF1, TCF4, AXIN1 and β -catenin were identified to be nuclear abundant in the erythroleukemic K562 and HEL cells. The myeloid cell line U937 shows no expression of the described proteins. Wnt signaling activation by treatment with the GSK3 β inhibitor CHIR99021 led to the stabilization of β -catenin in K562 and HEL cells. The stabilization supports the translocation of β -catenin into the nucleus. This effect was not observed in the U937 cell line. The same studied analyzed primary AML patient blasts, which show LEF1 and β -catenin proteins localized in the cytoplasm and nucleus (Morgan et al., 2019).

In addition LEF1 has been identified to be crucial for neutrophil granulocytopoiesis (Skokowa et al., 2006). It could be shown that overexpression of LEF1 in CD34⁺ cells promoted increased cell proliferation. LEF1 directly activated the expression of *CCND1*, *Survivin* and *MYC*. It also promoted the proliferation of CD33⁺ granulocyte committed cells and activated target genes like *CEBPa* and *GCSR*. Knockdown of LEF1 revealed to be anti-proliferative and pro-apoptotic in CD34⁺ cells. Also, the expression of the mentioned target genes was severely reduced. Interestingly the knockdown of β -catenin did not lead to a reduced proliferation, suggesting a β -catenin independent effect of LEF1.

These experiments show that LEF1 is present in a variety of myeloid cells and particular in cells which are committed to the erythroid/megakaryocytic bifurcation. This observation was further analyzed by target gene identification of the LEF1 transcription factor.

PRMT6 was identified as important regulator in myeloid cells. PRMT6 controls the erythroid differentiation and gene expression in human hematopoietic progenitor cells (Herkt et al., 2018). The enzyme is recruited by RUNX1 to erythroid genes during megakaryocytic differentiation and represses genes like *glycophorin A (GYPA)*. It is also recruited to the *KLF1* promoter and represses its expression during megakaryocytic differentiation (Kuvardina et al., 2015). The expression of PRMT6 is down regulated during megakaryocytic differentiation which leads to the upregulation of its target *ITGA2B* (CD41) (Herglotz et al., 2013). LEF1 and PRMT6 are both important in myeloid differentiation as they both target genes of erythropoiesis and megakaryopoiesis.

4.4 Identification of target genes of LEF1 and PRMT6

In order to understand that LEF1 is expressed in erythroleukemic cell lines, ChIP-seq data from the ENCODE project (ENCODE Project Consortium, 2012; Davis et al., 2018) were analyzed. The analysis of LEF1 ChIP data revealed that the transcription factor is functional in K562 cells, and targets specifically the promoter regions of the genome. Nearly a quarter of peaks is directly located at the transcriptional start sites of genes. In addition, the gene ontology analysis revealed that LEF1 is targeting genes controlling the megakaryocyte differentiation (GO:0030219). Amongst other, the promoters of the megakaryocytic differentiation marker *ITGA2B* (CD41), the transcription factor *TAL1* and the megakaryocyte growth factor Thrombopoietin (*THPO*) are targeted by the transcription factor LEF1. This global genomic analysis of LEF1 in the erythroleukemic cell line K562 revealed that the transcription factor has a currently unknown role in the megakaryocytic differentiation.

The specific LEF1 peaks of different cell lines were compared in order to analyses if the binding to megakaryocytic promoters is specific for hematopoietic cell lines. The peaks of erythroleukemic K562

cells were compared with peaks of human embryonic kidney HEK293T cells. Interestingly, LEF1 targets the promoter of *Axin2* in K562 and HEK293T cells. *Axin2* expression is increased after Wnt/ β -catenin signaling activation and operates in a negative feedback loop to destabilize the localization of β catenin in the nucleus (Jho et al., 2002). These findings show that LEF1 mediates this feedback loop in different cell lines, and presumably in a universal manner in all LEF1 expressing cell types. On the other hand, LEF1 shows specific binding on megakaryocytic promoters in the hematopoietic cell line, which is absent in the embryonic kidney cell line, suggesting a cell type specific recruitment of the transcription factor. The promoters of *ITGA2B* and *THPO* are only targeted in K562 cells. This difference can be explained with the fact that megakaryocytic genes are targeted by an orchestra of different transcription factors (Tijssen et al., 2011). Compared analysis of different ChIP seq experiments from ENCODE showed that *ITGA2B* is targeted by the hematopoietic transcription factors GATA1, LEF1 and TAL1. Also, the interaction partner RUNX1 is directly binding to the promoter (Herglotz et al., 2013). The comparison of different TCF/LEF transcription factors showed that the *ITGA2B* promoter is targeted only by LEF1. Binding of the factors TCF7 and TCF7L2 could not be shown, which suggests that LEF1 is the important transcription factor of the TCF/LEF family in the megakaryocytic differentiation. The common Wnt/ β -catenin target *Axin2* instead showed binding of all three factors: LEF1, TCF7 and TCF7L2.

The newly identified LEF1 target *ITGA2B* (CD41) was verified in ChIP qPCR experiments in K562 cells. The peak at the transcription start site could be validated. The lentiviral overexpression of LEF1 in K562 cells even increased the binding to the promoter, supporting the findings. Also, it seems that LEF1 is recruiting PRMT6 to the promoter region, as after LEF1 overexpression, the PRMT6 binding is slightly increased at the LEF1 binding peak. This agrees with the observation, that the LEF1 interaction partner RUNX1 is recruiting PRMT6 to the *ITGA2B* promoter (Herglotz et al., 2013).

The important transcription factor RUNX1 is crucial in the control of the megakaryocyte/erythroid branching point (Kuvardina et al., 2015), by regulating important factors like *KLF1*. The RUNX1 locus itself is rather complex, spanning an area of about 260 kb. The expression is controlled by two different promoters, which are located 160 kb apart from each other (Levanon et al., 2001). A putative enhancer 20 kb upstream of the TSS was identified, which is occupied by the hematopoietic transcription factors RUNX1, TAL1, GATA2 and LEF1. Lentiviral overexpression of LEF1 increased the binding of LEF1 and PRMT6 at the enhancer. Therefore, *RUNX1* itself was identified as a new target of the Wnt/ β -catenin pathway.

The *CCND1* promoter has been identified as a direct target of TCF/LEF1 transcription factors (Tetsu and McCormick, 1999). β -catenin controls the expression of *CCND1* in colon carcinoma cells, mediated by members of the LEF1/TCF family. The promoter has been chosen as positive control for LEF1 binding, and after overexpression of LEF1 in K562 cells the binding of the transcription factor was increased. Overexpression also resulted in the increased recruitment of PRMT6 to the *CCND1* promoter. Given the fact that LEF1 overexpression increased the *CCND1* expression by itself, it could be possible that PRMT6 is supporting this effect. Conditional PRMT-overexpressing mouse models

show a similar effect (Bao et al., 2018). Overexpression of PRMT1 or PRMT6 in mice increased the amount of CCND1 protein. Overexpression of PRMT4 had no effect on CCND1.

4.5 Verification of LEF1-PRMT6 target genes

The analysis of ChIP-seq data showed that *ITGA2B* (CD41) is a direct target of the transcription factor LEF1. These findings were verified with pGIPZ shRNA vectors. K562 were lentiviral transduced with to different knockdown shLEF1 RNAs. The reduced LEF1 expression led to a reduced *ITGA2B* expression and verified it as a LEF1 target. The expression of the known target genes *MYC* (He et al., 1998) and *CCND1* (Tetsu and McCormick, 1999) were also reduced. The transduction of human CD34⁺ progenitors with a LEF1 knockdown construct showed similar results (Skokowa et al., 2006). The authors showed that the expression of the target genes *CCND1* and *MYC* were significantly reduced after the knockdown. The knockdown of β -catenin had no effect on the expression of the LEF1 target genes. Similar knockdown experiments with shPRMT6 in K562 cells showed that PRMT6 targets *ITGA2B*. Downregulation of the expression of PRMT6 reduced the repressive effect of PRMT6 and *ITGA2B* was upregulated (Herglotz et al., 2013). This effect could be connected to the transcription factor LEF1.

The full length LEF1 and the truncated dominant negative LEF1 constructs were lentiviral transduced into K562 cells, in order to verify an opposite effect as the knockdown. Remarkably, the overexpression did not lead to an altered expression profile of the megakaryocytic target genes *ITGA2B* and *RUNX1*, suggesting that LEF1 is not able to recruit activators of gene expression to the promoters. Although the ChIP PCRs showed that overexpressed LEF1 is binding to the promoter regions but is by itself as a transcription factor unable to alter the expression of the target gene.

On the other hand, the positive control *CCND1* was upregulated by the overexpression of LEF1. This effect was shown also in CD34⁺ cells; lentiviral overexpression of LEF1 in human CD34⁺ progenitors directly promoted the upregulation of *CCND1* (Skokowa et al., 2006). This is particularly interesting as the truncated dominant negative LEF1 gene is missing the β -catenin binding motive and is therefore unable to recruit this activator to the *CCND1* gene. Nevertheless, also the truncated LEF1 protein increases the *CCND1* expression, suggesting that LEF1 recruits other activation proteins beside β -catenin to the promoter region.

This protein is probably PRMT6, the enzyme was identified as an activator of CCND1 expression. A PRMT6 overexpression mouse model revealed that PRMT6 upregulates the expression of *CCND1* and *ITGA2B* (Bao et al., 2018). Both genes are direct target genes of LEF1. Also, a group of protein arginine methyltransferases has been identified to regulate the Wnt/ β -catenin-signaling pathway (Cha and Jho, 2012). The results of this thesis suggest that PRMT6 and β -catenin target common megakaryocytic genes to regulate their expression.

4.6 LEF1 participates in the megakaryocytic differentiation

The overexpression of LEF1 in K562 cells did not increase the expression of megakaryocytic target genes like *ITGA2B* and *RUNX1*. Although the analysis of transcription factor promoter binding through ChIP-qPCR revealed that the overexpressed LEF1 is binding directly to these targets. This

question was addressed by the overexpression of a LEF1 coactivator. The truncated constantly active Δ N89 β -catenin was lentiviral overexpressed in K562. The truncated β -catenin lacks GSK-3 β phosphorylation sites and therefore cannot be degraded and the Wnt signaling pathway is stabilized. After overexpression of β -catenin the expression of *Axin2* increased. *Axin2* functions as a negative feedback loop of Wnt signaling (Jho et al., 2002), proving that the overexpression successfully activated the Wnt signaling pathway.

β -catenin also increased the expression of *LEF1* in K562 cells but did not activate any other transcription factor of the LEF/TCF family. The expression of *TCF7*, *TCF7L1* and *TCF7L2* kept unaltered. This data suggests that LEF1 is the sole important member of the transcription factor family in the erythroleukemic K562 cells, when the Wnt/ β -catenin signaling pathway is activated.

LEF1 activated together with β -catenin the expression of the megakaryocytic target genes *ITGA2B* (CD41) and *RUNX1*, revealing the importance of the Wnt pathway on megakaryopoiesis. This effect is restricted on megakaryocytic genes, as the analysis showed that important erythroid target genes were unaffected. The expression of *TAL1*, *KLF1* and *BCL6*, all important erythroid transcription factors stayed unaffected after β -catenin overexpression. The same genes are targeted by the enzyme PRMT6. *ITGA2B* (CD41) (Herglotz et al., 2013), *KLF1* and *GYP A* (Herkt et al., 2018) are regulated by PRMT6. Therefore, PRMT6 controls megakaryocytic differentiation.

4.7 LEF1-PRMT6 interaction in megakaryocytic cells

The finding that LEF1/ β -catenin support the expression of megakaryocytic genes was tested in TPO differentiated primary human CD34⁺ cells. Western blot analysis of LEF1 expression showed that the transcription factor is abundant through the TPO differentiation, supporting the theory that it is functional in megakaryopoiesis. CHIP-qPCR analysis of TPO differentiated CD34⁺ cells reveal that the *ITGA2B* (CD41) promoter is occupied by LEF1. Undifferentiated cells did not show LEF1 binding on the promoter. PRMT6 which was identified as a LEF1 interaction is recruited to the promoter region as well. This suggests that PRMT6 is recruited by LEF1 to the *ITGA2B* (CD41) promoter in order to activate its transcription during megakaryocytic differentiation.

The previous experiment showed that overexpression of constantly active β -catenin increases the expression of LEF1 and other megakaryocytic genes in K562 cells. This experiment was repeated in primary human TPO differentiated CD34⁺ cells. The activation of the Wnt signaling pathway through β -catenin led to the same results. The LEF1 expression was increased as also the expression of the megakaryocytic marker *ITAG2B* (CD41) and the megakaryocytic transcription factor *RUNX1*. This proves that the Wnt signaling is directly promoting megakaryocytic differentiation.

Similar results were shown in a double transgenic mouse model (Yalcin, 2018). Wnt-signaling was activated by the stabilization of the β -catenin protein in hematopoietic cells. The stabilization was driven by the promoter of the platelet derived growth factor b (PDGFb) which is only active in megakaryocytes and platelets. The specific activation of the Wnt-signaling pathway increased the expression of the megakaryocytic transcription factors *RUNX1* and *FLI1*. Stabilization of β -catenin increased the abundance of megakaryocytes in the spleen and the bone marrow. Despite the

increased amount of megakaryocytes, thrombopoiesis was not affected in this mouse model. Thrombocytes were not increased in the blood samples, suggesting that the Wnt-signaling pathway controls the maturation of megakaryocytes, but not the release of thrombocytes into the blood stream.

The impact of the LEF1/ β -catenin/Wnt signaling was further analyzed in primary hematopoietic cells. Primary human CD34⁺ cells were differentiated with EPO treatment to erythroid cells and with TPO treatment to megakaryocytic cells. Successful differentiation was confirmed with enhanced *GYP A* (CD235a) expression in erythroid cells and enhanced *ITGA2B* (CD41) expression in megakaryocytic cells. *LEF1* and *β -catenin* expression were highly increased in megakaryocytic cells, supporting the theory that the Wnt signaling pathway is significant for platelet production. The expression of the target gene *CCND1* was highest in the TPO treated cells possibly promoting polyploidization in the megakaryocytes.

4.8 PRMT6 targets the cell cycle regulator CCND1

CCND1 was identified as a GATA1 target in megakaryocytic but not in erythroid differentiation (Muntean et al., 2007). *CCND1* expression is necessary for polyploidization of the megakaryocytes. GATA1 deficient megakaryocytes show a reduced *CCND1* expression as well as growth and ploidy defects. Ectopic *CCND1* expression rescues the phenotype in part, by increasing cell size and polyploidization. Other defects of the GATA1 deficiency like terminal maturation and proplatelet production were unaffected. Similar to LEF1, the megakaryocytic transcription factor RUNX1 activates the expression of *CCND1* (Strom et al., 2000). As it was shown that LEF1 and RUNX1 directly interact with each other (Kahler and Westendorf, 2003) and are both able to recruit activators like β -catenin (Li et al., 2019) to the promoter, it can be assumed that both transcription factors work in orchestra with GATA1 to activate *CCND1* expression to promote endomitosis and polyploidization in megakaryocytic cells (Muntean et al., 2007).

It has been shown that the protein arginine methyltransferase 6 activates the expression of *CCND1* and *ITGA2B* in an overexpression mouse model (Bao et al., 2018). This suggest that the interacting transcription factors RUNX1 and LEF1 are recruited to these promoters to activate their expression. The knockdown of LEF1 and PRMT6 led both to a reduction of the *CCND1* expression. The knockdown of PRMT6 itself increased the number of cells residing in the G1 phase. This leads to a cell cycle arrest and decreases proliferation. This is in line with other studies which show that PRMT6 is recruited to promoter elements of important cell cycle regulators like CDKN1A, CDKN1B, CDKN2A and *CCND1* (Kleinschmidt et al., 2012; Neault et al., 2012; Phalke et al., 2012).

4.9 The bone marrow microenvironment (BMM)

The bone marrow microenvironment (BMM) controls the development and differentiation of hematopoietic stem cells (HSCs). This stem cell niche receives different growth factors and cytokines from the surrounding cell types such as osteoblasts and other mesenchymal stroma cells (Kumar et al., 2018). Osteoblasts control the fate of HSCs through the Wnt inhibitor Dkk1 (Dickkopf-related protein 1). A fine-tuned secretion of Wnt signals plays multiple roles in the maintenance and

quiescence of the stem cells (Fleming et al., 2008). Overexpression of Dkk1 in osteoblasts leads to an inhibited Wnt signal in HSCs and accelerates their cell cycle. On the other hand, overexpression of β -catenin likewise reduces the quiescence, resulting in the exhaustion of the HSC pool. These findings suggest a very fine-tuned Wnt signaling pathway is necessary to sustain the HSC stem cell niche (Suda and Arai, 2008). Further it has been shown that the osteoblastic lineages are able to control the HSC maintenance through N-cadherins. These cadherins create cell-cell adhesions with neighboring HSCs. These adherens junctions build protein complexes with β -catenin, directly targeting the Wnt Signaling pathway (Nakamura-Ishizu and Suda, 2019).

Besides the control of the quiescence of HSCs, Wnt signals are known to influence a great part of the immune system and hematopoiesis. From the 19 mammalian WNT proteins, 8 are known to directly activate the canonical β -catenin signaling. Already 6 of them were identified to take part in CD34⁺ differentiation and T- and B-cell development (Staal et al., 2008)

The factors Wnt3a and Wnt10a were identified to be present in the bone marrow (Reya et al., 2000). Stimulation with the factors led to an increased proliferation of human bone marrow B-cell progenitors. Wnt3a was identified as possible myeloid growth factor (Luis et al., 2009). Progenitor cell differentiation was impaired in Wnt3a deficient mice. The frequency of common myeloid progenitors (CMPs) and granulocyte/monocyte progenitors (GMPs) was severely reduced, megakaryocyte erythroid progenitors (MEPs) on the other hand were unaffected. These findings suggest, that reduced Wnt signaling affects the development of primitive progenitor cells, but terminal differentiation is not impaired.

Although the β -catenin/Wnt signaling pathway is well studied in the different hematopoietic branches, only a few studies were performed on its impact on megakaryopoiesis. Experiments in the human megakaryocytic cell line CHRF288-11 showed that dose-dependent treatment with Wnt3a led to the stabilization β -catenin (Macaulay et al., 2013). The noncanonical agonist Wnt5a and the Wnt inhibitor DKK1 destabilized β -catenin. Murine fetal liver megakaryocytes were treated *ex vivo* with Wnt3a. The activation of the Wnt signaling pathway led to a dose-dependent increase of proplatelets. Furthermore, mouse experiments showed that low-density lipoprotein receptor-related protein 6 (LRP6) deficient fetal liver cells produce a reduced number of megakaryocytes. This confirms that a functionally Wnt pathway is necessary for platelet production.

TPO treatment in the thrombopoietin-dependent megakaryocytic cell line UT-7/TPO showed upregulation of the Wnt pathway (Soda et al., 2008). TPO induces the phosphorylation of GSK-3 β in a dose-dependent manner. This led to the stabilization of β -catenin in the megakaryocytic cells. Similar effects were achieved with Wnt3a treatment, which also led to β -catenin stabilization, showing that the megakaryocytic cells possess a functional Wnt signaling pathway. Treatment with TPO induced the expression of the LEF1 target gene *CCND1*, supporting the results of this thesis.

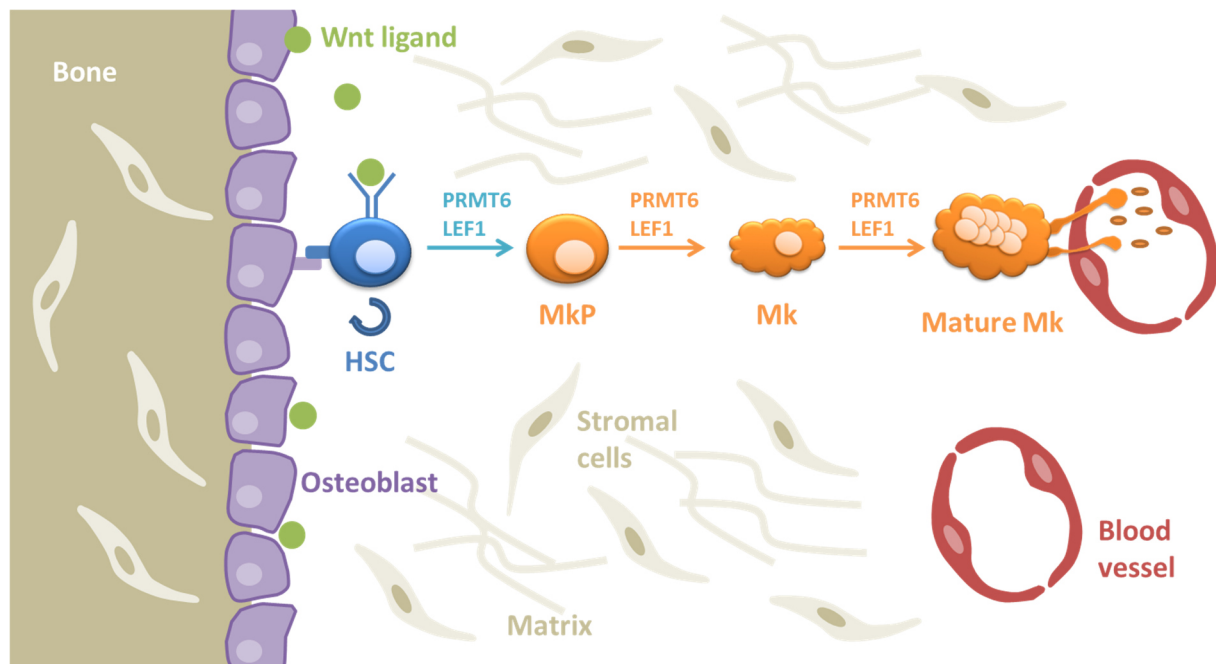


Figure 52: The bone marrow microenvironment (BMM): Osteoblasts use the β -catenin/Wnt signaling pathway to control the cell fate of HSCs. Osteoblasts secrete Wnt inhibitors and Wnt proteins to control the maintenance and quiescence of the stem cells. Additionally, osteoblasts create cell-cell adherens junctions with N-cadherins, directly interacting with intracellular β -catenin. The differentiation of the HSCs to megakaryocytes is facilitated by the transcription factor LEF1 and the cofactor PRMT6. The Wnt signals controlling this process are currently unknown. HSC: hematopoietic stem cell; MkP: megakaryocytic progenitor; Mk: megakaryocyte; modified after (Moore and Lemischka, 2006).

The cells of the bone marrow microenvironment like osteoblasts directly control the fate of the hematopoietic system through the LEF1/ β -catenin/Wnt signaling pathway shown in Figure 52. The results of this thesis show that LEF1 is an important transcription factor in the megakaryocytic differentiation. Important megakaryocytic genes like *ITGA2B* (CD41), *RUNX1* and *CCND1* are directly activated by LEF1/ β -catenin. The process which controls the Wnt signaling pathway to activate this differentiation is not determined yet. The current research shows that the bone marrow microenvironment regulates hematopoiesis through stromal cells like osteoblasts. These findings suggest that megakaryocytic differentiation could be controlled through Wnt signals secreted from osteoblasts and other mesenchymal stroma cells which control the sinusoidal-megakaryocyte niche (Day and Link, 2014). Also, the enzyme PRMT6 controls the important megakaryocytic genes like *ITGA2B* (CD41) and *CCND1* by directly being recruited to the promoters. PRMT6 was identified in this work as an interaction partner of LEF1. A group of PRMTs was identified to be directly associated with the Wnt signaling pathway (Cha and Jho, 2012). This is now also proven for PRMT6. The activation of the LEF1/ β -catenin/Wnt signaling pathway could activate the recruitment of PRMT6 to the LEF1 target genes in order to activate their expression.

4.10 Implications and outlook

This thesis revealed that LEF1 is an important transcription factor of the megakaryocytic development, under the control of the Wnt signaling pathway. LEF1 is able to interact with a variety of cofactors like PRMT6 and β -catenin and other megakaryocytic transcription factors like RUNX1. It must be assumed that LEF1 is recruited to each target promoter with an orchestra of different transcription factors, which all recruit a different set of cofactors, making the impact of on single transcription factor highly modular. This question should be addressed by comparing ChIP-seq data of a core group of megakaryocytic transcription factors like LEF1, RUNX1, TAL1, FLI1, GATA1 and GATA2 with the cofactor PRMT6. These results will set a clear view on the impact of LEF1 and PRMT6 to megakaryocytic target genes.

Cell-cell crosstalk through Wnt signaling is a very complex and important mechanism in the bone marrow microenvironment to control all aspects of hematopoiesis. This is well studied for hematopoietic stem cells and the lymphoid development. Important regulators like osteoblasts were identified to control this process with Wnt signaling. The interacting cell type which controls megakaryocytic development through Wnt secretion has still to be identified. Therefore, the bone marrow microenvironment has to be examined to discover the cells of the megakaryocytic microenvironment. This information cannot be retrieved through cell culture experiments, making mouse models necessary.

It has been shown that a group of protein arginine methyltransferases is directly regulating the Wnt signaling pathway. This thesis showed that PRMT6 is a newly identified member of this interacting group. PRMT6 is directly recruited to LEF1, which is a key transcription factor of the Wnt signaling pathway. Further research has to be performed, to investigate the impact of PRMT6 on this important pathway.

Understanding the exact influence of PRMT6 and Wnt signaling on megakaryopoiesis will enable to improve the treatment of abnormal levels of thrombocytes, such as thrombocythemia and thrombocytopenia. In order to be able to produce platelets *in vitro*, it will be necessary to understand the necessary Wnt signal protein dosage in detail, to mimic the *in vivo* environment of megakaryocytes.

5 Supplements

Table 14: Command line arguments of the R script. The MACS peak coordinates were reduced to a 3 columns BED file and transferred to Granges with the Bioconductor package ChIPpeakAnno, (V.3.10). Only peaks which overlap +/- 500 bp around the transcription start site were extracted. The peaks were annotated with entrez IDs and the enriched GO-terms were calculated.

```
#Install the following libraries
library(ChIPpeakAnno)
library(EnsDb.Hsapiens.v75)
library(TxDb.Hsapiens.UCSC.hg19.knownGene)
library(org.Hs.eg.db)

#Transfer the ChIP-peaks to GRanges
annoData <- toGRanges(EnsDb.Hsapiens.v75, feature="gene")
macs <- system.file("extdata", "K562_conservative_diss.txt", package="ChIPpeakAnno")
K562_peaks <- toGRanges(macs, format="BED")

#Extract the peaks overlapping the TSS +/- 500 bp
overlaps.anno <- annotatePeakInBatch(K562_peaks,
                                   AnnotationData=annoData,
                                   output="nearestBiDirectionalPromoters",
                                   bindingRegion=c(-500, 500))

#Add the Entrez ID to the peaks
overlaps.anno <- addGeneIDs(overlaps.anno,
                           "org.Hs.eg.db",
                           IDs2Add = "entrez_id")

write.csv(as.data.frame(unname(overlaps.anno)), "anno_K562_diss.csv")

#Calculate the enriched GO-terms
over <- getEnrichedGO(overlaps.anno, orgAnn="org.Hs.eg.db",
                     maxP=.05, minGOTerm=10,
                     multiAdjMethod="BH", condense=TRUE)

write.csv(as.data.frame(unname(over[["bp"]][, -c(8, 16)])), "over_K562_diss.csv")

#Calculate the peak distribution
write.csv(as.data.frame(unname(binOverFeature(K562_peaks, annotationData=annoData,
                                             radius=5000, nbins=500, FUN=length,
                                             errFun=0, ylab="count")
))), "K562_bins_diss.csv")

#Calculate the distribution over the Chromosome Regions
aCR<-assignChromosomeRegion(K562_peaks, nucleotideLevel=FALSE,
                           precedence=c("Promoters", "immediateDownstream",
                                         "fiveUTRs", "threeUTRs",
                                         "Exons", "Introns"),
                           TxDb=TxDb.Hsapiens.UCSC.hg19.knownGene)

write.csv(as.data.frame(unname(aCR)), "K562_Chromosome_region.csv")
```


Table 15: Possible members of the PRMT6 interactome, sorted by normalized H/L ratio

	protein names	gene symbol	Ratio H/L normalized
1	Protein arginine N-methyltransferase 6	PRMT6	21,145
2	YLP motif-containing protein 1	YLPM1	17,832
3	Angiomotin-like protein 1	AMOTL1	14,280
4	Dual specificity protein kinase CLK4	CLK4	10,244
5	Thyroid hormone receptor-associated protein 3	THRAP3	8,429
6	Interleukin enhancer-binding factor 2	ILF2	8,073
7	YLP motif-containing protein 1	YLPM1	7,458
8	Luc7-like protein 3	LUC7L3	7,250
9	Spermatid perinuclear RNA-binding protein	STRBP	7,233
10	Protein TFG;Tyrosine-protein kinase receptor	TFG	7,163
11	Transcription cofactor vestigial-like protein 4	VGLL4	6,277
12	ADAMTS-like protein 4	ADAMTSL4	6,261
13	Serine/arginine repetitive matrix protein 1	SRRM1	6,174
14	Non-POU domain-containing octamer-binding protein	NONO	6,061
15	Polymerase delta-interacting protein 3	POLDIP3	6,045
16	Lymphoid enhancer-binding factor 1	LEF1	5,950
17	Bcl-2-associated transcription factor 1	BCLAF1	5,416
18	Pre-mRNA-splicing regulator WTAP	WTAP	5,359
19	Methyl-CpG-binding domain protein 1	MBD1	5,203
20	Thyroid hormone receptor-associated protein 3	THRAP3	5,156
21	Corepressor interacting with RBPJ 1	CIR1	5,149
22	G patch domain-containing protein 8	GPATCH8	5,147
23	PHD and RING finger domain-containing protein 1	PHRF1	5,058
24	Interleukin enhancer-binding factor 3	ILF3	5,042
25	Splicing factor, arginine/serine-rich 19	SRA1	5,041
26	Coiled-coil domain-containing protein 86	CCDC86	4,838
27	POLDIP3	POLDIP3	4,794
28	Enhancer of rudimentary homolog	ERH	4,701
29	Protein SON	SON	4,608
30	WD40 repeat-containing protein SMU1	SMU1	4,590
31	FERM domain-containing protein 4A	FRMD4A	4,506
32	Peptidyl-prolyl cis-trans isomerase G	PPIG	4,314
33	RNA-binding protein 45	RBM45	4,122
34	RNA-binding protein 34	RBM34	4,106
35	Heterogeneous nuclear ribonucleoprotein H	HNRNPH1	4,004
36	Sentrin-specific protease 2	SEN2	4,001
37	Pre-mRNA-splicing factor RBM22	RBM22	3,966

38	Poly(A) RNA polymerase GLD2	PAPD4	3,964
39	Nuclease-sensitive element-binding protein 1	YBX1	3,917
40	Ubiquitin carboxyl-terminal hydrolase	USP42	3,890
41	Bcl-2-associated transcription factor 1	BCLAF1	3,867
42	DNA dC->dU-editing enzyme APOBEC-3B	APOBEC3B	3,861
43	Zinc finger protein RFP	TRIM27	3,790
44	Zinc finger protein 638	ZNF638	3,732
45	Heterogeneous nuclear ribonucleoprotein U-like protein 2	HNRNPUL2	3,697
46	E3 ubiquitin-protein ligase RING1	RING1	3,691
47	40S ribosomal protein S28	RPS28	3,656
48	U3 small nucleolar RNA-interacting protein 2	RRP9	3,615
49	Glutamate-rich WD repeat-containing protein 1	GRWD1	3,614
50	Cylicin-1	CYLC1	3,603
51	Zinc finger protein 579	ZNF579	3,589
52	RNA-binding protein Raly	RALY	3,567
53	THO complex subunit 4	ALYREF	3,545
54	Ribosomal RNA-processing protein 8	RRP8	3,496
55	Myoneurin	MYNN	3,475
56	Surfeit locus protein 6	SURF6	3,474
57	Heterogeneous nuclear ribonucleoprotein F	HNRPF	3,470
58	Pre-mRNA-splicing factor CWC25 homolog	CWC25	3,442
59	RNA exonuclease 4	REXO4	3,423
60	Serine/arginine repetitive matrix protein 2	SRRM2	3,387
61	Dual specificity protein kinase CLK3	CLK3	3,357
62	RNA-binding motif protein, X chromosome	RBMX	3,324
63	NK-tumor recognition protein	NKTR	3,310
64	Heterogeneous Nuclear Ribonucleoprotein C	HNRNPC	3,281
65	Probable RNA-binding protein 23	RBM23	3,272
66	Protein LSM14 homolog B	LSM14B	3,254
67	Ribosome biogenesis protein WDR12	WDR12	3,218
68	Suppressor of SWI4 1 homolog	PPAN	3,206
69	Zinc finger CCCH domain-containing protein 13	ZC3H13	3,169
70	Crossover junction endonuclease MUS81	MUS81	3,169
71	H/ACA ribonucleoprotein complex subunit 3	NOP10	3,148
72	Pre-mRNA-processing factor 19	PRPF19	3,071
73	Splicing factor U2AF 65 kDa subunit	U2AF2	3,038
74	F-box only protein 11	FBXO11	3,032
75	Probable ATP-dependent RNA helicase DDX28	DDX28	3,027
76	Centromere protein U	CENPU	2,973

77	Zinc finger protein 444	ZNF444	2,954
78	Endogenous retrovirus group K3 member 1	ERVK31	2,953
79	Microprocessor complex subunit DGCR8	DGCR8	2,946
80	KRR1 small subunit processome component homolog	KRR1	2,900
81	Zinc finger protein 106	ZFP106	2,860
82	TATA-binding protein-associated factor 2N	TAF15	2,846
83	Arginine/serine-rich coiled-coil protein 2	RSRC2	2,840
84	Ribosomal RNA processing protein 1 homolog A	RRP1	2,823
85	DNA/RNA-binding protein KIN17	KIN	2,812
86	Ribonuclease P protein subunit p14	RPP14	2,801
87	NF-kappa-B-activating protein	NKAP	2,770
88	Glutamine and serine-rich protein 1	QSER1	2,769
89	Serine/arginine-rich splicing factor 4	SFRS4	2,768
90	Protein PRRC2A	PRRC2A	2,760
91	Histone-lysine N-methyltransferase	NSD1	2,747
92	Protein arginine N-methyltransferase 1	PRMT1	2,724
93	tRNA-splicing ligase RtcB homolog	RTCB	2,693
94	Small nuclear ribonucleoprotein F	SNRPF	2,693
95	Protein FAM83A	FAM83A	2,681
96	Interferon-inducible ds RNA-dependent protein kinase activator A	PRKRA	2,670
97	RNA binding protein fox-1 homolog	RBFOX1	2,651
98	Deoxynucleotidyltransferase terminal-interacting protein 2	DNTTIP2	2,646
99	A-kinase anchor protein 17A	AKAP17A	2,633
100	NAD-dependent protein deacetylase sirtuin-7	SIRT7	2,619
101	Splicing factor 45	RBM17	2,606
102	Chromodomain-helicase-DNA-binding protein 2	CHD2	2,590
103	Telomeric repeat-binding factor 1	TERF1	2,578
104	RNA-binding protein 6	RBM6	2,575
105	Ribonuclease 3	DROSHA	2,574
106	Bifunctional lysine-specific demethylase and histidyl-hydroxylase	MINA	2,572
107	IQ motif and SEC7 domain-containing protein 1	IQSEC1	2,565
108	Breast cancer type 2 susceptibility protein	BRCA2	2,562
109	Lupus La protein	SSB	2,538
110	Kinesin-like protein KIF23	KIF23	2,532
111	Coiled-coil domain-containing protein 9	CCDC9	2,527
112	Probable helicase with zinc finger domain	HELZ	2,504
113	RNA-binding protein 12B	RBM12B	2,480

114	RNA-binding protein 4B	RBM4B	2,477
115	Splicing factor 3B subunit 4	SF3B4	2,473
116	Periphilin-1	PPHLN1	2,472
117	Small nuclear ribonucleoprotein E	SNRPE	2,435
118	Transducin beta-like protein 2	TBL2	2,434
119	Serum response factor-binding protein 1	SRFBP1	2,433
120	RNA-binding protein FUS	FUS	2,426
121	Dual specificity protein kinase CLK2	CLK2	2,425
122	E3 ubiquitin-protein ligase TRAIP	TRAIP	2,380
123	RNA methyltransferase-like protein 1	RNMTL1	2,369
124	60S ribosomal protein L37a	RPL37A	2,358
125	Cip1-interacting zinc finger protein	CIZ1	2,358
126	Protein virilizer homolog	KIAA1429	2,350
127	Nuclear valosin-containing protein-like	NVL	2,347
128	Shugoshin-like 2	SGOL2	2,336
129	Protein PRRC2B	PRRC2B	2,334
130	Protein DEK	DEK	2,328
131	Neudesin	NENF	2,312
132	Protein SCAF11	SCAF11	2,309
133	Serine/arginine-rich splicing factor 8	SRSF8	2,306
134	RNA-binding protein EWS	EWSR1	2,282
135	Endothelial transcription factor GATA-2	GATA2	2,270
136	Zinc finger protein 385A	ZNF385A	2,268
137	Double-stranded RNA-specific adenosine deaminase	ADAR	2,257
138	Zinc finger protein 184	ZNF184	2,239
139	Apoptosis-enhancing nuclease	AEN	2,233
140	Scaffold attachment factor B1	SAFB	2,228
141	Putative RNA-binding protein Luc7-like 1	LUC7L	2,228
142	PNMA-like protein 1	PNMAL1	2,221
143	60S ribosomal protein L4	RPL4	2,221
144	G-rich sequence factor 1	GRSF1	2,220
145	Splicing factor, proline- and glutamine-rich	SFPQ	2,205
146	Putative helicase MOV-10	MOV10	2,204
147	GON-4-like protein	GON4L	2,195
148	A-kinase anchor protein 8-like	AKAP8L	2,187
149	Protein FAM98A	FAM98A	2,178
150	Probable ATP-dependent RNA helicase DDX47	DDX47	2,176
151	UAP56-interacting factor	FYTTD1	2,176
152	Fragile X mental retardation protein 1	FMR1	2,162
153	Zinc finger protein 845	ZNF845	2,154

154	Putative RNA-binding protein 15B	RBM15B	2,154
155	Cell growth-regulating nucleolar protein	LYAR	2,150
156	Runt-related transcription factor 1	RUNX1	2,122
157	Chromatin target of PRMT1 protein	CHTOP	2,118
158	Abnormal spindle-like microcephaly-associated protein	ASPM	2,117
159	Putative RNA-binding protein Luc7-like 2	LUC7L2	2,116
160	Zinc finger and SCAN domain-containing protein 29	ZSCAN29	2,116
161	Nucleolar complex protein 4 homolog	NOC4L	2,112
162	Heterogeneous nuclear ribonucleoprotein Q	SYNCRIP	2,103
163	Telomerase-binding protein EST1A	SMG6	2,098
164	Uncharacterized protein C17orf85	C17orf85	2,088
165	Scaffold attachment factor B2	SAFB2	2,078
166	Heterogeneous nuclear ribonucleoprotein R	HNRNPR	2,077
167	Chromosome transmission fidelity protein 8 homolog isoform 2	CHTF8	2,068
168	Heterogeneous nuclear ribonucleoprotein D-like	HNRPDL	2,067
169	Heterogeneous nuclear ribonucleoprotein H3	HNRPH3	2,059
170	39S ribosomal protein L15, mitochondrial	MRPL15	2,050
171	Protein FAM208A	FAM208A	2,043
172	Nucleolar protein 12	NOL12	2,041
173	Transformer-2 protein homolog alpha	TRA2A	2,038
174	Zinc finger CCHC domain-containing protein 7	ZCCHC7	2,033
175	Zinc finger RNA-binding protein	ZFR	2,027
176	Twinkle protein, mitochondrial	PEO1	2,024
177	Ribosome biogenesis protein BMS1 homolog	BMS1	2,022
178	Heterogeneous nuclear ribonucleoprotein A/B	HNRNPAB	2,008
179	Krueppel-like factor 1	KLF1	2,004

6 References

- Arce, L., Yokoyama, N.N., and Waterman, M.L. (2006). Diversity of LEF/TCF action in development and disease. *Oncogene* 25, 7492-7504.
- Avasarala, S., Wu, P.-Y., Khan, S.Q., Yanlin, S., van Scoyk, M., Bao, J., Di Lorenzo, A., David, O., Bedford, M.T., and Gupta, V., et al. (2020). PRMT6 Promotes Lung Tumor Progression via the Alternate Activation of Tumor-Associated Macrophages. *Molecular cancer research : MCR* 18, 166-178.
- Balazs, A.B., Fabian, A.J., Esmon, C.T., and Mulligan, R.C. (2006). Endothelial protein C receptor (CD201) explicitly identifies hematopoietic stem cells in murine bone marrow. *Blood* 107, 2317-2321.
- Bao, J., Di Lorenzo, A., Lin, K., Lu, Y., Zhong, Y., Sebastian, M.M., Muller, W.J., Yang, Y., and Bedford, M.T. (2018). Mouse models of overexpression reveal distinct oncogenic roles for different type I protein arginine methyltransferases. *Cancer research* 79, 21-32.
- Bedford, M.T. (2007). Arginine methylation at a glance. *Journal of cell science* 120, 4243-4246.
- Bedford, M.T., and Richard, S. (2005). Arginine methylation an emerging regulator of protein function. *Molecular cell* 18, 263-272.
- Bissels, U., Bosio, A., and Wagner, W. (2012). MicroRNAs are shaping the hematopoietic landscape. *Haematologica* 97, 160-167.
- Blythe, S.A., Cha, S.-W., Tadjuidje, E., Heasman, J., and Klein, P.S. (2010). beta-Catenin primes organizer gene expression by recruiting a histone H3 arginine 8 methyltransferase, Prmt2. *Developmental cell* 19, 220-231.
- Bouchard, C., Sahu, P., Meixner, M., Nötzold, R.R., Rust, M.B., Kremmer, E., Feederle, R., Hart-Smith, G., Finkernagel, F., and Bartkuhn, M., et al. (2018). Genomic Location of PRMT6-Dependent H3R2 Methylation Is Linked to the Transcriptional Outcome of Associated Genes. *Cell reports* 24, 3339-3352.
- Boulanger, M.-C., Liang, C., Russell, R.S., Lin, R., Bedford, M.T., Wainberg, M.A., and Richard, S. (2005). Methylation of Tat by PRMT6 regulates human immunodeficiency virus type 1 gene expression. *Journal of virology* 79, 124-131.
- Bowman, G.D., and Poirier, M.G. (2014). Post-Translational Modifications of Histones That Influence Nucleosome Dynamics. *Chemical Reviews* 115, 2274-2295.
- Cantù, C., Ierardi, R., Alborelli, I., Fugazza, C., Cassinelli, L., Piconese, S., Bosè, F., Ottolenghi, S., Ferrari, G., and Ronchi, A. (2011). Sox6 enhances erythroid differentiation in human erythroid progenitors. *Blood* 117, 3669-3679.
- Cha, B., and Jho, E.-h. (2012). Protein arginine methyltransferases (PRMTs) as therapeutic targets. *Expert opinion on therapeutic targets* 16, 651-664.

- Cha, B., Kim, W., Kim, Y.K., Hwang, B.N., Park, S.Y., Yoon, J.W., Park, W.S., Cho, J.W., Bedford, M.T., and Jho, E.-h. (2011). Methylation by protein arginine methyltransferase 1 increases stability of Axin, a negative regulator of Wnt signaling. *Oncogene* *30*, 2379-2389.
- Chagraoui, H., Kassouf, M., Banerjee, S., Goardon, N., Clark, K., Atzberger, A., Pearce, A.C., Skoda, R.C., Ferguson, D.J.P., and Watson, S.P., et al. (2011). SCL-mediated regulation of the cell-cycle regulator p21 is critical for murine megakaryopoiesis. *Blood* *118*, 723-735.
- Chung, J., Karkhanis, V., Baiocchi, R.A., and Sif, S. (2019). Protein arginine methyltransferase 5 (PRMT5) promotes survival of lymphoma cells via activation of WNT/ β -catenin and AKT/GSK3 β proliferative signaling. *The Journal of biological chemistry* *294*, 7692-7710.
- Clevers, H. (2006). Wnt/beta-catenin signaling in development and disease. *Cell* *127*, 469-480.
- Corrigan, P.M., Dobbin, E., Freeburn, R.W., and Wheadon, H. (2009). Patterns of Wnt/Fzd/LRP gene expression during embryonic hematopoiesis. *Stem cells and development* *18*, 759-772.
- Daniels, D.L., and Weis, W.I. (2005). Beta-catenin directly displaces Groucho/TLE repressors from Tcf/Lef in Wnt-mediated transcription activation. *Nature structural & molecular biology* *12*, 364-371.
- Davis, C.A., Hitz, B.C., Sloan, C.A., Chan, E.T., Davidson, J.M., Gabdank, I., Hilton, J.A., Jain, K., Baymuradov, U.K., and Narayanan, A.K., et al. (2018). The Encyclopedia of DNA elements (ENCODE): data portal update. *Nucleic acids research* *46*, D794-D801.
- Day, R.B., and Link, D.C. (2014). Megakaryocytes in the hematopoietic stem cell niche. *Nature medicine* *20*, 1233-1234.
- Di Lorenzo, A., Yang, Y., Macaluso, M., and Bedford, M.T. (2014). A gain-of-function mouse model identifies PRMT6 as a NF- κ B coactivator. *Nucleic acids research* *42*, 8297-8309.
- Donze, D., Townes, T.M., and Bieker, J.J. (1995). Role of erythroid Kruppel-like factor in human gamma- to beta-globin gene switching. *The Journal of biological chemistry* *270*, 1955-1959.
- Doré, L.C., and Crispino, J.D. (2011). Transcription factor networks in erythroid cell and megakaryocyte development. *Blood* *118*, 231-239.
- El-Andaloussi, N., Valovka, T., Toueille, M., Steinacher, R., Focke, F., Gehrig, P., Covic, M., Hassa, P.O., Schär, P., and Hübscher, U., et al. (2006). Arginine methylation regulates DNA polymerase beta. *Molecular cell* *22*, 51-62.
- Emmanuel, A.O., Arnovitz, S., Haghi, L., Mathur, P.S., Mondal, S., Quandt, J., Okoreeh, M.K., Maienschein-Cline, M., Khazaie, K., and Dose, M., et al. (2018). Tcf-1 and HEB cooperate to establish the epigenetic and transcription profile of CD4+CD8+ thymocytes. *Nature immunology* *19*, 1366-1378.

ENCODE Project Consortium (2012). An integrated encyclopedia of DNA elements in the human genome. *Nature* 489, 57-74.

Evans, T., Reitman, M., and Felsenfeld, G. (1988). An erythrocyte-specific DNA-binding factor recognizes a regulatory sequence common to all chicken globin genes. *Proceedings of the National Academy of Sciences of the United States of America* 85, 5976-5980.

Felsenfeld, G., and Groudine, M. (2003). Controlling the double helix. *Nature* 421, 448-453.

Ferreira, R., Ohneda, K., Yamamoto, M., and Philipsen, S. (2005). GATA1 function, a paradigm for transcription factors in hematopoiesis. *Molecular and cellular biology* 25, 1215-1227.

Fleming, H.E., Janzen, V., Lo Celso, C., Guo, J., Leahy, K.M., Kronenberg, H.M., and Scadden, D.T. (2008). Wnt signaling in the niche enforces hematopoietic stem cell quiescence and is necessary to preserve self-renewal in vivo. *Cell stem cell* 2, 274-283.

Frankel, A., and Clarke, S. (2000). PRMT3 is a distinct member of the protein arginine N-methyltransferase family. Conferral of substrate specificity by a zinc-finger domain. *The Journal of biological chemistry* 275, 32974-32982.

Fujiwara, Y., Browne, C.P., Cunniff, K., Goff, S.C., and Orkin, S.H. (1996). Arrested development of embryonic red cell precursors in mouse embryos lacking transcription factor GATA-1. *Proceedings of the National Academy of Sciences of the United States of America* 93, 12355-12358.

Gary, J.D., and Clarke, S. (1998). RNA and protein interactions modulated by protein arginine methylation. *Progress in nucleic acid research and molecular biology* 61, 65-131.

Gillette, T.G., and Hill, J.A. (2015). Readers, writers, and erasers: chromatin as the whiteboard of heart disease. *Circulation research* 116, 1245-1253.

Goessling, W., North, T.E., Loewer, S., Lord, A.M., Lee, S., Stoick-Cooper, C.L., Weidinger, G., Puder, M., Daley, G.Q., and Moon, R.T., et al. (2009). Genetic interaction of PGE2 and Wnt signaling regulates developmental specification of stem cells and regeneration. *Cell* 136, 1136-1147.

Graf, T., and Enver, T. (2009). Forcing cells to change lineages. *Nature* 462, 587-594.

Guccione, E., Bassi, C., Casadio, F., Martinato, F., Cesaroni, M., Schuchlantz, H., Lüscher, B., and Amati, B. (2007). Methylation of histone H3R2 by PRMT6 and H3K4 by an MLL complex are mutually exclusive. *Nature* 449, 933-937.

Hall, M.A., Curtis, D.J., Metcalf, D., Elefanty, A.G., Sourris, K., Robb, L., Gothert, J.R., Jane, S.M., and Begley, C.G. (2003). The critical regulator of embryonic hematopoiesis, SCL, is vital in the adult for megakaryopoiesis, erythropoiesis, and lineage choice in CFU-S12. *Proceedings of the National Academy of Sciences of the United States of America* 100, 992-997.

Hattangadi, S.M., Wong, P., Zhang, L., Flygare, J., and Lodish, H.F. (2011). From stem cell to red cell: regulation of erythropoiesis at multiple levels by multiple proteins, RNAs, and chromatin modifications. *Blood* 118, 6258-6268.

He, T.C., Sparks, A.B., Rago, C., Hermeking, H., Zawel, L., da Costa, L.T., Morin, P.J., Vogelstein, B., and Kinzler, K.W. (1998). Identification of c-MYC as a target of the APC pathway. *Science (New York, N.Y.)* 281, 1509-1512.

Heller, P.G., Glembotsky, A.C., Gandhi, M.J., Cummings, C.L., Pirola, C.J., Marta, R.F., Kornblihtt, L.I., Drachman, J.G., and Molinas, F.C. (2005). Low Mpl receptor expression in a pedigree with familial platelet disorder with predisposition to acute myelogenous leukemia and a novel AML1 mutation. *Blood* 105, 4664-4670.

Herglotz, J., Kuvardina, O.N., Kolodziej, S., Kumar, A., Hussong, H., Grez, M., and Lausen, J. (2013). Histone arginine methylation keeps RUNX1 target genes in an intermediate state. *Oncogene* 32, 2565-2575.

Herkt, S.C., Kuvardina, O.N., Herglotz, J., Schneider, L., Meyer, A., Pommerenke, C., Salinas-Riester, G., Seifried, E., Bonig, H., and Lausen, J. (2018). Protein arginine methyltransferase 6 controls erythroid gene expression and differentiation of human CD34+ progenitor cells. *Haematologica* 103, 18-29.

Herrmann, F., Pably, P., Eckerich, C., Bedford, M.T., and Fackelmayer, F.O. (2009). Human protein arginine methyltransferases in vivo--distinct properties of eight canonical members of the PRMT family. *Journal of cell science* 122, 667-677.

Higgins, J.M. (2015). Red blood cell population dynamics. *Clinics in laboratory medicine* 35, 43-57.

Hua, W.-K., Chang, Y.-I., Yao, C.-L., Hwang, S.-M., Chang, C.-Y., and Lin, W.-J. (2013). Protein arginine methyltransferase 1 interacts with and activates p38 α to facilitate erythroid differentiation. *PloS one* 8, e56715.

Huang, D.W., Sherman, B.T., and Lempicki, R.A. (2009a). Bioinformatics enrichment tools: paths toward the comprehensive functional analysis of large gene lists. *Nucleic acids research* 37, 1-13.

Huang, D.W., Sherman, B.T., and Lempicki, R.A. (2009b). Systematic and integrative analysis of large gene lists using DAVID bioinformatics resources. *Nature protocols* 4, 44-57.

Huber, O., Korn, R., McLaughlin, J., Ohsugi, M., Herrmann, B.G., and Kemler, R. (1996). Nuclear localization of beta-catenin by interaction with transcription factor LEF-1. *Mechanisms of development* 59, 3-10.

Hughes, R.M., and Waters, M.L. (2006). Model systems for beta-hairpins and beta-sheets. *Current opinion in structural biology* 16, 514-524.

- Hyllus, D., Stein, C., Schnabel, K., Schiltz, E., Imhof, A., Dou, Y., Hsieh, J., and Bauer, U.-M. (2007). PRMT6-mediated methylation of R2 in histone H3 antagonizes H3 K4 trimethylation. *Genes & development* 21, 3369-3380.
- Iguchi, H., Urashima, Y., Inagaki, Y., Ikeda, Y., Okamura, M., Tanaka, T., Uchida, A., Yamamoto, T.T., Kodama, T., and Sakai, J. (2007). SOX6 suppresses cyclin D1 promoter activity by interacting with beta-catenin and histone deacetylase 1, and its down-regulation induces pancreatic beta-cell proliferation. *The Journal of biological chemistry* 282, 19052-19061.
- Jelkmann, W. (2007). Erythropoietin after a century of research: younger than ever. *European journal of haematology* 78, 183-205.
- Jho, E.-h., Zhang, T., Domon, C., Joo, C.-K., Freund, J.-N., and Costantini, F. (2002). Wnt/beta-catenin/Tcf signaling induces the transcription of Axin2, a negative regulator of the signaling pathway. *Molecular and cellular biology* 22, 1172-1183.
- Kahler, R.A., and Westendorf, J.J. (2003). Lymphoid enhancer factor-1 and beta-catenin inhibit Runx2-dependent transcriptional activation of the osteocalcin promoter. *The Journal of biological chemistry* 278, 11937-11944.
- Kassouf, M.T., Hughes, J.R., Taylor, S., McGowan, S.J., Soneji, S., Green, A.L., Vyas, P., and Porcher, C. (2010). Genome-wide identification of TAL1's functional targets: insights into its mechanisms of action in primary erythroid cells. *Genome research* 20, 1064-1083.
- Katz, J.E., Dlakić, M., and Clarke, S. (2003). Automated identification of putative methyltransferases from genomic open reading frames. *Molecular & cellular proteomics : MCP* 2, 525-540.
- Kaushansky, K. (1997). Thrombopoietin the primary regulator of platelet production. *Trends in endocrinology and metabolism: TEM* 8, 45-50.
- Kaushansky, K., Lok, S., Holly, R.D., Broudy, V.C., Lin, N., Bailey, M.C., Forstrom, J.W., Buddle, M.M., Oort, P.J., and Hagen, F.S. (1994). Promotion of megakaryocyte progenitor expansion and differentiation by the c-Mpl ligand thrombopoietin. *Nature* 369, 568-571.
- Kirstetter, P., Anderson, K., Porse, B.T., Jacobsen, S.E.W., and Nerlov, C. (2006). Activation of the canonical Wnt pathway leads to loss of hematopoietic stem cell repopulation and multilineage differentiation block. *Nature immunology* 7, 1048-1056.
- Kleinschmidt, M.A., Graaf, P. de, van Teeffelen, H.A.A.M., and Timmers, H.T.M. (2012). Cell cycle regulation by the PRMT6 arginine methyltransferase through repression of cyclin-dependent kinase inhibitors. *PLoS one* 7, e41446.
- Kolligs, F.T., Hu, G., Dang, C.V., and Fearon, E.R. (1999). Neoplastic transformation of RK3E by mutant beta-catenin requires deregulation of Tcf/Lef transcription but not activation of c-myc expression. *Molecular and cellular biology* 19, 5696-5706.

Kolodziej, S., Kuvardina, O.N., Oellerich, T., Herglotz, J., Backert, I., Kohrs, N., La Buscató, E., Wittmann, S.K., Salinas-Riester, G., and Bonig, H., et al. (2014). PADI4 acts as a coactivator of Tal1 by counteracting repressive histone arginine methylation. *Nature communications* 5, 3995.

Kumar, R., Godavarthy, P.S., and Krause, D.S. (2018). The bone marrow microenvironment in health and disease at a glance. *Journal of cell science* 131.

Kuvardina, O.N., Herglotz, J., Kolodziej, S., Kohrs, N., Herkt, S., Wojcik, B., Oellerich, T., Corso, J., Behrens, K., and Kumar, A., et al. (2015). RUNX1 represses the erythroid gene expression program during megakaryocytic differentiation. *Blood* 125, 3570-3579.

Kzhyshkowska, J., Schütt, H., Liss, M., Kremmer, E., Stauber, R., Wolf, H., and Dobner, T. (2001). Heterogeneous nuclear ribonucleoprotein E1B-AP5 is methylated in its Arg-Gly-Gly (RGG) box and interacts with human arginine methyltransferase HRMT1L1. *The Biochemical journal* 358, 305-314.

Lancrin, C., Sroczynska, P., Serrano, A.G., Gandillet, A., Ferreras, C., Kouskoff, V., and Lacaud, G. (2010). Blood cell generation from the hemangioblast. *Journal of molecular medicine (Berlin, Germany)* 88, 167-172.

Lancrin, C., Sroczynska, P., Stephenson, C., Allen, T., Kouskoff, V., and Lacaud, G. (2009). The haemangioblast generates haematopoietic cells through a haemogenic endothelium stage. *Nature* 457, 892-895.

Lento, W., Congdon, K., Voermans, C., Kritzik, M., and Reya, T. (2013). Wnt signaling in normal and malignant hematopoiesis. *Cold Spring Harbor perspectives in biology* 5.

Levanon, D., Glusman, G., Bangsow, T., Ben-Asher, E., Male, D.A., Avidan, N., Bangsow, C., Hattori, M., Taylor, T.D., and Taudien, S., et al. (2001). Architecture and anatomy of the genomic locus encoding the human leukemia-associated transcription factor RUNX1/AML1. *Gene* 262, 23-33.

Levanon, D., Goldstein, R.E., Bernstein, Y., Tang, H., Goldenberg, D., Stifani, S., Paroush, Z., and Groner, Y. (1998). Transcriptional repression by AML1 and LEF-1 is mediated by the TLE/Groucho corepressors. *Proceedings of the National Academy of Sciences of the United States of America* 95, 11590-11595.

Li, Q., Lai, Q., He, C., Fang, Y., Yan, Q., Zhang, Y., Wang, X., Gu, C., Wang, Y., and Ye, L., et al. (2019). RUNX1 promotes tumour metastasis by activating the Wnt/ β -catenin signalling pathway and EMT in colorectal cancer. *Journal of experimental & clinical cancer research : CR* 38, 334.

Litt, M., Qiu, Y., and Huang, S. (2009). Histone arginine methylations: their roles in chromatin dynamics and transcriptional regulation. *Bioscience reports* 29, 131-141.

Livak, K.J., and Schmittgen, T.D. (2001). Analysis of relative gene expression data using real-time quantitative PCR and the 2^{-Delta Delta C(T)} Method. *Methods (San Diego, Calif.)* 25, 402-408.

Lu, P., Hankel, I.L., Hostager, B.S., Swartzendruber, J.A., Friedman, A.D., Brenton, J.L., Rothman, P.B., and Colgan, J.D. (2011). The developmental regulator protein Gon4l associates with protein YY1, co-repressor Sin3a, and histone deacetylase 1 and mediates transcriptional repression. *The Journal of biological chemistry* 286, 18311-18319.

Luger, K., Mäder, A.W., Richmond, R.K., Sargent, D.F., and Richmond, T.J. (1997). Crystal structure of the nucleosome core particle at 2.8 Å resolution. *Nature* 389, 251-260.

Luger, K., and Richmond, T.J. (1998). The histone tails of the nucleosome. *Current opinion in genetics & development* 8, 140-146.

Luis, T.C., Ichij, M., Brugman, M.H., Kincade, P., and Staal, F.J.T. (2012). Wnt signaling strength regulates normal hematopoiesis and its deregulation is involved in leukemia development. *Leukemia* 26, 414-421.

Luis, T.C., Naber, B.A.E., Roozen, P.P.C., Brugman, M.H., Haas, E.F.E. de, Ghazvini, M., Fibbe, W.E., van Dongen, J.J.M., Fodde, R., and Staal, F.J.T. (2011). Canonical wnt signaling regulates hematopoiesis in a dosage-dependent fashion. *Cell stem cell* 9, 345-356.

Luis, T.C., Weerkamp, F., Naber, B.A.E., Baert, M.R.M., Haas, E.F.E. de, Nikolic, T., Heuvelmans, S., Krijger, R.R. de, van Dongen, J.J.M., and Staal, F.J.T. (2009). Wnt3a deficiency irreversibly impairs hematopoietic stem cell self-renewal and leads to defects in progenitor cell differentiation. *Blood* 113, 546-554.

Macaulay, I.C., Thon, J.N., Tijssen, M.R., Steele, B.M., MacDonald, B.T., Meade, G., Burns, P., Rendon, A., Salunkhe, V., and Murphy, R.P., et al. (2013). Canonical Wnt signaling in megakaryocytes regulates proplatelet formation. *Blood* 121, 188-196.

MacDonald, B.T., Tamai, K., and He, X. (2009). Wnt/beta-catenin signaling: components, mechanisms, and diseases. *Developmental cell* 17, 9-26.

Medvinsky, A.L., and Dzierzak, E.A. (1998). Development of the definitive hematopoietic hierarchy in the mouse. *Developmental and comparative immunology* 22, 289-301.

Michaud-Levesque, J., and Richard, S. (2009). Thrombospondin-1 is a transcriptional repression target of PRMT6. *The Journal of biological chemistry* 284, 21338-21346.

Molenaar, M., van de Wetering, M., Oosterwegel, M., Peterson-Maduro, J., Godsave, S., Korinek, V., Roose, J., Destrée, O., and Clevers, H. (1996). XTcf-3 transcription factor mediates beta-catenin-induced axis formation in *Xenopus* embryos. *Cell* 86, 391-399.

Moore, K.A., and Lemischka, I.R. (2006). Stem cells and their niches. *Science (New York, N.Y.)* 311, 1880-1885.

- Morgan, R.G., Ridsdale, J., Payne, M., Heesom, K.J., Wilson, M.C., Davidson, A., Greenhough, A., Davies, S., Williams, A.C., and Blair, A., et al. (2019). LEF-1 drives aberrant β -catenin nuclear localization in myeloid leukemia cells. *Haematologica* *104*, 1365-1377.
- Morrison, S.J., and Scadden, D.T. (2014). The bone marrow niche for haematopoietic stem cells. *Nature* *505*, 327-334.
- Mulroy, T., Xu, Y., and Sen, J.M. (2003). beta-Catenin expression enhances generation of mature thymocytes. *International immunology* *15*, 1485-1494.
- Muntean, A.G., Pang, L., Poncz, M., Dowdy, S.F., Blobel, G.A., and Crispino, J.D. (2007). Cyclin D-Cdk4 is regulated by GATA-1 and required for megakaryocyte growth and polyploidization. *Blood* *109*, 5199-5207.
- Nagarajan, P., Onami, T.M., Rajagopalan, S., Kania, S., Donnell, R., and Venkatachalam, S. (2009). Role of chromodomain helicase DNA-binding protein 2 in DNA damage response signaling and tumorigenesis. *Oncogene* *28*, 1053-1062.
- Nakamura-Ishizu, A., and Suda, T. (2019). Dynamic Changes in the Niche with N-Cadherin Revisited: The HSC "Niche Herein". *Cell stem cell* *24*, 355-356.
- Neault, M., Mallette, F.A., Vogel, G., Michaud-Levesque, J., and Richard, S. (2012). Ablation of PRMT6 reveals a role as a negative transcriptional regulator of the p53 tumor suppressor. *Nucleic acids research* *40*, 9513-9521.
- North, T.E., Stacy, T., Matheny, C.J., Speck, N.A., and Bruijn, M.F.T.R. de (2004). Runx1 is expressed in adult mouse hematopoietic stem cells and differentiating myeloid and lymphoid cells, but not in maturing erythroid cells. *Stem cells (Dayton, Ohio)* *22*, 158-168.
- Nötzold, R.R. (2015). Identifikation der Genom-weiten Bindungsstellen für die Argininmethyltransferase PRMT6 mittels ChIP-Seq. Dissertation (Marburg).
- Okamura, R.M., Sigvardsson, M., Galceran, J., Verbeek, S., Clevers, H., and Grosschedl, R. (1998). Redundant regulation of T cell differentiation and TCRalpha gene expression by the transcription factors LEF-1 and TCF-1. *Immunity* *8*, 11-20.
- Ong, S.-E., Blagoev, B., Kratchmarova, I., Kristensen, D.B., Steen, H., Pandey, A., and Mann, M. (2002). Stable isotope labeling by amino acids in cell culture, SILAC, as a simple and accurate approach to expression proteomics. *Molecular & cellular proteomics : MCP* *1*, 376-386.
- Orkin, S.H. (1992). GATA-binding transcription factors in hematopoietic cells. *Blood* *80*, 575-581.
- Orkin, S.H., and Zon, L.I. (2008). Hematopoiesis: an evolving paradigm for stem cell biology. *Cell* *132*, 631-644.

Ou, C.-Y., LaBonte, M.J., Manegold, P.C., So, A.Y.-L., Ianculescu, I., Gerke, D.S., Yamamoto, K.R., Ladner, R.D., Kahn, M., and Kim, J.H., et al. (2011). A coactivator role of CARM1 in the dysregulation of β -catenin activity in colorectal cancer cell growth and gene expression. *Molecular cancer research* : MCR 9, 660-670.

Pajerowski, A.G., Nguyen, C., Aghajanian, H., Shapiro, M.J., and Shapiro, V.S. (2009). NKAP is a transcriptional repressor of notch signaling and is required for T cell development. *Immunity* 30, 696-707.

Pazin, M.J., and Kadonaga, J.T. (1997). What's up and down with histone deacetylation and transcription? *Cell* 89, 325-328.

Perkins, A.C., Sharpe, A.H., and Orkin, S.H. (1995). Lethal beta-thalassaemia in mice lacking the erythroid CACCC-transcription factor EKLF. *Nature* 375, 318-322.

Pfaffl, M.W. (2001). A new mathematical model for relative quantification in real-time RT-PCR. *Nucleic acids research* 29, e45.

Phalke, S., Mzoughi, S., Bezzi, M., Jennifer, N., Mok, W.C., Low, D.H.P., Thike, A.A., Kuznetsov, V.A., Tan, P.H., and Voorhoeve, P.M., et al. (2012). p53-Independent regulation of p21Waf1/Cip1 expression and senescence by PRMT6. *Nucleic acids research* 40, 9534-9542.

Pippa, R., Dominguez, A., Malumbres, R., Endo, A., Arriazu, E., Marcotegui, N., Guruceaga, E., and Odero, M.D. (2017). MYC-dependent recruitment of RUNX1 and GATA2 on the SET oncogene promoter enhances PP2A inactivation in acute myeloid leukemia. *Oncotarget* 8, 53989-54003.

Psaila, B., and Mead, A.J. (2019). Single-cell approaches reveal novel cellular pathways for megakaryocyte and erythroid differentiation. *Blood* 133, 1427-1435.

Rainer, J., Gatto, L., and Weichenberger, C.X. (2019). *ensemldb*: an R package to create and use Ensembl-based annotation resources. *Bioinformatics (Oxford, England)* 35, 3151-3153.

Rakow, S., Pullamsetti, S.S., Bauer, U.-M., and Bouchard, C. (2019). Assaying epigenome functions of PRMTs and their substrates. *Methods (San Diego, Calif.)*.

Reed, S.E., Staley, E.M., Mayginnes, J.P., Pintel, D.J., and Tullis, G.E. (2006). Transfection of mammalian cells using linear polyethylenimine is a simple and effective means of producing recombinant adeno-associated virus vectors. *Journal of virological methods* 138, 85-98.

Reya, T., Duncan, A.W., Ailles, L., Domen, J., Scherer, D.C., Willert, K., Hintz, L., Nusse, R., and Weissman, I.L. (2003). A role for Wnt signalling in self-renewal of haematopoietic stem cells. *Nature* 423, 409-414.

Reya, T., O'Riordan, M., Okamura, R., Devaney, E., Willert, K., Nusse, R., and Grosschedl, R. (2000). Wnt signaling regulates B lymphocyte proliferation through a LEF-1 dependent mechanism. *Immunity* 13, 15-24.

- Robinson, J.T., Thorvaldsdóttir, H., Winckler, W., Guttman, M., Lander, E.S., Getz, G., and Mesirov, J.P. (2011). Integrative genomics viewer. *Nature biotechnology* 29, 24-26.
- Rodriguez, P., Bonte, E., Krijgsveld, J., Kolodziej, K.E., Guyot, B., Heck, A.J.R., Vyas, P., Boer, E. de, Grosveld, F., and Strouboulis, J. (2005). GATA-1 forms distinct activating and repressive complexes in erythroid cells. *The EMBO journal* 24, 2354-2366.
- Samols, D., Thornton, C.G., Murtif, V.L., Kumar, G.K., Haase, F.C., and Wood, H.G. (1988). Evolutionary conservation among biotin enzymes. *The Journal of biological chemistry* 263, 6461-6464.
- Scheller, M., Huelsken, J., Rosenbauer, F., Taketo, M.M., Birchmeier, W., Tenen, D.G., and Leutz, A. (2006). Hematopoietic stem cell and multilineage defects generated by constitutive beta-catenin activation. *Nature immunology* 7, 1037-1047.
- Schlaeger, T.M., Mikkola, H.K.A., Gekas, C., Helgadottir, H.B., and Orkin, S.H. (2005). Tie2Cre-mediated gene ablation defines the stem-cell leukemia gene (SCL/tal1)-dependent window during hematopoietic stem-cell development. *Blood* 105, 3871-3874.
- Shivdasani, R.A., Fujiwara, Y., McDevitt, M.A., and Orkin, S.H. (1997). A lineage-selective knockout establishes the critical role of transcription factor GATA-1 in megakaryocyte growth and platelet development. *The EMBO journal* 16, 3965-3973.
- Singhroy, D.N., Mesplède, T., Sabbah, A., Quashie, P.K., Falgueyret, J.-P., and Wainberg, M.A. (2013). Automethylation of protein arginine methyltransferase 6 (PRMT6) regulates its stability and its anti-HIV-1 activity. *Retrovirology* 10, 73.
- Skokowa, J., Cario, G., Uenal, M., Schambach, A., Germeshausen, M., Battmer, K., Zeidler, C., Lehmann, U., Eder, M., and Baum, C., et al. (2006). LEF-1 is crucial for neutrophil granulocytopenia and its expression is severely reduced in congenital neutropenia. *Nature medicine* 12, 1191-1197.
- Soda, M., Willert, K., Kaushansky, K., and Geddis, A.E. (2008). Inhibition of GSK-3beta promotes survival and proliferation of megakaryocytic cells through a beta-catenin-independent pathway. *Cellular signalling* 20, 2317-2323.
- Songdej, N., and Rao, A.K. (2017). Hematopoietic transcription factor mutations: important players in inherited platelet defects. *Blood* 129, 2873-2881.
- Spyropoulos, D.D., Pharr, P.N., Lavenburg, K.R., Jackers, P., Papas, T.S., Ogawa, M., and Watson, D.K. (2000). Hemorrhage, impaired hematopoiesis, and lethality in mouse embryos carrying a targeted disruption of the Fli1 transcription factor. *Molecular and cellular biology* 20, 5643-5652.
- Staal, F.J.T., Luis, T.C., and Tiemessen, M.M. (2008). WNT signalling in the immune system: WNT is spreading its wings. *Nature reviews. Immunology* 8, 581-593.

- Starck, J., Cohet, N., Gonnet, C., Sarrazin, S., Doubeikovskaia, Z., Doubeikovski, A., Verger, A., Duterque-Coquillaud, M., and Morle, F. (2003). Functional cross-antagonism between transcription factors FLI-1 and EKLF. *Molecular and cellular biology* *23*, 1390-1402.
- Stein, C. (2011). Charakterisierung der Repressorfunktion von PRMT6 und deren Rolle bei der Differenzierung, Proliferation und Seneszenz. Dissertation (Marburg).
- Stein, C., Nötzold, R.R., Riedl, S., Bouchard, C., and Bauer, U.-M. (2016). The Arginine Methyltransferase PRMT6 Cooperates with Polycomb Proteins in Regulating HOXA Gene Expression. *PloS one* *11*, e0148892.
- Stein, C., Riedl, S., Rühnick, D., Nötzold, R.R., and Bauer, U.-M. (2012). The arginine methyltransferase PRMT6 regulates cell proliferation and senescence through transcriptional repression of tumor suppressor genes. *Nucleic acids research* *40*, 9522-9533.
- Strom, D.K., Nip, J., Westendorf, J.J., Linggi, B., Lutterbach, B., Downing, J.R., Lenny, N., and Hiebert, S.W. (2000). Expression of the AML-1 oncogene shortens the G(1) phase of the cell cycle. *The Journal of biological chemistry* *275*, 3438-3445.
- Suda, T., and Arai, F. (2008). Wnt signaling in the niche. *Cell* *132*, 729-730.
- Tallack, M.R., Whittington, T., Yuen, W.S., Wainwright, E.N., Keys, J.R., Gardiner, B.B., Nourbakhsh, E., Cloonan, N., Grimmond, S.M., and Bailey, T.L., et al. (2010). A global role for KLF1 in erythropoiesis revealed by ChIP-seq in primary erythroid cells. *Genome research* *20*, 1052-1063.
- Tetsu, O., and McCormick, F. (1999). Beta-catenin regulates expression of cyclin D1 in colon carcinoma cells. *Nature* *398*, 422-426.
- Thomas, D., Lakowski, T.M., Pak, M.L., Kim, J.J., and Frankel, A. (2010). Förster resonance energy transfer measurements of cofactor-dependent effects on protein arginine N-methyltransferase homodimerization. *Protein science : a publication of the Protein Society* *19*, 2141-2151.
- Tijssen, M.R., Cvejic, A., Joshi, A., Hannah, R.L., Ferreira, R., Forrai, A., Bellissimo, D.C., Oram, S.H., Smethurst, P.A., and Wilson, N.K., et al. (2011). Genome-wide analysis of simultaneous GATA1/2, RUNX1, FLI1, and SCL binding in megakaryocytes identifies hematopoietic regulators. *Developmental cell* *20*, 597-609.
- Valenta, T., Hausmann, G., and Basler, K. (2012). The many faces and functions of β -catenin. *The EMBO journal* *31*, 2714-2736.
- van den Berg, D.J., Sharma, A.K., Bruno, E., and Hoffman, R. (1998). Role of members of the Wnt gene family in human hematopoiesis. *Blood* *92*, 3189-3202.
- van Genderen, C., Okamura, R.M., Fariñas, I., Quo, R.G., Parslow, T.G., Bruhn, L., and Grosschedl, R. (1994). Development of several organs that require inductive epithelial-mesenchymal interactions is impaired in LEF-1-deficient mice. *Genes & development* *8*, 2691-2703.

Veeman, M.T., Slusarski, D.C., Kaykas, A., Louie, S.H., and Moon, R.T. (2003). Zebrafish prickles, a modulator of noncanonical Wnt/Fz signaling, regulates gastrulation movements. *Current biology : CB* *13*, 680-685.

Verbeek, S., Izon, D., Hofhuis, F., Robanus-Maandag, E., te Riele, H., van de Wetering, M., Oosterwegel, M., Wilson, A., MacDonald, H.R., and Clevers, H. (1995). An HMG-box-containing T-cell factor required for thymocyte differentiation. *Nature* *374*, 70-74.

Wang, X., Crispino, J.D., Letting, D.L., Nakazawa, M., Poncz, M., and Blobel, G.A. (2002). Control of megakaryocyte-specific gene expression by GATA-1 and FOG-1: role of Ets transcription factors. *The EMBO journal* *21*, 5225-5234.

Weber, K., Bartsch, U., Stocking, C., and Fehse, B. (2008). A multicolor panel of novel lentiviral "gene ontology" (LeGO) vectors for functional gene analysis. *Molecular therapy : the journal of the American Society of Gene Therapy* *16*, 698-706.

Wu, H., Zheng, W., Eram, M.S., Vhuyian, M., Dong, A., Zeng, H., He, H., Brown, P., Frankel, A., and Vedadi, M., et al. (2016). Structural basis of arginine asymmetrical dimethylation by PRMT6. *The Biochemical journal* *473*, 3049-3063.

Xu, Y., Banerjee, D., Huelsken, J., Birchmeier, W., and Sen, J.M. (2003). Deletion of beta-catenin impairs T cell development. *Nature immunology* *4*, 1177-1182.

Yalcin, B.H. (2018). Wnt/ β -catenin signalling modulates megakaryopoiesis in the haematopoietic system. Dissertation (Frankfurt am Main).

Yang, Y., and Bedford, M.T. (2013). Protein arginine methyltransferases and cancer. *Nature reviews. Cancer* *13*, 37-50.

Yang, Y., Hadjikyriacou, A., Xia, Z., Gayatri, S., Kim, D., Zurita-Lopez, C., Kelly, R., Guo, A., Li, W., and Clarke, S.G., et al. (2015). PRMT9 is a type II methyltransferase that methylates the splicing factor SAP145. *Nature communications* *6*, 6428.

Yoshimatsu, M., Toyokawa, G., Hayami, S., Unoki, M., Tsunoda, T., Field, H.I., Kelly, J.D., Neal, D.E., Maehara, Y., and Ponder, B.A.J., et al. (2011). Dysregulation of PRMT1 and PRMT6, Type I arginine methyltransferases, is involved in various types of human cancers. *International journal of cancer* *128*, 562-573.

Zhang, W., Bone, J.R., Edmondson, D.G., Turner, B.M., and Roth, S.Y. (1998). Essential and redundant functions of histone acetylation revealed by mutation of target lysines and loss of the Gcn5p acetyltransferase. *The EMBO journal* *17*, 3155-3167.

Zhang, X., and Cheng, X. (2003). Structure of the predominant protein arginine methyltransferase PRMT1 and analysis of its binding to substrate peptides. *Structure (London, England : 1993)* *11*, 509-520.

Zhang, X., Zhou, L., and Cheng, X. (2000). Crystal structure of the conserved core of protein arginine methyltransferase PRMT3. *The EMBO journal* 19, 3509-3519.

Zhang, Y., Liu, T., Meyer, C.A., Eeckhoute, J., Johnson, D.S., Bernstein, B.E., Nusbaum, C., Myers, R.M., Brown, M., and Li, W., et al. (2008). Model-based analysis of ChIP-Seq (MACS). *Genome biology* 9, R137.

Zhao, X., Jankovic, V., Gural, A., Huang, G., Pardanani, A., Menendez, S., Zhang, J., Dunne, R., Xiao, A., and Erdjument-Bromage, H., et al. (2008). Methylation of RUNX1 by PRMT1 abrogates SIN3A binding and potentiates its transcriptional activity. *Genes & development* 22, 640-653.

Zhu, J., and Emerson, S.G. (2002). Hematopoietic cytokines, transcription factors and lineage commitment. *Oncogene* 21, 3295-3313.

Zhu, L.J. (2013). Integrative analysis of ChIP-chip and ChIP-seq dataset. *Methods in molecular biology* (Clifton, N.J.) 1067, 105-124.

7 List of tables

Table 1: Cell lines.....	23
Table 2: Cell culture media and supplements.....	23
Table 3: Chemicals, Reagents.....	24
Table 4: Enzymes.....	25
Table 5: Plasmids.....	26
Table 6: Oligonucleotides.....	30
Table 7: Antibodies.....	32
Table 8: Equipment.....	33
Table 9: Components and thermocycling conditions of the PCR.....	35
Table 10: Components and thermocycling conditions of the quantitative real-time PCR.....	36
Table 11: Analyzed CHIP-sequencing experiments.....	43
Table 12: List of the 9 proteins with annotation in hematopoietic or lymphoid organ development.....	52
Table 13: List of LEF1 peaks in GO:0030219 (megakaryocyte differentiation).....	61
Table 14: Command line arguments of the R script.....	98
Table 15: Possible members of the PRMT6 interactome, sorted by normalized H/L ratio.....	99

8 List of figures

Figure 1: Hierarchical model of human hematopoiesis	6
Figure 2: Schematic representation of megakaryopoiesis and platelet production.....	7
Figure 3: Schematic representation of erythropoiesis.....	8
Figure 4: Different assembly levels of chromatin packaging.	10
Figure 5: Family of mammalian PRMT enzymes	11
Figure 6: Schematic representation of the protein domain structure of PRMT6	12
Figure 7: Mechanisms of arginine methylation of PRMTs.	13
Figure 8: The transcription factor RUNX1 recruits PRMT6 to genes involved in the regulation of erythroid and megakaryocytic differentiation.. ..	14
Figure 9: Family of mammalian TCF/LEF transcription factors	17
Figure 10: Schematic representation of the canonical Wnt signaling pathway.....	18
Figure 11: Protein structure of β -catenin.....	19
Figure 12: Schematic representation of PRMT family enzymes regulating the LEF1 Wnt β -catenin-signaling pathway.....	21
Figure 13: Plasmid vector map of the pGL3-Basic vector.....	27
Figure 14: Plasmid vector map of the pcDNA3 vector	27
Figure 15: Plasmid vector map of the LeGO-iG2 vector	28
Figure 16: Plasmid vector map of the pRRLsAVI-MCS-iGFP-BirA vector	29
Figure 17: Plasmid vector map of the pGIPZ vector.....	30
Figure 18: The flow diagram shows the schematic procedure of the identification of novel PRMT6 interaction partners	45
Figure 19: Schematic overview of combined Co-Streptavidin Precipitation (Co-SP) with subsequent Stable Isotope Labeling with Amino acids in Cell culture (SILAC).. ..	47
Figure 20: RNA expression of PRMT6 in different hematopoietic cell lines.	48
Figure 21: RNA expression of PRMT6 in transduced K562 cells.....	49
Figure 22: Western Blot showing the Co-Streptavidin Precipitation (Co-SP) of biotinylated PRMT6 protein (Bio-PRMT6) from stable transduced K562 cells	50
Figure 23: The PRMT6 interactome; The Database for Annotation, Visualization and Integrated Discovery (DAVID) v6.8 was used for Functional Annotation Clustering.....	51
Figure 24: Functional Annotation Clustering of the PRMT6 interactome	52
Figure 25: Analysis of PRMT6 protein network.....	53
Figure 26: Protein interactions of the identified protein network were verified with Co-Streptavidin Precipitation (Co-SP)	54
Figure 27: Protein interactions of the identified protein network were verified with Co-Streptavidin Precipitation (Co-SP)	56
Figure 28: PRMT6 TOP-flash assay	58
Figure 29: RNA expression of <i>LEF1</i> in different hematopoietic cell lines.....	59
Figure 30: LEF1 ChIP-Seq analysis in K562 cells.....	60
Figure 31: Comparison of LEF1 peaks in different cell lines.....	63

Figure 32: Comparison of different TCF/LEF peaks in K562 cells	64
Figure 33: Verification of the identified LEF1 peak at the <i>ITGA2B</i> promoter	65
Figure 34: Verification of the identified LEF1 peak at the <i>RUNX1</i> enhancer	67
Figure 35: Verification of the putative LEF1 peak at the <i>CCND1</i> promoter.	68
Figure 36: RNA expression of two separate pGIPZ shLEF1 knockdown vectors in erythroleukemic K562 cells.....	69
Figure 37: Western blot of the two separate pGIPZ shLEF1 knockdown vectors in erythroleukemic K562 cells.....	70
Figure 38: RNA expression of two LEF1 overexpression vectors in erythroleukemic K562 cells.....	71
Figure 39: RNA expression of two LEF1 overexpression vectors in erythroleukemic K562 cells.....	72
Figure 40: Western blot of the LEF1 over-expressing erythroleukemic K562 cells.....	73
Figure 41: RNA expression of β -catenin overexpression vectors in erythroleukemic K562 cells	74
Figure 42: RNA expression of β -catenin over-expression vectors in erythroleukemic K562 cells.....	75
Figure 43: RNA expression of β -catenin over-expression vectors in erythroleukemic K562 cells.....	76
Figure 44: Western blot of the LEF1 expression in TPO differentiated CD34 ⁺ cells.....	77
Figure 45: LEF1 binding during megakaryocytic differentiation	78
Figure 46: RNA expression of β -catenin overexpression vectors in TPO treated CD34 ⁺ cells.....	80
Figure 47: RNA expression of differentiated hematopoietic cells	81
Figure 48: RNA expression of differentiated hematopoietic cells.	83
Figure 49: RNA expression of differentiated hematopoietic cells..	84
Figure 50: RNA expression of two separate pGIPZ shPRMT6 knockdown vectors in erythroleukemic K562 cells.....	85
Figure 51: Cell cycle analysis of transduced K562 cells	86
Figure 52: The bone marrow microenvironment (BMM)	96

9 Abbreviations

A	Adenine
aa	Amino acid
ADMA	asymmetric dimethyl-arginine
ALL	Acute lymphoblastic leukemia
AML	Acute myeloid leukemia
APC	Sdenomatous polyposis coli
arg	Arginine
Avi	Avidin
BCL6	B-cell lymphoma 6 protein
BED	Browser extensible data
Bio	Biotin
BirA	Biotin holoenzyme synthetase
BIRC5	Baculoviral inhibitor of apoptosis repeat-containing 5
BMM	Bone marrow microenvironment
C	Cytosine
c	Carboxy
CCND1	Cyclin D1
CD	Cluster of differentiation
cDNA	Complementary DNA
CEBPA	CCAAT/enhancer-binding protein alpha
CHD2	Chromodomain helicase DNA binding protein 2
ChIP	Chromatin immunoprecipitation
CLP	Common lymphoid progenitor
CMEP	Common myeloid erythroid progenitor
CRC	colorectal cancer
CRD	Context-dependent regulatory domain
CTNNB1	Catenin Beta 1; β -Catenin
DAVID	Database for annotation, visualization and integrated discovery
Dkk1	Dickkopf-related protein 1
dn	Dominant negative
DNA	Deoxyribonucleic acid
Dvl	Dishevelled
ENCODE	Encyclopedia of DNA elements
EP	Erythroid progenitor
EPO	erythropoetin
FACS	Fluorescence-activated cell sorting
FcR	Fc receptor
FCS	Fetal calf serum
FLI1	Friend leukemia integration 1 transcription factor

G	Guanine
GAPDH	Glyceraldehyde 3-phosphate dehydrogenase
GAR	Glycine- and arginine-rich
GATA	GATA-binding factor
G-CSF	Granulocyte-colony stimulating factor
GCSR	Glucagon receptor
GFP	Green fluorescent protein
GMP	Granulocyte-macrophage progenitor
GO	Gene Ontology
GON4L	GON-4-like protein
GPIb	Glycoprotein Ib
GRCh	Genome reference consortium human build
GSK3 β	Glycogen synthase kinase 3 beta
GYP A	Glycophorin A
H	Histone
h	Human
H/L	Heavy-to-light ratio
HBP1	HMG-box transcription factor 1
HEL	Human erythroleukemia
hg	Human genome
HMG	High-mobility group
HSC	Hematopoietic stem cell
ID	Identifier
IgG	Immunoglobulin G
IGV	Integrative Genomics Viewer
IL	Interleukin
ILF	Interleukin-enhancer binding protein
IR	infrared
ITGA2B	Integrin alpha-IIb
ITGB3	Integrin beta-3
K	Lysine
KIT	Proto-oncogene c-KIT
KLF1	Krüppel-like factor 1
LEF1	Lymphoid enhancer-binding factor 1
LeGO	Lentiviral gene ontology vectors
LRP	Lipoprotein receptor related protein
LRP6	Lipoprotein receptor-related protein 6
LT	Long-term
lys	Lysine
m/z	Mass-to-charge ratio

MCS	Multiple cloning site
MEF	Mouse embryonic fibroblasts
MEP	Megakaryocytic-erythroid progenitor
miRNA	Micro ribonucleic acid
Mk	megakaryocyte
MkP	Megakaryocytic progenitor
MLL1	Acute lymphoblastic leukemia 1
MMA	monomethyl-arginine
MPP	Multipotent progenitor
mRNA	Messenger RNA
N	Amino
NF-E2	Transcription factor NF-E2 45 kDa subunit
NKAP	NF-kappa-B-activating protein
NLS	Nuclear localization signal
ns	not significant
OD	Infrared
PCR	polymerase chain reaction
PDGFb	Platelet derived growth factor b
PI	Protease Inhibitor
POLG	Polymerase subunit gamma
PRC2	Polycomb repressive complex 2
PRMT	Protein arginine N-methyltransferase
PU.1	Transcription factor PU.1
p-value	Probability value
qPCR	quantitative PCR
R	Arginine
RARA	Retinoic acid receptor alpha
RBC	Red blood cells
Rc	Reticulocytes
RefSeq	Reference sequence
RHD	Runt homology domain
Rnase	Ribonuclease
RT	Room temperature
RUNX1	Runt-related transcription factor 1
SAM	S-Adenosyl methionine
SCF	Stem cell factor
SD	Standard deviation
SDMA	symmetric dimethyl-arginine
seq	Sequencing
Ser	Serine

SFFV	Silencing-prone spleen focus forming virus
SILAC	Stable isotope labeling by amino acids in cell culture
SOX6	SRY-box transcription factor 6
SP	Streptavidin precipitation
ST	Short-term
T	Thymine
TAL1	T-cell acute lymphocytic leukemia protein 1
TCF7	Transcription factor 7
TCF7L1	Transcription factor 7-like 1
TCF7L2	Transcription factor 7-like 2
TCR	T cell receptor
TF	Transcription factor
Thr	Threonine
TLE	Transducin-like enhancer protein
TOP-flash	TCL/LEF-firefly luciferase
TPO	thrombopoetin
TSP1	Thrombospondin 1
TSS	Transcription start site
UCSC	University of California, Santa Cruz
UTR	Untranslated region
V-ERBA	V-erbA-related protein 2
W	Adenine or thymine
Wnt	Wingless
WRE	Wnt-responsive element
YY1	Yin Yang 1

Publications

Herkt SC, Kuvardina ON, Herglotz J, **Schneider L**, Meyer A, Pommerenke C, Salinas-Riester G, Seifried E, Bonig H, Lausen J (2018) Protein arginine methyltransferase 6 controls erythroid gene expression and differentiation of human CD34+ progenitor cells. **Haematologica** 103: 18–29.

Hiss M, Meyberg R, Westermann J, Haas FB, **Schneider L**, Schallenberg-Rüdinger M, Ullrich KK, Rensing SA (2017a) Sexual reproduction, sporophyte development and molecular variation in the model moss *Physcomitrella patens*: introducing the ecotype Reute. **Plant J** 90: 606–620.

Hiss M, **Schneider L**, Grosche C, Barth MA, Neu C, Symeonidi A, Ullrich KK, Perroud P-F, Schallenberg-Rüdinger M, Rensing SA (2017b) Combination of the Endogenous *lhcsr1* Promoter and Codon Usage Optimization Boosts Protein Expression in the Moss *Physcomitrella patens*. **Front Plant Sci** 8: 1842.

Kuvardina ON, Herkt S, Meyer A, **Schneider L**, Yillah J, Kohrs N, Bonig H, Seifried E, Müller-Tidow C, Lausen J (2017) Hematopoietic transcription factors and differential cofactor binding regulate PRKACB isoform expression. **Oncotarget** 8: 71685–71698.

Lang D, Ullrich KK, Murat F, Fuchs J, Jenkins J, Haas FB, Piednoel M, Gundlach H, van Bel M, Meyberg R, Vives C, Morata J, Symeonidi A, Hiss M, Muchero W, Kamisugi Y, Saleh O, Blanc G, Decker EL, van Gessel N, Grimwood J, Hayes RD, Graham SW, Gunter LE, McDaniel SF, Hoernstein SNW, Larsson A, Li F-W, Perroud P-F, Phillips J, Ranjan P, Rokshar DS, Rothfels CJ, **Schneider L**, Shu S, Stevenson DW, Thümmel F, Tillich M, Villarreal Aguilar JC, Widiez T, Wong GK-S, Wymore A, Zhang Y, Zimmer AD, Quatrano RS, Mayer KFX, Goodstein D, Casacuberta JM, Vandepoele K, Reski R, Cuming AC, Tuskan GA, Maumus F, Salse J, Schmutz J, Rensing SA (2018) The *Physcomitrella patens* chromosome-scale assembly reveals moss genome structure and evolution. **Plant J** 93: 515–533.

Meyberg R, Perroud P-F, Haas FB, **Schneider L**, Heimerl T, Renzaglia KS, Rensing SA (2020) Characterization of evolutionarily conserved key players affecting eukaryotic flagellar motility and fertility using a moss model. **New Phytol.**

Roth H, **Schneider L**, Eberle R, Lausen J, Modlich U, Blümel J, Baylis SA (2020) Zika virus infection studies with CD34+ hematopoietic and megakaryocyte-erythroid progenitors, red blood cells and platelets. **Transfusion**

Steiner M, **Schneider L**, Yillah J, Gerlach K, Kuvardina ON, Meyer A, Maring A, Bonig H, Seifried E, Zörnig M, Lausen J (2019) FUSE binding protein 1 (FUBP1) expression is upregulated by T-cell acute lymphocytic leukemia protein 1 (TAL1) and required for efficient erythroid differentiation. **PLoS ONE** 14: e0210515.

Curriculum vitae

Personal data:

Lucas Schneider

Schwalbacher Str. 13
D-60326 Frankfurt
Phone: +49-69 -6782376
lucas.schneider@iig.uni-stuttgart.de
l.schneider@blutspende.de

Date of birth: 27.09.1988 in Bad Säckingen

Education:

- | | |
|-------------------|-----------------------------------------------------------------------------------------|
| 10/2019 – 08/2020 | Research assistant at the University of Stuttgart |
| 05/2016 – 09/2019 | Research assistant at the DRK blood donation service Frankfurt am Main |
| 01/2015 - 02/2016 | Research assistant at the Philipps University Marburg |
| 10/2012 - 12/2014 | M.Sc. in Molecular and Cellular Biology at the Philipps University Marburg |
| 10/2009 - 09/2012 | B.Sc. in Biology at the Albert Ludwig University of Freiburg |
| 08/2008 - 09/2009 | Alternative civilian service in the house St. Gabriel, Caritas Freiburg e.V. |
| 08/2005 - 06/2008 | High School for nutritional science at the Justus von Liebig School in Waldshut-Tiengen |

Acknowledgements

I want to thank Prof. Dr. Jörn Lausen for providing me with the opportunity to do this work and the excellent supervision of my thesis.

I also would like to thank Prof. Dr. Monilola Olayioye for being the second reviewer of my thesis.

My special thanks go to the Lausen lab group for all the support and the great atmosphere in the laboratory and the research meetings.

I want to thank the group of Prof. Dr. med. Thomas Oellerich and Dr. Björn Häupl for their execution of the SILAC based mass spectrometry.

I want to thank Univ.-Prof. Dr. med. habil. Dr. med. Halvard B. Bönig for giving me the opportunity to work in his laboratory. I want to thank his team for all the support and warmth.

I also would like to thank Univ.-Prof. Dr. med. Dr. h. c. Erhard Seifried for making it possible for me to work at the Institute for Transfusion Medicine and Immunohaematology in Frankfurt am Main.

Ehrenwörtliche Erklärung

Hiermit erkläre ich, dass ich die beigefügte Dissertation selbstständig verfasst und keine anderen als die angegebenen Hilfsmittel genutzt habe. Alle wörtlich oder inhaltlich übernommenen Stellen habe ich als solche gekennzeichnet.

Ich versichere außerdem, dass ich die beigefügte Dissertation nur in diesem und keinem anderen Promotionsverfahren eingereicht habe und dass diesem Promotionsverfahren keine endgültig gescheiterten Promotionsverfahren vorausgegangen sind.

Ort, Datum

Unterschrift

Name / Anschrift
Lucas Schneider
Schwalbacher Str. 13
60326 Frankfurt